

Correlated Spin Transport in Nanostructures: Entanglement Creation and Spin Filtering

Inauguraldissertation
zur
Erlangung der Würde eines Doktors der Philosophie

vorgelegt der
Philosophisch-Naturwissenschaftlichen Fakultät
der Universität Basel

von
Patrik Recher
aus Basel

Basel, 2003

Genehmigt von der Philosophisch-Naturwissenschaftlichen Fakultät auf Antrag
von

Prof. Dr. Daniel Loss

Prof. Dr. C.J.W. Beenakker

Prof. Dr. Christoph Bruder

Basel, den 21. Oktober 2003

Prof. Dr. Marcel Tanner
Dekan

Acknowledgements

It is a great pleasure to thank Prof. Daniel Loss for his continuous support and guidance during my time as a PhD-student. His physical intuition and broad knowledge impress me deeply. I have enjoyed working on exciting and timely research projects. Parts of my projects were also in close collaboration with Dr. Eugene Sukhorukov. To work with him was pleasant and very valuable for me, thanks Zhenya. In addition, I would like to thank Profs. Carlo Beenakker and Christoph Bruder for kindly agreeing to co-referee this Thesis, and Prof. F.-K. Thielemann for charing the defense exam.

The atmosphere in the Basel group has always been very friendly and stimulating. In particular, I would like to thank my office mate Oliver Gywat for numerous discussions about physics and shared insights on our research projects. Aside from this, we have also had many conversations about topics outside of physics which were as fun and interesting. I thank Dr. Florian Meier for joint runs along the river Rhine and, of course, for his friendship, discussions, and the nice coffee breaks. I would like to thank Hanno Gassmann for repeatedly having dinner with me in St. Johannis Restaurant during the writing of this Thesis. Finally, I would like to thank all the other members of the group which made my time as a PhD-student very enjoyable and even more memorable. Thank you to Audrius Alkauskas, Dr. Wolfgang Belzig, Dr. Guido Burkard, Verónica Cerletti, Bill Coish, Dr. Audrey Cottet, Dr. Carlos Egues, Hans-Andreas Engel, Vitaly Golovach, Dr. Alexander Khaetskii, Dr. Michael Leuenberger, Dr. Daniel Saraga, Dr. John Schliemann, Christian Schroll and Dr. Pascal Simon. And last but not least, I would like to thank Bill Coish, Hanno Gassmann, Dr. Florian Marquardt and Dr. Florian Meier for reading parts of the manuscript, and Hans-Andreas Engel for providing me with his references sort routine. The print of this Thesis was financially supported by the "Dissertationenfonds" of the University of Basel.

Abstract

The electron spin for electronics has only recently attracted much interest. The idea to use spin—as opposed to charge—as the fundamental data carrier was motivated by recent experiments that showed unusually long spin-dephasing times up to microseconds for electrons in semiconductors as well as phase coherent transport over distances exceeding one hundred micrometers. In addition, experiments demonstrated the injection of spin-polarized carriers—electrons and holes—from a magnetic into a non-magnetic semiconductor which opens the door for various applications in spin electronics (spintronics). Besides the broad use of the electron spin in conventional devices, like in giant magnetoresistance (GMR) based magnetic read-out heads for computer hard drives or for non-volatile memories, the spin of the electron confined in nanostructures such as semiconductor quantum dots serves as a natural realization of a quantum bit (qubit). A quantum computer uses explicitly the quantum nature of systems where phase coherence and entanglement play a crucial role which requires a radically new design of the underlying computer hardware. In particular, entangled spin qubits, combined with the ability to control them via their charges, can serve as electronic EPR (Einstein-Podolsky-Rosen)-pairs in wires, i.e. pairs of electrons which are spatially separated (and uncorrelated) but still correlated with respect to their spins. Such entangled particles are the resource for secure quantum communication protocols which have been experimentally implemented using photons—the quantized units of light. The equivalent experiments for *massive* particles like electrons in a solid-state environment have not yet been performed, although their need cannot be overestimated, both from a practical point of view and also from a more fundamental one.

In this Thesis, we address the question of creating such nonlocal spin-entangled electron pairs in a way that is suitable to detect the produced entanglement in transport experiments via their current-noise properties. We

discuss various setups—entanglers— where Cooper pairs in a superconductor with spin singlet wave functions act as the source of spin-entanglement. In the presence of a voltage bias between the superconductor and two spatially separated normal conducting leads which are weakly tunnel-coupled to the superconductor, the electrons of a Cooper pair can tunnel coherently—in an Andreev (pair-)tunneling process—from the superconductor to the normal leads thereby remaining in the spin singlet state. This produces a current carried by pairs of spin-entangled electrons in the leads. In these setups, superconducting pair-correlations and Coulomb interaction between the two electrons are competing features. On the one hand, the orbital wave function of a Cooper pair is symmetric which favors the tunneling of both electrons into the same outgoing arm of the entangler. Such processes are unwanted since they do not lead to nonlocality. On the other hand, in small low-dimensional quantum confined nanostructures, electron-electron interaction becomes sizable and can be used to separate the two electrons of a Cooper pair. We exploit such strong correlations between the electron charges of a pair by using either quantum dots in the Coulomb blockade regime, one dimensional wires with Luttinger liquid properties or resistive outgoing leads coupled to the superconductor. We calculate the two competing tunneling currents from the superconductor to different leads (desired pair-split process) and to the same lead (unwanted local process) in detail. By comparing their ratio, we can estimate the efficiency of the entangler and see how it depends on various system parameters. This then allows us to identify a regime of experimental accessibility where the pair-split process is dominant.

The ability to have (coherent) control over single electron spins in semiconductor nanostructures is crucial in view of quantum computing with electron spins. In particular, spin-filtering and spin read-out is of great importance. For this we consider a quantum dot in the Coulomb blockade regime weakly coupled to current leads and show that in the presence of a magnetic field the dot acts as an efficient spin filter (at the single-spin level) which produces a spin-polarized current. Conversely, if the leads are fully spin-polarized, the magnitude of the transport current through the dot depends on the spin state of the dot. Quantum dots permit the control of charge down to single electrons. It is therefore feasible to consider a single spin $1/2$ on the dot—a spin qubit—which can be read out by a current. Combined with electron spin resonance (ESR) techniques this allows one to operate the quantum dot as a single spin memory with read-in and read-out capabilities.

Contents

Acknowledgements	i
Abstract	iii
1 Introduction	1
1.1 The electron spin for electronics	1
1.2 Entanglement and nonlocality	4
1.3 Detection of spin-entanglement	6
1.4 Ways of creating spin-entanglement	7
1.5 Outline	10
2 Creation of mobile spin-entangled electrons using superconductors	13
2.1 Introduction	13
2.2 Andreev Entangler with quantum dots	14
2.2.1 Qualitative description of the entangler	15
2.2.2 Hamiltonian	19
2.2.3 Stationary current and T-matrix	21
2.2.4 Current due to tunneling into different leads	22
2.2.5 Tunneling via the same dot	28
2.2.6 Efficiency and discussion	32
2.2.7 Aharonov-Bohm oscillations	34
2.2.8 Conclusion	37
2.3 Andreev Entangler with Luttinger liquid leads	38
2.3.1 About Fermi liquids and Luttinger liquids	38
2.3.2 Setup of entangler	43
2.3.3 Hamiltonian	45
2.3.4 Stationary current	48

2.3.5	T-matrix	48
2.3.6	Current for tunneling into different leads	50
2.3.7	Current for tunneling into the same lead	58
2.3.8	Efficiency and discussion	62
2.3.9	Decay of the electron-singlet due to interactions	64
2.3.10	Propagation of charge and spin	65
2.3.11	Conclusion and outlook	68
2.4	Andreev Entangler with high-resistance leads	69
2.4.1	Introduction	70
2.4.2	Setup and formalism	71
2.4.3	Current for tunneling into different leads	74
2.4.4	Current for tunneling into the same lead	76
2.4.5	Discussion and conclusion	78
3	Quantum dot as spin filter and spin memory	81
3.1	Introduction	81
3.2	Hamiltonian and formalism	83
3.3	Spin filter in the sequential tunneling regime	88
3.4	Spin filter in the cotunneling regime	89
3.5	Efficiency of spin filter in the sequential tunneling regime	91
3.6	Spin read-out and spin memory	91
3.7	Switchable spin filter in carbon nanotubes	94
3.8	Using the spin filter to measure Bell inequalities	95
3.9	Conclusion	100
A	Suppression of virtual states with both electrons in the leads	101
B	Electron hole pair excitation	103
C	Finite size diagonalization of the Luttinger liquid-Hamiltonian	105
D	Two-particle correlation function for a Luttinger liquid	109
E	Exact results for time integrals	113
F	Response function $\chi_{\phi\phi}(\omega)$	115

References

119

Curriculum Vitae

129

Chapter 1

Introduction

1.1 The electron spin for electronics

The ongoing reduction of the size of electronic devices down to length scales which become comparable to the Fermi wavelength $\lambda = h/p_F$ of electrons in the host material, where p_F is the Fermi momentum and $h = 6.63 \times 10^{-34}$ Js Planck's constant, leads to discrete energy levels which requires a quantum mechanical treatment of transport processes, e.g. to calculate the conductance of a small quantum wire [1, 2]. This wavelength is on the order of several nanometers in low dimensional semiconductor structures. Further, in quantum-confined nanostructures, the quantization of charge becomes relevant and allows the control of charge transport down to single electrons [3]. While the charge of the electron is well established in electronics, the idea to use its spin as the basic unit of information storage has only recently attracted much interest [4–6]. The suggestion to use spin in electronic devices has received strong experimental support [7–9] showing unusually long spin dephasing times [7] in semiconductors (~ 150 ns), the injection of spin-polarized currents from a magnetic- to a non-magnetic semiconductor [8, 9], as well as phase-coherent spin transport over distances exceeding 100 micrometers [7].

The electron spin allows fundamental improvements of conventional devices, e.g. in magnetic read-out heads for computer hard drives based on the giant magnetoresistance (GMR) effect [10], non-volatile memories, or in spin-polarized field-effect transistors [11] which are based on injected spin currents and are controlled via spin orbit interaction—a combination of charge and

spin control. Further, electron spins in quantum-confined structures such as semiconductor quantum dots [3], atoms, or molecules can be used as a quantum bit (qubit) [12] for quantum computing [13–15] and quantum communication [14–16], where a radically new design of the necessary hardware is required.

A quantum computer processes quantum bits (qubits) rather than classical bits like 0 and 1. A qubit $|\psi\rangle$ can be in any superposition of its underlying basis states $|0\rangle$ and $|1\rangle$, i.e.

$$|\psi\rangle = \alpha|0\rangle + \beta|1\rangle, \quad (1.1)$$

where the complex amplitudes α and β satisfy the normalization condition $|\alpha|^2 + |\beta|^2 = 1$. A spin $1/2$ of an electron represents a natural realization of such a two level system since the spin of an electron has only two basis states $|\uparrow\rangle$ and $|\downarrow\rangle$ with respect to an arbitrary quantization axis. These states can then be identified as $|0\rangle$ and $|1\rangle$, respectively. A state of N qubits is a vector in a space of 2^N dimensions with basis $|0\dots 00\rangle$, $|0\dots 01\rangle$, $|0\dots 10\rangle$, \dots . The power of a quantum computer comes from the quantum parallelism since a quantum computer processes coherent superpositions of computational basis states rather than just binary strings of zeros and ones. The two most important examples of a quantum algorithm that outperforms any known classical algorithm for the same problem are Shor's factoring algorithm [17] and Grover's algorithm [18] for searching an unsorted database.

Already a large number of proposals for the implementation of a quantum computer exist. Among many others, qubits encoded in the internal degrees of freedom of cold trapped ions [19] or in specific nuclear spins of a molecule (liquid-state NMR) [20–23] are studied. Very promising systems to search for implementations of a quantum bit are solid-state systems. They have the advantage that once the basic building blocks of a quantum computer are realized, the upscaling to a functional device containing many qubits seems likely (e.g. on-chip production in semiconductor systems). It was proposed by Loss and DiVincenzo [12] that arrays of semiconducting quantum dots, each dot containing a single electron spin, can be used for a quantum computer. The coupling between two spins on neighboring quantum dots is achieved by spin-exchange interaction which is controlled by varying the tunnel barriers between the dots or by external magnetic and/or electric fields. Realistic ideas for the implementation of this proposal are under investigation [24]. A subsequent proposal which uses the same principles

is given by nuclear spins in donor atoms in silicon [25]. In addition, ESR transistors in SiGe heterostructures [26], electrons trapped by surface acoustic waves [27] and charge degrees of freedom in quantum dots [28–32] have been considered as potential realizations of a qubit. In superconducting devices, flux states [33] or charge states [34–36] in coupled Josephson junctions, and d-wave Josephson junctions [37] have been proposed as the fundamental building blocks of a quantum computer.

To perform a quantum computation, each qubit should be addressable individually. During a calculation, the state of a quantum computer is in general in a complicated quantum superposition which should stay phase coherent, i.e. the superposition of computational basis states should remain unaffected. In this sense, the qubit should be as “microscopic” as possible. By this we mean that the qubit degrees of freedom should couple only very weakly to the environment. On the other hand, we want to manipulate a qubit which requires some coupling to the outside world. In addition, at the end of every calculation, the qubit has to be read out. This demands mechanisms with control at the level of a single qubit, e.g. a spin 1/2 particle. This issue we address in Chapter 3 where we show that a single electron spin on a quantum dot can be read out via (charge) transport measurements. Here, the basic idea is to measure the spin of an electron via its charge [12]. This is feasible since the orbital degrees of freedom of an electron are connected to its spin degrees of freedom via the Pauli principle.

In addition to single-qubit operations, coupling between any two (neighboring) qubits is required. The most important two-qubit quantum gate is the XOR gate [21] since any quantum algorithm can be decomposed into XOR gates and single-qubit operations. It has been shown in Ref. [12] that this gate can be described by a (unitary) quantum operation containing a sequence of single-qubit rotations and, very essential, the so-called square-root-of-swap operation $U_{sw}^{1/2}$. It acts on a two-qubit basis state as follows: E.g. for the $|01\rangle$ state, $U_{sw}^{1/2} |01\rangle = (|01\rangle + i|10\rangle)/(1+i)$. The state $(|01\rangle + i|10\rangle)/(1+i)$ is an entangled state, since it is not separable into a product of single qubit states. Thus, the creation of entanglement is needed for the explicit construction of the XOR gate.

These entangled qubits combined with the possibility of transporting them in wires via their charge then allows the creation of mobile and *nonlocal* entangled states which represent the fundamental resource for secure quantum communication [16]. This is particularly interesting for electron spins

in quantum confined semiconductors with long spin decoherence lengths on the order of $100 \mu\text{m}$ [7]. The decoherence length is the transport length over which a qubit of the form Eq. (1.1) stays phase coherent. It should be noted that quantum communication protocols, like dense coding or quantum teleportation [15], only require two or a few qubits. Their implementation is therefore less demanding than a quantum computer where $\sim 10^5$ qubits should be controlled phase coherently.

1.2 Entanglement and nonlocality

Nonlocality and entanglement are two of the most peculiar features of quantum mechanics. We call a quantum state of two particles entangled if it cannot be written as a product of single-particle wave functions. As an illustrative and most simple example we consider the two electrons in a Helium atom. In the ground state, both electrons occupy the lowest orbital state $|\Phi_0\rangle$ (the 1s-state) and therefore the (approximate) wave function is

$$\begin{aligned} \psi(x_1\sigma_1, x_2\sigma_2) &= \psi_{orb}(x_1, x_2) \times \psi_{spin}(\sigma_1, \sigma_2) \\ &= \Phi_0(x_1)\Phi_0(x_2) \times \frac{1}{\sqrt{2}}\{\chi_\uparrow(\sigma_1)\chi_\downarrow(\sigma_2) - \chi_\downarrow(\sigma_1)\chi_\uparrow(\sigma_2)\}, \end{aligned} \tag{1.2}$$

where x_i and σ_i denote the position and spin coordinates of particle $i = 1, 2$. The orbital wave function $\psi_{orb}(x_1, x_2)$ is a product of two single-particle wave functions and therefore is not entangled whereas the spin wave function is entangled (only the singlet state with total spin zero is allowed by the Pauli principle). Similar, the ground state of a single quantum dot which contains two electrons is also a spin singlet [38]. However, this state of the Helium atom or of the single quantum dot is not yet very interesting in the context of spin-entanglement, although the spin state is not a product state. The reason is that we cannot measure each electron individually since they occupy the same orbital state $|\Phi_0\rangle$. But if we could (somehow!) separate the electrons in a way that one electron gets transported to a point A and the other to a point B , we could create a wave function for the two electrons of the form

$$\begin{aligned} \psi_{AB}(x_1\sigma_1, x_2\sigma_2) &= \frac{1}{\sqrt{2}}\{\Phi_A(x_1)\Phi_B(x_2) + \Phi_B(x_1)\Phi_A(x_2)\} \\ &\times \frac{1}{\sqrt{2}}\{\chi_\uparrow(\sigma_1)\chi_\downarrow(\sigma_2) - \chi_\downarrow(\sigma_1)\chi_\uparrow(\sigma_2)\}, \end{aligned} \tag{1.3}$$

where Φ_A and Φ_B are wave functions which are located at points A and B , respectively. The spin wave function is assumed to be unaffected by the transport of electrons to A and B . If the distance between A and B is large so that the wave functions do not overlap, i.e. $\int d^3x \Phi_A(x)\Phi_B^*(x) = 0$, one of the two orbital terms in ψ_{AB} is always zero. Therefore, we know for certain that one electron is always located at A and the other at B . But what about the spin of the electron at A or B ? We do not know! The wave function in Eq. (1.3) has the form of the groundstate wave function (in the Heitler-London approximation) for the hydrogen molecule H_2 or also for a tunnel-coupled double quantum dot [39]. Although the dissociation of the two electrons is not complete—the small wave function overlap is needed for the exchange splitting favoring the singlet groundstate—the two wave functions are well separated in space and therefore can be addressed individually which could be exploited to finally dissociate the two entangled electrons completely. Exactly this situation we consider in Section 1.4 where a tunnel-coupled quantum dot is proposed to create mobile spin-entangled electrons in two spatially separated leads which are coupled to the double dot.

The state Eq. (1.3) is at first sight not alarming, since in quantum mechanics a state can be in a superposition of other states, but here it is more than just a superposition. It is clearer to write ψ_{AB} in second quantized form

$$|\psi_{AB}\rangle = \frac{1}{\sqrt{2}} \left(d_{A\uparrow}^\dagger d_{B\downarrow}^\dagger - d_{A\downarrow}^\dagger d_{B\uparrow}^\dagger \right) |0\rangle, \quad (1.4)$$

where $d_{A\sigma}^\dagger$ ($d_{B,-\sigma}^\dagger$) creates a spin σ ($-\sigma$) electron at A (B) and $|0\rangle$ is the particle vacuum. Since a measurement in quantum mechanics is a filtration process the spin measurements at A and B are unavoidably correlated even though A and B can be far apart such that there is no way of transporting information from A to B during the correlation measurements.

This paradox is known as the EPR paradox after a paper by A. Einstein, B. Podolsky, and N. Rosen in 1935 [40]. There it was concluded that quantum mechanics must be an incomplete theory where the true microscopic description can be understood in terms of so-called hidden variables [41] and has to obey the locality principle. The locality principle states that the outcome of a measurement of the particle at A should not be influenced by a measurement of the particle located at B if A and B are far apart, even if in the distant past the two particles might have interacted—e.g. in the H_2

molecule. In 1964, J.S. Bell formulated a testable inequality [42] between correlation measurements on two particle systems based on the locality principle which is in contradiction to quantum mechanics. The violation of the Bell inequality¹ could be demonstrated with photons [43] in favor of the quantum theory². To date no equivalent experiment exists for massive particles like electrons in a solid-state environment.

Apart from the philosophical interest in nonlocal quantum correlations, entanglement is used as a resource for various secure quantum communication schemes [16, 21]. Again such quantum communication protocols like dense coding [44] or quantum teleportation [45, 46] have been successfully implemented with photons but not yet with massive particles such as electrons.

1.3 Detection of spin-entanglement

In view of the quantum computing proposal by Loss and DiVincenzo [12] with electron spins in quantum dots it is interesting and desirable to test the entanglement between two electron spins which are spatially separated so that each spin can be manipulated independently. It has been shown in Refs. [12, 39] that two electron spins which reside on adjacent quantum dots can become entangled by lowering the tunneling barrier between the two dots which leads to an exchange interaction between the two spins on the dots. By measuring the exchange splitting (singlet-triplet splitting) one would obtain some information about entanglement in this system. Another way to test the entanglement between two electron spins is via transport experiments. It has been proposed in Ref. [47] that in a beamsplitter setup (see Fig. (1.1)) combined with noise measurements (i.e. current-current correlation measurements), entanglement can be detected via an enhancement of the shot noise (for singlets). A further possibility to measure entanglement is to measure spin-spin correlations between the two spatially separated electrons and show that the Bell inequality is violated. By using spin filters, the spin information can be converted into charge information [48], which then

¹There are different versions of “Bell inequalities”. In this Thesis, we sometimes refer to as the Bell inequality to honor Bell’s original idea to formulate such a testable inequality.

²For photons, the qubit basis states are defined as its polarization states, e.g. left and right circular polarization. The creation of polarization entangled photons is usually achieved via parametric downconversion processes in optical nonlinear crystals.

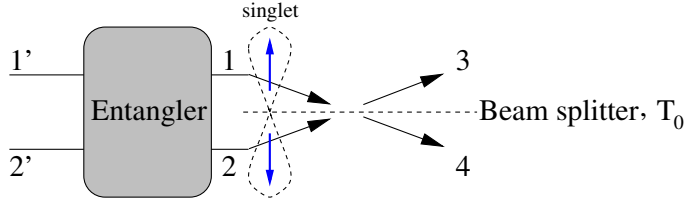


Figure 1.1: Setup to measure noise of spin-entangled electrons [47]: Uncorrelated electrons are fed into the entangler from leads 1' and 2' and transformed into entangled states, let's say spin singlets, which are injected into leads 1 and 2, one electron per lead. The entanglement of the spin singlet can then be detected using a beam splitter setup. Since the orbital wave function of the singlet is symmetric, the electrons leave the beamsplitter preferably in the same outgoing arms (3 or 4). This “bunching” of the electrons then leads to an enhancement of the shot noise in the outgoing arms compared to uncorrelated electrons.

allows us, to express the Bell inequality in terms of current-current correlation functions [49, 50]. This requires that a current of spin-entangled and spatially separated electrons (e.g. in two wires so that each wire contains one electron of the entangled pair) is available. In such a current of entangled pairs, the time separation between the arrival (in the measurement apparatus) of different pairs must be longer than the time delay between the electrons belonging to the same entangled spin-pair. This is very crucial for testing entanglement via transport measurements since they should only detect (cross) correlations between electrons from the same pair.

The major part of this Thesis is devoted to the creation of such currents carried by spin-entangled electrons in wires suitable for their detection via noise. We further discuss a possible spin filter which produces (or detects) spin-polarized currents if a quantum dot in the Coulomb blockade regime, and coupled to leads, is subjected to a magnetic field. We analyze the possibility to use such a spin filter for measuring Bell inequalities of spin-entangled electrons.

1.4 Ways of creating spin-entanglement

Entanglement is the rule rather than the exception in the groundstate of solid state systems. As we have learned in Section 1.2, the ground state of the Helium atom or of a single quantum dot is spin-entangled. However,

to make the entanglement useful for testing nonlocality or as a source for quantum communication protocols, we require separate control over each particle which takes part in the entangled state (e.g. to transport them to separate places). Obviously it is hard to have control over entangled states in a solid-state environment due to other electrons in the device structure that may interact with the entangled pair as well as coupling to the environment—the solid-state matrix.

For such a setup—to which we refer to as entangler—various proposals exist. The probably most natural candidate for such an entangler is a tunnel-coupled double quantum dot [12,39,51,52] where both dots are initially empty and coupled to separate outgoing drain leads and to the same source lead. By lowering the tunnel barrier, uncorrelated electrons from the source can then enter the dots (one electron in each dot due to Coulomb repulsion between the electrons) and become entangled via spin exchange interaction. The tunneling barrier to the source is raised again so that further electrons are prevented from entering when, in the next step, the barriers to the drain leads are opened and the entangled pair can leave the double dot to separate leads. By continuously repeating this procedure, we generate a current of entangled and nonlocal spin pairs. Although this idea is natural, it requires precise control of switching parameters [52], e.g. the switching of the tunneling barriers connecting the dots to the drains should be fast compared to the interdot tunneling. Otherwise one cannot assure that the electrons leave to different leads. This entangler scheme combined with the beamsplitter setup [47] as an entanglement detector is currently investigated experimentally by the Delft group, see Ref. [53]. Besides the tunneling mechanism to create spin-entangled electrons in nearby quantum dots there exist different means to couple two spins, e.g. via interaction to an optically excited virtual exciton in the host material surrounding the dot [54], by coupling spins in quantum dots via an optical cavity mode [55], or via coupling two quantum dots to the same s-wave superconductor. In equilibrium, the coupling to the superconductor then leads to an effective spin exchange which favors a spin singlet ground state for the double dot [56]. Therefore, superconductors provide another source of spin-entanglement (see below).

Single quantum dots can also be used as a spin-entangler. A single quantum dot in the cotunneling regime and coupled to one source and two drains with narrow energy band configurations was shown to give rise to a current of nonlocal spin-entangled electrons if the dot has a finite charging energy [57]. A further proposal with one quantum dot, contains two additional

dots tunnel-coupled to the first one, which themselves are coupled to outgoing leads [58].

In Chapter 2, we consider three setups where a superconductor acts as a source of mobile spin-entanglement. In an s-wave superconductor the electrons in the vicinity of the Fermi surface form Cooper pairs [59] where electrons of opposite momentum are paired up into a singlet spin-state due to an effective attractive interaction between electrons mediated by phonons. If the superconductor is tunnel-coupled to a normal conductor, the two electrons forming the Cooper pair in the superconductor can tunnel by means of an Andreev (pair)-tunneling [60] event into the normal conductor, thereby remaining in the spin singlet state. Thus, an applied voltage bias between the superconductor and the normal region results in a stationary current of spin-entangled electrons from the superconductor to the normal region. If two separate outgoing normal leads are tunnel-coupled to the superconductor the pair can split and each of the two electrons will tunnel into a separate lead which gives rise to an electronic EPR pair. Several proposals including Coulomb blockade effects in quantum dots [61], (see Section 2.2), in Luttinger liquid leads [62, 63], (see Section 2.3), or in circuits with resistive leads [64], (see Section 2.4), were proposed in order to separate the two electrons of a pair such that they preferably enter separate leads. A related proposal makes use of energy filters in the normal leads (e.g. produced in quantum dots) [65] and does not use Coulomb interaction to separate the two electrons of a pair. In this proposal, the SN-junction is transparent and therefore subsequent spin-entangled pairs are not separated in time. In addition, the injection energy predetermined by the filters have to be different.

There exist further means to create spin-entangled electrons, e.g. in Ref. [66] generic quantum interference effects in a beamsplitter setup are used. Very recently, entanglement was also considered in the orbital sector of Cooper pairs [67], and in a degenerate electron gas where entangled electron-hole pairs are created by a tunneling barrier [68]. The latter proposal does not require an interaction mechanism to create the entanglement in the first place. The electron-hole pairs become separated spatially by the propagation along edge channels in a quantum Hall regime setup and are entangled in the quantum numbers of two edge channels which can either refer to orbital or to spin degrees of freedom [68]. In these systems, where orbital entanglement is created, one can also find a violation of the Bell inequality similar to the case for spins. Here, the spin filters are replaced by beamsplitters with variable reflection and transmission amplitudes. The successful detection of a charge

in a specific outgoing arm of the beamsplitter then depends on the orbital degree of freedom in which the pair is entangled [67, 68].

1.5 Outline

The outline of this Thesis is as follows.

In Chapter 2, we present a detailed description of three setups where an s-wave superconductor acts as a spin-entangler. In Section 2.2 (Refs. [61, 69]), the superconductor is coupled to two quantum dots each of which is tunnel-coupled to normal Fermi liquid leads. We show that in the presence of a voltage bias and in the Coulomb blockade regime two correlated electrons provided by the Andreev process can coherently tunnel from the superconductor via different dots into different leads. The spin singlet coming from the Cooper pair remains preserved in this process, and the setup provides a source of mobile and nonlocal spin-entangled electrons.

The transport current is calculated and shown to be dominated by a two-particle Breit-Wigner resonance which allows the injection of two spin-entangled electrons into different leads at exactly the same orbital energy, which is a crucial requirement for the detection of spin-entanglement via noise measurements. The coherent tunneling of both electrons into the same lead is suppressed by the on-site Coulomb repulsion and/or the superconducting gap, while the tunneling into different leads is suppressed through the initial separation of the tunneling electrons. This latter suppression depends crucially on the effective dimensionality of the superconductor and is characteristic also for the subsequent proposals. In the regime of interest the particle-hole excitations of the leads are shown to be negligible.

The Aharonov-Bohm oscillations in the current are shown to contain single- and two-electron periods with amplitudes that both vanish with increasing Coulomb repulsion albeit differently fast. This feature can be used as a probe of the spatial separation of two spin-entangled electrons. In Section 2.3 (Ref. [62]), we consider a superconductor which is tunnel-coupled to two spatially separated Luttinger liquid leads, i.e. we replace the Coulomb blockade effects of the quantum dots by strong Luttinger liquid correlations present in one-dimensional quantum wires (e.g. in metallic carbon nanotubes). Here, the coherent tunneling of two electrons into the same Luttinger liquid is suppressed compared to single-electron tunneling into a Luttinger liquid in a characteristic interaction dependent power law if the

voltage bias between the superconductor and the leads is much smaller than the superconductor gap.

We further determine the decay of the singlet state of two electrons injected into different Luttinger liquids caused by the Luttinger liquid correlations. Although the electron is not a proper quasiparticle of the Luttinger liquid, we show that the spin information can still be transported via the spin-density fluctuations produced by the injected spin-entangled electrons. In a third proposal presented in Section 2.4 (Ref. [64]), the necessary mechanism to separate the two electrons coming from the same Cooper pair is achieved by coupling the superconductor to leads with a finite resistance. The resulting dynamical Coulomb blockade effect, which we describe phenomenologically in terms of an electromagnetic environment, is shown to be enhanced for tunneling of two spin-entangled electrons into the same lead compared to the process where the pair splits and each electron tunnels into a different lead.

In Chapter 3, we consider a quantum dot in the Coulomb blockade regime weakly coupled to current leads and show that in the presence of a magnetic field the dot acts as an efficient spin filter (at the single-spin level) which produces a spin-polarized current (Ref. [48]). Conversely, if the leads are fully spin-polarized the up or down state of the spin on the dot results in a large sequential or small cotunneling current, and thus, together with ESR techniques, the setup can be operated as a single-spin memory (Ref. [48]). The application of a single-wall carbon nanotube as a switchable spin filter (Ref. [70]) and the ability to use the spin filter effect of quantum dots to measure Bell inequalities of spin-entangled electrons is discussed.

Chapter 2

Creation of mobile spin-entangled electrons using superconductors

2.1 Introduction

In this chapter, we discuss possible setups which create a current of nonlocal spin-entangled electrons as needed for quantum communication and quantum computation. We have already given an overview of different proposals for the creation of such spin-entangled electrons in a solid-state environment in Section 1.4.

We consider an s-wave superconductor [59] where the electrons form Cooper pairs with spin singlet wave functions as a source of spin-entanglement. In a superconductor, the electrons with energies near the Fermi surface and of opposite momentum pair-up into Cooper pairs and share a spin singlet wave function. The pairing arises due to a phonon mediated attractive interaction between electrons. By tunnel-coupling the superconductor to a normal region, the two electrons of a Cooper pair can tunnel by means of an Andreev (pair-)tunneling event from the superconductor to the normal region [60] thereby maintaining their singlet wave function. At low temperature and voltage bias between the superconductor and the normal region only pair-tunneling is allowed, while single electron tunneling is strongly suppressed due to the gapped excitation spectrum of the superconductor. We consider two outgoing and spatially separated leads coupled to the superconductor

such that the two electrons of a pair can either tunnel as a whole into one lead or the pair can split and the electrons tunnel to different leads. The pair-split process leads to the creation of an electronic EPR pair, i.e. the two electrons are separated in orbital space but still entangled in spin space. Since we are interested in creating currents of nonlocal singlets, we have to suppress processes where both electrons enter the same lead. The Cooper pair wave function is symmetric in orbital space, and consequently the probability to find the two electrons close to each other is enhanced. This has the consequence, that the two electrons would rather tunnel both into the same lead. On the other hand, the electron also has charge, and therefore we can use the Coulomb repulsion between the electrons of a pair to separate them spatially. In the following we propose three setups where we exploit, in one way or the other, the Coulomb repulsion between the two electrons of a pair so that the residual current is carried by pair-split processes.

Apart from any entanglement properties, the calculations presented in this chapter give independent insights into correlated two-particle transport from a superconductor into two spatially separated normal leads where the combined effect of superconductivity and Coulomb blockade phenomena on the normal side of the SN-junction gives rise to interesting results in its own right.

2.2 Andreev Entangler with quantum dots

Here, we propose an electron-spin entangler where the superconductor is weakly tunnel-coupled to two separate quantum dots which are then weakly tunnel-coupled to outgoing Fermi liquid leads, see Fig. 2.1. The two electrons are forced to tunnel coherently into separate leads rather than both into the same, by the two intermediate quantum dots operated in the Coulomb blockade regime [3] so that the tunneling of two electrons via the same dot is suppressed by the on site repulsion U of the quantum dots. The current for tunneling of two electrons via different dots into different leads shows a two-particle Breit-Wigner resonance peaked at $\epsilon_l = \mu_S$ with ϵ_l being the chemical potential of dot $l = 1, 2$ which allows the injection of the two electrons into the leads at the same orbital energy. This ability was shown to be crucial if the spin-entanglement is detected via noise in a beamsplitter setup [47], see also Section 1.3. We start with a qualitative description of the entangler and its principal mechanism based on Andreev processes and

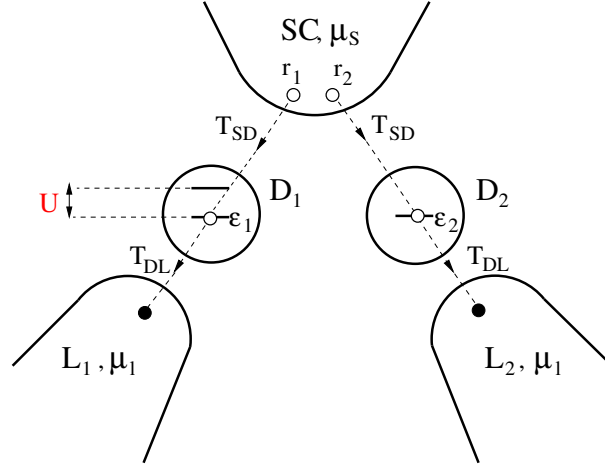


Figure 2.1: The entangler setup with quantum dots: Two spin-entangled electrons forming a Cooper pair can tunnel with amplitude T_{SD} from points \mathbf{r}_1 and \mathbf{r}_2 of the superconductor, SC, to two dots, D_1 and D_2 , by means of Andreev tunneling. The dots are tunnel-coupled to noninteracting normal leads L_1 and L_2 , with tunneling amplitude T_{DL} . The superconductor and leads are kept at chemical potentials μ_S and μ_l , respectively.

Coulomb blockade effects and also specify the necessary parameter regime for successful transport of the initial spin-entanglement of the Cooper pairs via the quantum dots to the outgoing leads. In subsequent sections we then introduce the Hamiltonian and calculate the stationary current for two competing transport channels which is followed by a discussion of the results. We further discuss an Aharonov-Bohm loop setup where the phase coherent part of the current contains two oscillation periods which distinguish interference processes stemming from different paths that the two spin-entangled electrons can take around the loop.

2.2.1 Qualitative description of the entangler

The s-wave superconductor with chemical potential μ_S is weakly coupled to two separate quantum dots D_1 and D_2 by tunnel barriers, which themselves are weakly coupled to Fermi liquid leads L_1 and L_2 , respectively, both held

at the same chemical potential $\mu_1 = \mu_2 = \mu_l$ ¹. The corresponding tunneling amplitudes between superconductor and dots, and dot-leads, are denoted by T_{SD} and T_{DL} , respectively which, for simplicity, we assume to be equal for both dots and leads. By applying a bias voltage $\delta\mu = \mu_S - \mu_l > 0$, transport of entangled electrons occurs from the superconductor via the dots to the leads. In general, the tunnel-coupling of a superconductor to a normal region allows for coherent transport of two electrons of opposite spins due to Andreev tunneling [60], while single-electron tunneling is suppressed in the regime $\Delta > \delta\mu, k_B T$, where Δ is the energy gap in the superconductor and T is the temperature. The gap Δ is the minimum energy to break up a Cooper pair into a quasiparticle in the superconductor and an electron in the normal region due to tunneling. According to the energy-time uncertainty relation, \hbar/Δ then defines the time delay between the two coherent tunneling steps in the Andreev process. In the present setup, we envision a situation where the two electrons are forced to tunnel coherently into *different* leads rather than both into the same lead. This situation can be enforced in the presence of two intermediate quantum dots which are assumed to be in the Coulomb blockade regime [3] so that the state with the two electrons being on the same quantum dot is strongly suppressed, and thus the electrons will preferably tunnel into separate dots and subsequently into separate leads—this will be quantified in the following.

The chemical potentials ϵ_1 and ϵ_2 of the quantum dots can be tuned by external gate voltages [3] such that the coherent tunneling of two electrons into different leads is at resonance if $\epsilon_1 + \epsilon_2 = 2\mu_S$, see Fig. 2.2. This current resonance condition reflects energy conservation in a tunneling process of a Cooper pair with energy $2\mu_S$ from the superconductor to the dots 1,2 (one electron on each dot) with chemical potentials ϵ_1, ϵ_2 and requires that the resonant dot levels have to be adjusted such that one is above μ_S and the other (by the same amount) below μ_S . This is very similar to the more familiar picture of Andreev reflection at a superconductor/normal interface. There, an electron on the normal side of the junction, and with energy ϵ above μ_S , is back reflected as a hole with energy ϵ below μ_S by the simultaneous creation of a Cooper pair in the superconductor [59]. In that sense the empty dot level below μ_S can be considered as the hole and the empty dot level above μ_S as the empty electron state. In contrast, we will see that the current for

¹If the chemical potentials of the leads were different, an unentangled single-particle current could flow from one lead to the other via the superconductor.

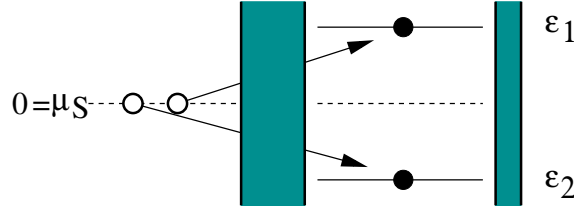


Figure 2.2: The energy situation of the superconductor with chemical potential μ_S and the two dots 1,2 with chemical potentials ϵ_1, ϵ_2 . Transport of the two members of a Cooper pair with energy $2\mu_S$ from the superconductor to *different* outgoing leads with chemical potential $\mu_l < \epsilon_l$ (not drawn) is at resonance if $\epsilon_1 + \epsilon_2 = 2\mu_S$.

the coherent tunneling of two electrons via the *same* dot into the *same* lead is suppressed by the on-site Coulomb U repulsion of a quantum dot and/or by the superconducting gap Δ .

Next, we introduce the relevant parameters describing the proposed device and specify their regime of interest. First we note that to avoid unwanted correlations with electrons already on the quantum dots, one could work in the cotunneling regime [3] where the number of electrons on the dots are fixed and the resonant levels ϵ_l , $l = 1, 2$ cannot be occupied, see also Chapter 3. However, we prefer to work at the particular resonance $\epsilon_l \simeq \mu_S$, since then the total current and the desired suppression of tunneling into the same lead is maximized. Also, the desired injection of the two electrons into different leads but at the *same* orbital energy is then achieved. In the resonant regime, we can avoid unwanted correlations between tunneling of subsequent Cooper pairs if we require that the dot-lead coupling is much stronger than the superconductor-dot coupling, i.e. $|T_{SD}| < |T_{DL}|$, so that electrons which enter the dots from the superconductor will leave the quantum dots to the leads much faster than new electrons can be provided from the superconductor. In addition, a stationary occupation due to the coupling to the leads is exponentially small if $\delta\mu > k_B T$, T being the temperature and k_B the Boltzmann constant. Thus, in this asymmetric barrier case, the resonant dot levels ϵ_l can be occupied only during a virtual process, see also Subsection 2.2.3. The quantum dots in the ground state are allowed to contain an arbitrary but even number of electrons, $N_D = \text{even}$, with total spin zero (i.e. antiferromagnetic filling of the dots). An odd number N_D must be excluded since a simple spin-flip on the quantum dot would be possible in the transport process and, as a result, the desired entanglement would be lost. Further,

we have to make sure that also spin flip processes of the following kind are excluded. Consider an electron that tunnels from the superconductor into a given dot. Now, it is possible in principle (e.g. in a sequential tunneling process [3]) that another electron with the opposite spin leaves the dot and tunnels into the lead, and, again, the desired entanglement would be lost. However, such spin flip processes will be excluded if the energy level spacing of the quantum dots, $\delta\epsilon$, (assumed to be similar for both dots) exceeds both, temperature $k_B T$ and bias voltage $\delta\mu$. A serious source of entanglement-loss is given by electron hole-pair excitations out of the Fermi sea of the leads during the resonant tunneling events. Since then a simple spin flip on the dot would be possible due to the coupling to the leads. However, we will show in Appendix B that such many-particle contributions can be suppressed if the resonance width $\gamma_l = 2\pi\nu_l|T_{DL}|^2$ is smaller than $\delta\mu$ (for $\epsilon_l \simeq \mu_S$), where ν_l is the density of states (DOS) per spin of the leads at the chemical potential μ_l .

To summarize, the regime of interest where the coherence of an initially entangled Cooper pair (spin singlet) is preserved during the transport to the leads is given by

$$\Delta, U, \delta\epsilon > \delta\mu > \gamma_l, k_B T, \quad \text{and} \quad \gamma_l > \gamma_S. \quad (2.1)$$

As regards possible experimental implementations of the proposed setup and its parameter regime, we would like to mention that, typically, quantum dots are made out of semiconducting heterostructures, which satisfy above inequalities [3]. Furthermore, in recent experiments, it has been shown that the fabrication of hybrid structures with semiconductor and superconductor being tunnel-coupled is possible [71, 72]. Other candidate materials are e.g. carbon nanotubes which also show Coulomb blockade behavior with U and $\delta\epsilon$ being in the regime of interest here [73–75], see also Section 3.7. The present work might provide further motivation to implement the structures proposed here.

Our goal in the following is to calculate the stationary charge current of pairwise spin-entangled electrons for two competing transport channels, first for the desired transport of two entangled electrons into different leads (I_1) and second for the unwanted transport of both electrons into the same lead (I_2). We compare then the two competing processes and show how their ratio, I_1/I_2 , depends on the various system parameters and how it can be made large. An important finding is that when tunneling of two electrons into different leads occurs, the current is suppressed due to the fact that

tunneling into the dots will typically take place from different points \mathbf{r}_1 and \mathbf{r}_2 on the superconductor (see Fig. 1) due to the spatial separation of the dots D_1 and D_2 . We show that the distance of separation $\delta r = |\mathbf{r}_1 - \mathbf{r}_2|$ leads to an exponential suppression of the current via different dots if $\delta r > \xi$ (see Eq. (2.24)), where $\xi = v_F/\pi\Delta$ is the coherence length of a Cooper pair. In the relevant regime, $\delta r < \xi$, however, the suppression is only polynomial in the parameter $k_F\delta r$, with k_F being the Fermi wavenumber in the superconductor, and depends sensitively on the dimension of the superconductor. We find (see Subsection 2.2.6) that the suppression is less dramatic in lower dimensional superconductors where we find asymptotically smoother power law suppressions in $k_F\delta r$.

On the other hand, tunneling via the same dot implies $\delta r = 0$, but suffers a suppression due to U and/or Δ . The suppression of this current is given by the small parameter $(\gamma_l/U)^2$ in the case $U < \Delta$, or by $(\gamma_l/\Delta)^2$, if $U > \Delta$ as will be derived in the following. Thus, to maximize the efficiency of the entangler, we also require $k_F\delta r < \Delta/\gamma_l, U/\gamma_l$.

Finally, we will discuss the effect of a magnetic flux on the entangled current in an Aharonov-Bohm loop, and we will see that this current contains both, single- and two-particle Aharonov-Bohm periods whose amplitudes have different parameter dependences. This allows us to distinguish processes where two electrons travel through the same arm of the loop from the desired processes where two electrons travel through different arms. The relative weight of the amplitudes of the two Aharonov-Bohm periods are directly accessible by flux-dependent current measurements which are then a direct probe of the desired nonlocality of the entangled electrons.

2.2.2 Hamiltonian

We use a tunneling Hamiltonian description [76] of the system, $H = H_0 + H_T$, where

$$H_0 = H_S + \sum_l H_{Dl} + \sum_l H_{Ll}, \quad l = 1, 2. \quad (2.2)$$

Here, the superconductor is described by the BCS-Hamiltonian [59]

$$H_S = \sum_{\mathbf{k}, \sigma} E_{\mathbf{k}} \gamma_{\mathbf{k}\sigma}^\dagger \gamma_{\mathbf{k}\sigma}, \quad (2.3)$$

where $\sigma = \uparrow, \downarrow$, and the quasiparticle operators $\gamma_{\mathbf{k}\sigma}$ describe excitations out of the BCS-ground state $|0\rangle_S$ defined by $\gamma_{\mathbf{k}\sigma}|0\rangle_S = 0$. They are related to

the electron annihilation and creation operators $c_{\mathbf{k}\sigma}$ and $c_{\mathbf{k}\sigma}^\dagger$ through the Bogoliubov transformation

$$\begin{aligned} c_{\mathbf{k}\uparrow} &= u_{\mathbf{k}}\gamma_{\mathbf{k}\uparrow} + v_{\mathbf{k}}\gamma_{-\mathbf{k}\downarrow}^\dagger \\ c_{-\mathbf{k}\downarrow} &= u_{\mathbf{k}}\gamma_{-\mathbf{k}\downarrow} - v_{\mathbf{k}}\gamma_{\mathbf{k}\uparrow}^\dagger, \end{aligned} \quad (2.4)$$

where $u_{\mathbf{k}} = (1/\sqrt{2})(1 + \xi_{\mathbf{k}}/E_{\mathbf{k}})^{1/2}$ and $v_{\mathbf{k}} = (1/\sqrt{2})(1 - \xi_{\mathbf{k}}/E_{\mathbf{k}})^{1/2}$ are the usual BCS coherence factors [59], and $\xi_{\mathbf{k}} = \epsilon_{\mathbf{k}} - \mu_S$ is the normal state single-electron energy counted from the Fermi level μ_S , and $E_{\mathbf{k}} = \sqrt{\xi_{\mathbf{k}}^2 + \Delta^2}$ is the quasiparticle energy. We choose energies such that $\mu_S = 0$ in this section. Both dots are represented as one localized (spin-degenerate) level with energy ϵ_l and is modeled by an Anderson-type Hamiltonian

$$H_{Dl} = \epsilon_l \sum_{\sigma} d_{l\sigma}^\dagger d_{l\sigma} + U n_{l\uparrow} n_{l\downarrow}, \quad l = 1, 2. \quad (2.5)$$

The resonant dot level ϵ_l can be tuned by the gate voltage. Other levels of the dots do not participate in transport if $\delta\epsilon > \delta\mu > k_B T$, where $\delta\mu = -\mu_l$, and μ_l is the chemical potential of lead $l = 1, 2$, and $\delta\epsilon$ is the single-particle energy level spacing of the dots. The leads $l = 1, 2$ are assumed to be non-interacting (normal) Fermi liquids, $H_{Ll} = \sum_{\mathbf{k}\sigma} \epsilon_{\mathbf{k}} a_{l\mathbf{k}\sigma}^\dagger a_{l\mathbf{k}\sigma}$. Tunneling from the dot l to the lead l or to the point \mathbf{r}_l in the superconductor is described by the tunnel Hamiltonian $H_T = H_{SD} + H_{DL}$ with

$$H_{SD} = \sum_{l\sigma} T_{SD} d_{l\sigma}^\dagger \psi_{\sigma}(\mathbf{r}_l) + \text{h.c.}, \quad (2.6)$$

$$H_{DL} = \sum_{l\mathbf{k}\sigma} T_{DL} a_{l\mathbf{k}\sigma}^\dagger d_{l\sigma} + \text{h.c.} \quad (2.7)$$

Here, $\psi_{\sigma}(\mathbf{r}_l)$ annihilates an electron with spin σ at site \mathbf{r}_l , and $d_{l\sigma}^\dagger$ creates it again (with the same spin) at dot l with amplitude T_{SD} . $\psi_{\sigma}(\mathbf{r}_l)$ is related to $c_{\mathbf{k}\sigma}$ by the Fourier transform $\psi_{\sigma}(\mathbf{r}_l) = \sum_{\mathbf{k}} e^{i\mathbf{k}\mathbf{r}_l} c_{\mathbf{k}\sigma}$. Tunneling from the dot to the state \mathbf{k} in the lead is described by the tunnel amplitude T_{DL} . We assume that the \mathbf{k} -dependence of T_{DL} can be safely neglected.

2.2.3 Stationary current and T-matrix

The stationary current of *two* electrons² passing from the superconductor via virtual dot states to the leads is given by³

$$I = 2e \sum_{f,i} W_{fi} \rho_i, \quad (2.8)$$

where W_{fi} is the transition rate from the superconductor to the leads. We calculate this transition rate in terms of a T-matrix approach [77],

$$W_{fi} = 2\pi |\langle f | T(\varepsilon_i) | i \rangle|^2 \delta(\varepsilon_f - \varepsilon_i). \quad (2.9)$$

Here, $T(\varepsilon_i) = H_T \frac{1}{\varepsilon_i + i\eta - H} (\varepsilon_i - H_0)$, is the on-shell transmission or T-matrix, with η being a small positive real number which we take to zero at the end of the calculation. Finally, ρ_i is the stationary occupation probability for the entire system to be in the state $|i\rangle$. The T-matrix $T(\varepsilon_i)$ can be written as a power series in the tunnel Hamiltonian H_T ,

$$T(\varepsilon_i) = H_T + H_T \sum_{n=1}^{\infty} \left[\frac{1}{\varepsilon_i + i\eta - H_0} H_T \right]^n, \quad (2.10)$$

where the initial energy is $\varepsilon_i = 2\mu_S \equiv 0$. We work in the regime defined in Eq. (2.1), i.e. $\gamma_l > \gamma_S$, and $\Delta, U, \delta\varepsilon > \delta\mu > \gamma_l, k_B T$, and around the resonance $\varepsilon_i \simeq \mu_S$. Further, $\gamma_S = 2\pi\nu_S |T_{SD}|^2$ and $\gamma_l = 2\pi\nu_l |T_{DL}|^2$ define the tunneling rates between superconductor and dots, and between dots and leads, respectively, with ν_S and ν_l being the DOS per spin at the chemical potentials μ_S and μ_l , respectively. We will show that the total effective tunneling rate from the superconductor to the leads is given by γ_S^2/γ_l due to the Andreev process. In the regime Eq. (2.1), the entire tunneling process becomes a two-particle problem where the many-particle effect of the reservoirs (leads) can be safely neglected and the coherence of an initially entangled Cooper pair (spin singlet) is maintained during the transport into the leads as we shall show below. Since the superconducting gap satisfies

²The charge q_e of an electron is $q_e = -e$ where e is the elementary charge $e = 1.6 \times 10^{-19}$ C.

³In explicit calculations we set $\hbar = 1$ in this Thesis but restore \hbar in fundamental quantities, like in the quantum resistance h/e^2 if these quantities appear in introductions or discussions.

$\Delta > \delta\mu, k_B T$, the superconductor contains no quasiparticle initially. Further, in the regime (2.1), the resonant dot levels ϵ_l are mostly empty, since in the assumed asymmetric case, $|T_{DL}| > |T_{SD}|$ (or $\gamma_l > \gamma_S$), the electron leaves the dot to the lead much faster than it can be replaced by another electron from the superconductor. In addition, we can neglect any stationary occupation of the dots induced by the coupling of the dots to the leads. Indeed, in the stationary limit and for given bias $\delta\mu$ this occupation probability is determined by the grand canonical distribution function $\propto \exp(-\delta\mu/k_B T) \ll 1$, and thus $\rho_i \simeq 0$ for any initial state where the resonant dot level is occupied. In this regime, the initial state $|i\rangle$ becomes $|i\rangle = |0\rangle_S |0\rangle_D |\mu_l\rangle_l$, where $|0\rangle_S$ is the quasiparticle vacuum for the superconductor, $|0\rangle_D$ means that both dot levels ϵ_l are unoccupied, and $|\mu_l\rangle_l$ defines the occupation of the leads which are filled with electrons up to the chemical potential μ_l . We remark that in our regime of interest no Kondo effects appear which could destroy the spin-entanglement, since our dots contain each an even number of electrons in the stationary limit.

2.2.4 Current due to tunneling into different leads

We now calculate the current for simultaneous coherent transport of two electrons into different leads. The final state for two electrons, one of them being in lead 1 the other in lead 2, can be classified according to their total spin S . This spin can be either a singlet (in standard notation) $|S\rangle = (|\uparrow\downarrow\rangle - |\downarrow\uparrow\rangle)/\sqrt{2}$ with $S = 0$, or a triplet with $S = 1$. Since the total spin is conserved, $[\mathbf{S}^2, H] = 0$, the singlet state of the initial Cooper pair will be conserved in the transport process and the final state must also be a singlet. That this is so can also be seen explicitly when we allow for the possibility that the final state could be the $S_z = 0$ triplet⁴ $|t_0\rangle = (|\uparrow\downarrow\rangle + |\downarrow\uparrow\rangle)/\sqrt{2}$. Therefore, we consider final two-particle states of the form

$$|f\rangle = (1/\sqrt{2})(a_{1\mathbf{p}\uparrow}^\dagger a_{2\mathbf{q}\downarrow}^\dagger \pm a_{1\mathbf{p}\downarrow}^\dagger a_{2\mathbf{q}\uparrow}^\dagger)|i\rangle, \quad (2.11)$$

where the $-$ and $+$ signs belong to the singlet $|S\rangle$ and triplet $|t_0\rangle$, respectively. Note that this singlet/triplet state is formed out of two electrons, one being in the \mathbf{p} -state in lead 1 and with energy $\epsilon_{\mathbf{p}}$, while the other one is in the

⁴The triplets $|t_+\rangle = |\uparrow\uparrow\rangle$ and $|t_-\rangle = |\downarrow\downarrow\rangle$ can be excluded right away since the tunnel Hamiltonian H_T conserves the spin-component σ and an Andreev process involves tunneling of two electrons with different spin σ .

\mathbf{q} -state in lead 2 with energy $\epsilon_{\mathbf{q}}$. Thus, the two electrons are entangled in spin space while separated in orbital space, thereby providing a nonlocal EPR pair. The tunnel process to different leads appears in the following order. A Cooper pair breaks up, where one electron with spin σ tunnels to one of the dots (with empty level ϵ_l) from the point of the superconductor nearest to this dot. This is a virtual state with energy deficit $E_{\mathbf{k}} > \Delta$. Since $\Delta > \gamma_l$, the second electron from the Cooper pair with spin $-\sigma$ tunnels to the other empty dot-level *before* the electron with spin σ escapes to the lead. Therefore, both electrons tunnel almost simultaneously to the dots (within the uncertainty time $1/\Delta$). Since we work at the resonance $\epsilon_l \simeq \mu_S = 0$, the energy denominators in (2.10) show divergences $\propto 1/\eta$ indicating that tunneling between the dots and the leads is resonant and we have to treat tunneling to all orders in H_{DL} in Eq. (2.10), eventually giving a finite result in which η will be replaced by $\gamma_l/2$. Tunneling back to the superconductor is unlikely since $|T_{SD}| < |T_{DL}|$. We can therefore write the transition amplitude between initial and final state as

$$\langle f|T_0|i\rangle = \frac{1}{\sqrt{2}}\langle a_{2\mathbf{q}\downarrow}a_{1\mathbf{p}\uparrow}T'd_{1\uparrow}^\dagger d_{2\downarrow}^\dagger\rangle\langle(d_{2\downarrow}d_{1\uparrow} \pm d_{2\uparrow}d_{1\downarrow})T''\rangle, \quad (2.12)$$

where $T_0 = T(\epsilon_i = 0)$, and the partial T-matrices T' and T'' are given by

$$T'' = \frac{1}{i\eta - H_0}H_{SD}\frac{1}{i\eta - H_0}H_{SD}, \quad (2.13)$$

and

$$T' = H_{DL}\sum_{n=0}^{\infty}\left(\frac{1}{i\eta - H_0}H_{DL}\right)^{2n+1}. \quad (2.14)$$

In Eq. (2.12) we used that the matrix element containing T' is invariant under spin exchange $\uparrow \leftrightarrow \downarrow$, and the abbreviation $\langle \dots \rangle$ stands for $\langle i|\dots|i\rangle$. The part containing T'' describes the Andreev process, while the part containing T' is the resonant dot \leftrightarrow lead tunneling.

We first consider the Andreev process. We insert a complete set of single-quasiparticle (virtual) states, i.e., $\mathbb{1} = \sum_{l\mathbf{k}\sigma}\gamma_{\mathbf{k}\sigma}^\dagger d_{l-\sigma}^\dagger|i\rangle\langle i|d_{l-\sigma}\gamma_{\mathbf{k}\sigma}$, between the two H_{SD} in Eq. (2.13) and use that the resulting energy denominator $|i\eta - E_{\mathbf{k}} - \epsilon_l| \approx |E_{\mathbf{k}}|$, since we work close to the resonance $\epsilon_l \simeq 0$ and $E_{\mathbf{k}} > \Delta$. The triplet contribution vanishes since $u_{\mathbf{k}}v_{\mathbf{k}} = u_{-\mathbf{k}}v_{-\mathbf{k}}$ for an

s-wave superconductor. For the final state being a singlet we then get

$$\begin{aligned} & \langle (d_{2\downarrow}d_{1\uparrow} - d_{2\uparrow}d_{1\downarrow})T'' \rangle \\ &= \frac{4T_{SD}^2}{\epsilon_1 + \epsilon_2 - i\eta} \sum_{\mathbf{k}} \frac{u_{\mathbf{k}}v_{\mathbf{k}}}{E_{\mathbf{k}}} \cos(\mathbf{k} \cdot \delta\mathbf{r}), \end{aligned} \quad (2.15)$$

where $\delta\mathbf{r} = \mathbf{r}_1 - \mathbf{r}_2$ denotes the distance vector between the points on the superconductor from which electron 1 and 2 tunnel into the dots. To evaluate the sum over \mathbf{k} we use $u_{\mathbf{k}}v_{\mathbf{k}} = \Delta/(2E_{\mathbf{k}})$, linearize the spectrum around the Fermi level with Fermi wavenumber k_F , and obtain finally for the Andreev contribution

$$\langle (d_{2\downarrow}d_{1\uparrow} - d_{2\uparrow}d_{1\downarrow})T'' \rangle = \frac{2\pi\nu_S T_{SD}^2}{\epsilon_1 + \epsilon_2 - i\eta} \frac{\sin(k_F\delta r)}{k_F\delta r} e^{-\frac{\delta r}{\xi}}. \quad (2.16)$$

Dominant contribution of resonant tunneling

We turn to the calculation of the matrix element in Eq. (2.12) containing T' where tunneling is treated to all orders in H_{DL} . We introduce the ket notation $|12\rangle$, and, for simplicity, suppress the spin index σ . Here, 1 stands for quantum numbers of the electron on dot 1/lead 1 and similarly for 2. For example, $|pq\rangle$ stands for $a_{1\mathbf{p}\sigma}^\dagger a_{2\mathbf{q}-\sigma}^\dagger|i\rangle$, where \mathbf{p} is from lead 1 and \mathbf{q} from lead 2, or, correspondingly, $|pD\rangle$ stands for $a_{1\mathbf{p}\sigma}^\dagger d_{2,-\sigma}^\dagger|i\rangle$, etc. We restrict ourselves to the resummation of the following dot \leftrightarrow lead transitions $|DD\rangle \rightarrow |LD\rangle \rightarrow |DD\rangle$ or $|DD\rangle \rightarrow |DL\rangle \rightarrow |DD\rangle$. In this sequence, $|DD\rangle$ is the state with one electron on dot 1 and the other one on dot 2, and $|LD\rangle$ denotes a state where one electron is in lead 1 and the other one on dot 2. We thereby exclude tunneling sequences of the kind $|DD\rangle \rightarrow |LD\rangle \rightarrow |LL\rangle \rightarrow |LD\rangle \rightarrow |DD\rangle$ or $|DD\rangle \rightarrow |LD\rangle \rightarrow |LL\rangle \rightarrow |DL\rangle \rightarrow |DD\rangle$, where both electrons are *virtually* simultaneously in the leads as well as the creation of electron-hole pair excitations out of the Fermi sea. We show in Appendix A and B that such contributions are suppressed in the regime Eq. (2.1) considered here by the small parameter $\gamma_l/\delta\mu$. The dominant contributions are then resummed

in the following sequence

$$\begin{aligned}
& \langle pq|T'|DD\rangle \\
&= \left\{ \langle pq|H_{D_1L_1}|Dq\rangle \langle Dq| \sum_{n=0}^{\infty} \left(\frac{1}{i\eta-H_0} H_{D_1L_1}\right)^{2n} |Dq\rangle \langle Dq| \frac{1}{i\eta-H_0} H_{D_2L_2} |DD\rangle \right. \\
&\quad \left. + \langle pq|H_{D_2L_2}|pD\rangle \langle pD| \sum_{n=0}^{\infty} \left(\frac{1}{i\eta-H_0} H_{D_2L_2}\right)^{2n} |pD\rangle \langle pD| \frac{1}{i\eta-H_0} H_{D_1L_1} |DD\rangle \right\} \\
&\times \langle DD| \sum_{m=0}^{\infty} \left(\frac{1}{i\eta-H_0} H_{DL}\right)^{2m} |DD\rangle. \tag{2.17}
\end{aligned}$$

Since the sums for the transition $|DD\rangle \rightarrow |DD\rangle$ via the sequences $|DD\rangle \rightarrow |LD\rangle \rightarrow |DD\rangle$ and $|DD\rangle \rightarrow |DL\rangle \rightarrow |DD\rangle$ are independent, we can write all summations in Eq. (2.17) as geometric series which can be resummed explicitly. We begin with the two-particle process for which we find

$$\begin{aligned}
& \langle DD| \sum_{m=0}^{\infty} \left(\frac{1}{i\eta-H_0} H_{DL}\right)^{2m} |DD\rangle \\
&= \frac{1}{1 - \langle DD| \left(\frac{1}{i\eta-H_0} H_{DL}\right)^2 |DD\rangle}, \tag{2.18}
\end{aligned}$$

where

$$\langle DD| \left(\frac{1}{i\eta-H_0} H_{DL}\right)^2 |DD\rangle = \frac{\Sigma}{i\eta - \epsilon_1 - \epsilon_2}, \tag{2.19}$$

with Σ being the self-energy, $\Sigma = |T_{DL}|^2 \sum_{l\mathbf{k}} (i\eta - \epsilon_l - \epsilon_{\mathbf{k}})^{-1}$. In the presence of a Fermi sea in the leads, we introduce a cut-off in the sum in Σ at the Fermi level $\epsilon_{\mathbf{k}} \sim -\delta\mu$ and at the edge of the conduction band, ϵ_c . Then we obtain $\Sigma = \text{Re}\Sigma - i\gamma/2$, where $\gamma = \gamma_1 + \gamma_2$, and the logarithmic renormalization of the energy level is small, i.e. $|\text{Re}\Sigma| \sim \gamma_l \ln(\epsilon_c/\delta\mu) < \delta\mu$ and will be neglected. Finally, we arrive at the following expression

$$\langle DD| \sum_{m=0}^{\infty} \left(\frac{1}{i\eta-H_0} H_{DL}\right)^{2m} |DD\rangle = \frac{\epsilon_1 + \epsilon_2 - i\eta}{\epsilon_1 + \epsilon_2 - i\gamma/2}. \tag{2.20}$$

Similar results hold for the one-particle resummations in Eq. (2.17),

$$\langle pD| \sum_{n=0}^{\infty} \left(\frac{1}{i\eta-H_0} H_{D_2L_2}\right)^{2n} |pD\rangle = \frac{\epsilon_2 + \epsilon_{\mathbf{p}} - i\eta}{\epsilon_2 + \epsilon_{\mathbf{p}} - i\gamma_2/2}, \tag{2.21}$$

$$\langle Dq | \sum_{n=0}^{\infty} \left(\frac{1}{i\eta - H_0} H_{D_1 L_1} \right)^{2n} | Dq \rangle = \frac{\epsilon_1 + \epsilon_{\mathbf{q}} - i\eta}{\epsilon_1 + \epsilon_{\mathbf{q}} - i\gamma_1/2}. \quad (2.22)$$

Inserting the preceding results back into Eq. (2.17) we obtain

$$\langle pq | T' | DD \rangle = \frac{-T_{DL}^2 (\epsilon_1 + \epsilon_2 - i\eta)}{(\epsilon_1 + \epsilon_{\mathbf{q}} - i\gamma_1/2)(\epsilon_2 + \epsilon_{\mathbf{p}} - i\gamma_2/2)}. \quad (2.23)$$

Thus, we see that the resummations cancel all divergences like the $(\epsilon_1 + \epsilon_2 - i\eta)$ denominator appearing in Eqs. (2.15) and (2.16), and that, as expected, the resummation of divergent terms leads effectively to the replacement $i\eta \rightarrow i\gamma_l/2$ so that the limit $\epsilon_l \rightarrow 0$ is well-behaved. It is interesting to note that the two-particle resonance $(\epsilon_1 + \epsilon_2 - i\gamma/2)^{-1}$ occurring in Eq. (2.20) has canceled out in Eq. (2.23), and we finally obtain a product of two independent single-particle Breit-Wigner resonances. Still, we will just see that the two-particle correlation is reintroduced when we insert Eq. (2.23) into the expression for the current Eq. (2.8) due to the integrations over \mathbf{p} , \mathbf{q} , and the fact that the main contribution comes from the resonances. Indeed, making use of Eqs. (2.8,2.9), and energy conservation $\varepsilon_f = \varepsilon_i = 0$, i.e. $\epsilon_{\mathbf{p}} = -\epsilon_{\mathbf{q}}$, and of Eqs. (2.16) and (2.23), we finally obtain for the current (denoted by I_1) where each of the two entangled electrons tunnels into a *different* lead

$$I_1 = \frac{e\gamma_S^2\gamma}{(\epsilon_1 + \epsilon_2)^2 + \gamma^2/4} \left[\frac{\sin(k_F\delta r)}{k_F\delta r} \right]^2 \exp\left(-\frac{2\delta r}{\pi\xi}\right), \quad (2.24)$$

where, $\gamma = \gamma_1 + \gamma_2$. We note that Eq. (2.24) also holds for the case with $\gamma_1 \neq \gamma_2$. The current becomes exponentially suppressed with increasing distance δr between the tunneling points on the superconductor, the scale given by the Cooper pair coherence length ξ . This does not pose severe restrictions for conventional s-wave materials with ξ typically being on the order of micrometers. More severe is the restriction that $k_F\delta r$ should not be too large compared to unity, especially if k_F^{-1} of the superconductor assumes a typical value on the order of a few Angstroms. Still, since the suppression in $k_F\delta r$ is only power-law like there is a sufficiently large regime on the nanometer scale for δr where the current I_1 can assume a finite measurable value. The power law suppression of the current in $1/k_F\delta r$ is very sensitive to the dimension of the superconductor and we suspect that the suppression will be softened by going over to lower dimensional superconductors. We will address this issue in Subsection 2.2.6. The current Eq. (2.24) has a

two-particle Breit-Wigner resonance form which assumes its maximum value when $\epsilon_1 = -\epsilon_2$ (see also Fig. 2.2, and note that $\mu_S \equiv 0$),

$$I_1 = \frac{4e\gamma_S^2}{\gamma} \left[\frac{\sin(k_F \delta r)}{k_F \delta r} \right]^2 \exp\left(-\frac{2\delta r}{\pi\xi}\right). \quad (2.25)$$

This resonance at $\epsilon_1 = -\epsilon_2$ clearly shows that the current is a correlated two-particle effect (even apart from any spin correlation) as we should expect from the Andreev process involving the coherent tunneling of two electrons. Together with the single-particle resonances in Eq. (2.23) and by using energy conservation $\epsilon_i = \epsilon_f = 0$, which implies $\epsilon_{\mathbf{p}} = -\epsilon_{\mathbf{q}}$, we thus see that the current is carried by correlated pairs of electrons whose lead energies satisfy $|\epsilon_{\mathbf{p}} - \epsilon_1| \lesssim \gamma_1$ and $|\epsilon_{\mathbf{q}} - \epsilon_2| \lesssim \gamma_2$.

A particularly interesting case occurs when the energies of the dots, ϵ_1 and ϵ_2 , are both tuned to zero, i.e. $\epsilon_1 = \epsilon_2 = \mu_S = 0$. We stress that in this case the electron in lead 1 and its spin-entangled partner in lead 2 possess exactly the *same* orbital energy. It has been shown previously [47] that this degeneracy of orbital energies is a crucial requirement for noise measurements in which the singlets can be detected by an enhanced noise in the current (bunching) due to a symmetrical orbital wave function of the singlet state, whereas uncorrelated electrons, or, more generally, electrons in a triplet state, lead to a suppression of noise (antibunching). Note that not all triplets are entangled states. Only the triplet with $S_z = 0$ is entangled. Measurement of noise enhancement is therefore a unique signature of entanglement [47].

We remark again that the current I_1 is carried by electrons which are entangled in spin space and spatially separated in orbital space. In other words, the stationary current I_1 is a current of nonlocal spin-based EPR pairs. Finally, we note that due to the singlet character of the EPR pair we do not know whether the electron in, say, lead 1 carries an up or a down spin, this can be revealed only by a spin-measurement. Of course, any measurement of the spin of one (or both) electrons will immediately destroy the singlet state and thus the entanglement. Such a spin measurement (spin read-out) can be performed e.g. by making use of the spin filtering effect of quantum dots [48], explained in detail in Chapter 3. The singlet state will also be destroyed by spin-dependent scattering (but not by Coulomb exchange interaction in the Fermi sea [47]). However, it is known experimentally that electron spins in a semiconductor environment show unusually long dephasing times approaching microseconds and can be transported phase coherently

over distances exceeding $100 \mu\text{m}$ [7]. This distance is sufficiently long for experiments performed typically on the length scale of quantum confined nanostructures [3].

Negligible tunnel contributions

We turn now to a discussion of various tunnel processes which we have not taken into account so far and show that they are negligibly small compared to the ones we have retained. As we mentioned above we exclude virtual states where both electrons are simultaneously in the leads. This is justified in the regime Eq. (2.1) considered here. To show this we consider the process $|DD\rangle \rightarrow |DD\rangle$. This transition occurs either in a transition sequence of the type $|DD\rangle \rightarrow |LD\rangle \rightarrow |DD\rangle$, as considered above, leading to the amplitude $A_{DL} = -i\gamma_L - (\gamma_L/\pi) \ln(\epsilon_c/\delta\mu)$ (see Eq. (A.1) in Appendix A), or in a sequence of the type $|DD\rangle \rightarrow |LD\rangle \rightarrow |LL\rangle \rightarrow |DL\rangle \rightarrow |DD\rangle$, where both electrons are simultaneously in the leads ($|LL\rangle$ -state), leading to the amplitude

$$A_{LL} = \frac{\gamma_L^2}{2\pi^2\delta\mu} \left[i\pi + \ln\left(\frac{\epsilon_c}{\delta\mu}\right) \right] \quad (2.26)$$

(see Eq. (A.3) in Appendix A). However, this amplitude A_{LL} is suppressed by a factor $\gamma_L/\delta\mu < 1$ compared to A_{DL} . Above we used $\gamma_1 = \gamma_2 = \gamma_L$ for simplicity. Further, a process where we create an electron-hole pair out of the Fermi sea of the leads could, in principle, destroy the spin-correlation of the entangled electron pair when an electron with the “wrong” spin (coming from the Fermi sea) hops on the dot. But such contributions cost additional energy of at least $\delta\mu$, and again such particle-hole processes are suppressed by a factor $(\gamma_l/\delta\mu)^2$ as we show in detail in Appendix B.

2.2.5 Tunneling via the same dot

The two electrons of a Cooper pair can also tunnel via the *same* dot into the same lead. In this section, we calculate the current induced by this process. We show that we obtain a suppression of such processes by a factor $(\gamma_l/U)^2$ and/or $(\gamma_l/\Delta)^2$ compared to the process discussed in the preceding section. However, in contrast to the previous case, we do not get a suppression resulting from the spatial separation of the Cooper pair on the superconductor, since here the two electrons tunnel from the same point either from \mathbf{r}_1 or \mathbf{r}_2 , see Fig. 2.3). As before, a tunnel process starts by breaking up a Cooper pair

followed by an Andreev process with two possible sequences, see Fig. 2.3. a) In a first step, one electron tunnels from the superconductor to, say, dot 1, and in a second step the second electron also tunnels to dot 1. There are now two electrons on the *same* dot which costs additional Coulomb repulsion energy U , thus this virtual state is suppressed by $1/U$. Finally, the two electrons leave dot 1 and tunnel into lead 1. b) There is an alternative competing process which avoids the double occupancy. Here, one electron tunnels to, say, dot 1, and then the same electron tunnels further into lead 1, leaving an excitation on the superconductor which costs additional gap energy Δ (instead of U), before finally the second electron tunnels from the superconductor via dot 1 into lead 1. We first concentrate on the tunneling process b), and note that the leading contribution comes from the processes where both electrons have left the superconductor so that the system has no energy deficit anymore. We still have to resum the tunnel processes from the dot to the lead to all orders in the tunnel Hamiltonian H_{DL} . In what follows we suppress the label $l = 1, 2$ since the setup is assumed to be symmetric and tunneling into either lead 1 or lead 2 gives the same result. The transition amplitude $\langle f|T_0|i\rangle$ including only leading terms is

$$\begin{aligned}
\langle f|T_0|i\rangle &= \sum_{\mathbf{p}''\sigma} \langle f|H_{DL}|D\mathbf{p}''\sigma\rangle \\
&\times \langle D\mathbf{p}''\sigma | \sum_{n=0}^{\infty} \left(\frac{1}{i\eta - H_0} H_{DL}\right)^{2n} |D\mathbf{p}''\sigma\rangle \\
&\times \langle D\mathbf{p}''\sigma | \frac{1}{i\eta - H_0} H_{SD} \frac{1}{i\eta - H_0} H_{DL} \frac{1}{i\eta - H_0} H_{SD} |i\rangle, \quad (2.27)
\end{aligned}$$

where again $|f\rangle = (1/\sqrt{2})(a_{\mathbf{p}\uparrow}^\dagger a_{\mathbf{p}'\downarrow}^\dagger \pm a_{\mathbf{p}\downarrow}^\dagger a_{\mathbf{p}'\uparrow}^\dagger)|i\rangle$, with \pm denoting the triplet (+) and singlet (-), resp., and the intermediate state $|D\mathbf{p}''\sigma\rangle = d_{-\sigma}^\dagger a_{\mathbf{p}''\sigma}^\dagger|i\rangle$. The index σ appearing together with the tunnel Hamiltonians in Eq. (2.27) determines the spin of the electron that tunnels. There are some remarks in order regarding Eq. (2.27). The electron which tunnels to the state $|\mathbf{p}''\sigma\rangle$ —via step 1 and 2 in panel b) of Fig. 2.3—has not to be resummed further since this would lead either to a double occupancy of the dot which is suppressed by $1/U$, or to the state with two electrons simultaneously in the lead with a *virtual* summation over the state \mathbf{p}'' . But we already showed that the latter process is suppressed by $\gamma_l/\delta\mu$. Making then use of Eq. (2.22), we obtain for

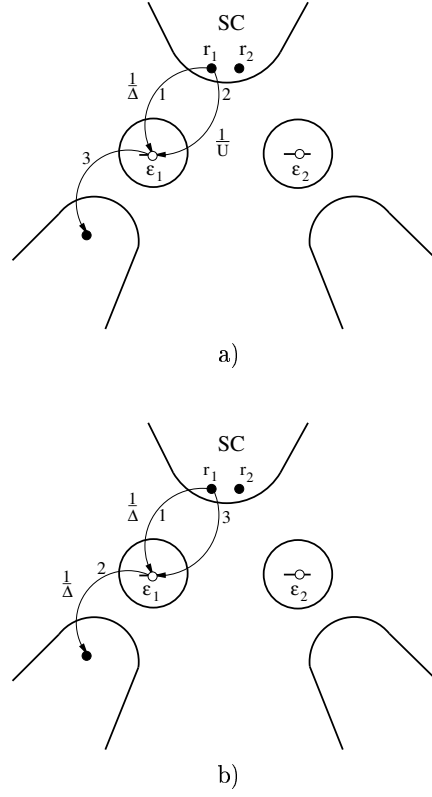


Figure 2.3: Two competing virtual processes are shown when the two electrons tunnel via the same dot: a) Andreev process leading to a double occupancy of the dot with virtual energy $1/U$, and b) the process which differs by the sequence of tunneling leading to an additional virtual energy $1/\Delta$ instead of $1/U$.

the first factor in Eq. (2.27)

$$\begin{aligned}
 \langle f | H_{DL} \sum_{n=0}^{\infty} \left(\frac{1}{i\eta - H_0} H_{DL} \right)^{2n} | D\mathbf{p}'' \uparrow \rangle \\
 = -\frac{T_{DL}}{\sqrt{2}} \frac{\epsilon_l + \epsilon_{\mathbf{p}''} - i\eta}{\epsilon_l + \epsilon_{\mathbf{p}''} - i\gamma_l/2} (\delta_{\mathbf{p}''\mathbf{p}} \mp \delta_{\mathbf{p}''\mathbf{p}'}), \quad (2.28)
 \end{aligned}$$

$$\begin{aligned}
\langle f|H_{DL} \sum_{n=0}^{\infty} \left(\frac{1}{i\eta - H_0} H_{DL}\right)^{2n} |D\mathbf{p}'' \downarrow\rangle \\
= \frac{T_{DL}}{\sqrt{2}} \frac{\epsilon_l + \epsilon_{\mathbf{p}''} - i\eta}{\epsilon_l + \epsilon_{\mathbf{p}''} - i\gamma_l/2} (\delta_{\mathbf{p}''\mathbf{p}'} \mp \delta_{\mathbf{p}''\mathbf{p}}), \quad (2.29)
\end{aligned}$$

where again in Eqs. (2.28) and (2.29) the upper sign belongs to the triplet and the lower sign to the singlet. The terms in Eqs. (2.28) and (2.29) describe repeated dot \leftrightarrow lead tunneling events of the second electron of the pair⁵ which eventually also tunnels to the lead. For the third line of Eq. (2.27) containing the superconductor-dot transitions we obtain

$$\begin{aligned}
\langle D\mathbf{p}'' \uparrow | \frac{1}{i\eta - H_0} H_{SD} \frac{1}{i\eta - H_0} H_{DL} \frac{1}{i\eta - H_0} H_{SD} |i\rangle \\
= -\langle D\mathbf{p}'' \downarrow | \frac{1}{i\eta - H_0} H_{SD} \frac{1}{i\eta - H_0} H_{DL} \frac{1}{i\eta - H_0} H_{SD} |i\rangle \\
= \frac{T_{DL} T_{SD}^2 \nu_S}{\Delta(\epsilon_l + \epsilon_{\mathbf{p}''} - i\eta)}. \quad (2.30)
\end{aligned}$$

Combining the results of Eqs. (2.28)-(2.30) we obtain for the amplitude in Eq. (2.27)

$$\langle f|T_0|i\rangle = -\frac{2^{3/2} \nu_S (T_{SD} T_{DL})^2 (\epsilon_l - i\gamma_l/2)}{\Delta(\epsilon_l + \epsilon_{\mathbf{p}} - i\gamma_l/2)(\epsilon_l + \epsilon_{\mathbf{p}'} - i\gamma_l/2)} \quad (2.31)$$

for the final state $|f\rangle$ being a singlet, whereas we get again zero for the triplet.

Next we consider the process a) where the tunneling involves a double occupancy of the dot (see panel a) in Fig. 2.3). In this case the transition amplitude can be written as

$$\begin{aligned}
\langle f|T_0|i\rangle &= \sum_{\mathbf{p}''\sigma} \langle f|H_{DL}|D\mathbf{p}''\sigma\rangle \\
&\times \langle D\mathbf{p}''\sigma | \sum_{n=0}^{\infty} \left(\frac{1}{i\eta - H_0} H_{DL}\right)^{2n} |D\mathbf{p}''\sigma\rangle \\
&\times \langle D\mathbf{p}''\sigma | \frac{1}{i\eta - H_0} H_{DL} \frac{1}{i\eta - H_0} H_{SD} \frac{1}{i\eta - H_0} H_{SD} |i\rangle. \quad (2.32)
\end{aligned}$$

As before, the transition amplitude $\langle f|T_0|i\rangle$ is only nonzero for the final lead state $|f\rangle$ being a singlet state. Repeating a similar calculation as before we

⁵—the electron that leaves the superconductor as second—

find that the amplitude is given by Eq. (2.31) but with Δ being replaced by U/π . We note that the two amplitudes in Eqs. (2.31) and (2.32) have the same initial and same final states. Thus, to obtain the total current due to processes a) and b) we need to add these two amplitudes. Then, using Eq. (2.8) we find for the total current I_2 in case of tunneling of two electrons into the same lead,

$$I_2 = \frac{e\gamma_S^2\gamma}{\mathcal{E}^2}, \quad \frac{1}{\mathcal{E}} = \frac{1}{\pi\Delta} + \frac{1}{U}. \quad (2.33)$$

We see that the effect of the quantum dots consists in the suppression factor $(\gamma/\mathcal{E})^2$ for tunneling into the *same* lead. We remark that in contrast to the previous case (tunneling into different leads) the current does not have a resonant behavior since the virtual dot states are no longer at resonance due the energy costs U or Δ in the tunneling process. Our final goal is to compare I_1 given in Eq. (2.25) with I_2 . Thus, forming the ratio of the currents of the two competing processes, we obtain

$$\frac{I_1}{I_2} = \frac{4\mathcal{E}^2}{\gamma^2} \left[\frac{\sin(k_F\delta r)}{k_F\delta r} \right]^2 \exp\left(-\frac{2\delta r}{\pi\xi}\right). \quad (2.34)$$

From this ratio we see that the desired regime with I_1 dominating I_2 is obtained when $\mathcal{E}/\gamma > k_F\delta r$, and $\delta r < \xi$. We would like to emphasize that the relative suppression of I_2 (as well as the absolute value of the current I_1) is maximized by working around the resonances $\epsilon_l \simeq \mu_S = 0^6$.

2.2.6 Efficiency and discussion

The current I_1 and therefore the ratio Eq. (2.34) suffers an exponential suppression on the scale of ξ if the tunneling of the two (coherent) electrons takes place from different points \mathbf{r}_1 and \mathbf{r}_2 of the superconductor. For conventional s-wave superconductors the coherence length ξ is typically on the order of micrometers (see e.g. Ref. [78]) and therefore poses not severe restrictions. So in the interesting regime, the suppression of the Andreev amplitude is only polynomial $\propto 1/k_F\delta r$. It was predicted theoretically in Ref. [79] and shown experimentally in Ref. [80] that a superconductor on top of a two-dimensional

⁶We remark that incoherent transport (sequential tunneling) is negligible as long as the scattering rate inside the dots, Γ_φ , is much smaller than γ_l , since $I_{\text{seq}}/I_{\text{coh}} \simeq \Gamma_\varphi/\gamma_l$, see page 260 in Ref. [2].

electron gas (2DEG) can induce superconductivity (by the proximity effect) in the 2DEG with a finite order parameter Δ . The 2DEG then becomes a two-dimensional (2D) superconductor. One could then desire to implement the two quantum dots in the 2DEG directly. More recently, it was suggested that superconductivity should also be present in ropes of single-walled carbon nanotubes [81] which are strictly one-dimensional (1D) systems. It is therefore interesting to calculate the sum over \mathbf{k} -vectors in Eq. (2.15) also in 2D and 1D. In the case of a 2D superconductor we find in leading order in $\delta r/\pi\xi$

$$\begin{aligned} & \sum_{\mathbf{k}(2D)} \frac{u_{\mathbf{k}}v_{\mathbf{k}}}{E_{\mathbf{k}}} \cos(\mathbf{k} \cdot \delta\mathbf{r}) \\ &= \frac{\pi}{2}\nu_S \left(J_0(k_F\delta r) + 2 \sum_{\nu=1}^{\infty} \frac{J_{2\nu}(k_F\delta r)}{\pi\nu} \right). \end{aligned} \quad (2.35)$$

In the limit of large $k_F\delta r$, the right-hand side of Eq. (2.35) can be approximated by $(\pi/2)\nu_S J_0(k_F\delta r)(1 - (2/\pi)\ln 2)$ which is exact to leading order in $1/k_F\delta r$. For large $k_F\delta r$, the behavior of the zeroth-order Besselfunction is $J_0(k_F\delta r) \sim \sqrt{2/\pi k_F\delta r} \cos(k_F\delta r - (\pi/4))$. So the amplitude decays asymptotically only $\propto 1/\sqrt{k_F\delta r}$, or the current I_1 by a factor $\propto 1/k_F\delta r$, respectively. In one dimension we obtain

$$\sum_{\mathbf{k}(1D)} \frac{u_{\mathbf{k}}v_{\mathbf{k}}}{E_{\mathbf{k}}} \cos(\mathbf{k} \cdot \delta\mathbf{r}) = \frac{\pi}{2}\nu_S \cos(k_F\delta r) e^{-(\delta r/\pi\xi)}, \quad (2.36)$$

where there are only oscillations and no decay of the Andreev amplitude (for $\delta r/\pi\xi < 1$). We see that the suppression due to the finite separation of the tunneling points on the superconductor can be reduced considerably, or even excluded completely, by going over to lower-dimensional superconductors. By taking into account the dependence on the dimension of the superconductor we can relax the condition for the entangler to be efficient to

$$(\mathcal{E}/\gamma)^2 > (k_F\delta r)^{d-1}, \quad (2.37)$$

where d is the dimension of the superconductor.

We emphasize that the coherent injection of the two spin-entangled electrons by an Andreev process via the dots into the leads allows for a time resolved detection of *individual* Cooper pairs in the leads since the delay time between

the two partner electrons of a Cooper pair is given by \hbar/Δ whereas the average time separation of subsequent Cooper pairs is given by⁷ $2e/I_1 \sim \hbar\gamma_l/\gamma_S^2$. Since $\Delta > \gamma_S$ and, in addition, $\gamma_l > \gamma_S$ the time delay between the two partners of a Cooper pair is much shorter than the time difference between subsequent Cooper pairs. It is therefore crucial to have weak coupling to the superconductor so that subsequent correlation measurements only report correlations within the same (spin-entangled) pair. The detection of spin-entanglement via noise measurements in a beamsplitter geometry as discussed in Ref. [47] as well as measuring Bell inequalities requires current-current correlation measurements [47, 49, 50, 67, 68]. We also discuss this issue in the last section of Chapter 3. In Ref. [67] it was pointed out that if the injection of electrons into the leads appears with an uncertainty energy $\Delta\varepsilon$, the current-current correlation measurements of pairs is in addition correlated during the correlation time $\tau_c = \hbar/\Delta\varepsilon$ which is larger than \hbar/Δ but still much shorter than $2e/I_1$ since in our case $\Delta\varepsilon \sim \gamma_l$, and $\gamma_l > \gamma_S$. To estimate the current amplitudes we use tunneling rates in the range of rates obtained in tunneling experiments through Coulomb blockaded quantum dots [82]. For $\gamma_S \sim \gamma_l/10 \sim 1 \mu\text{eV}$ we get a pair in average every 40 ns, again neglecting geometrical factors.

2.2.7 Aharonov-Bohm oscillations

In this subsection, we show that the different tunneling paths of the two electrons from the superconductor to the leads can be detected via the flux-dependent Aharonov-Bohm oscillations in the current flowing through a closed loop, see Fig. 2.4. We show that due to the possibility that two electrons can tunnel either via different dots into different leads (non-local process) or via the same dot into the same lead (local process), the current as a function of magnetic flux ϕ penetrating the loop contains h/e and $h/2e$ oscillation periods. To be concrete, we consider a setup where the two leads 1 and 2 are connected such that they form an Aharonov-Bohm loop, (see Fig. 2.4), where the electrons are injected from the left via the superconductor, traversing the upper (lead 1) and lower (lead 2) arm of the loop before they rejoin to interfere and then exit into the same lead, where the current is then measured as a function of varying magnetic flux ϕ . In

⁷We neglect here the geometrical factor containing δr in I_1 which would make $2e/I_1$ even smaller.

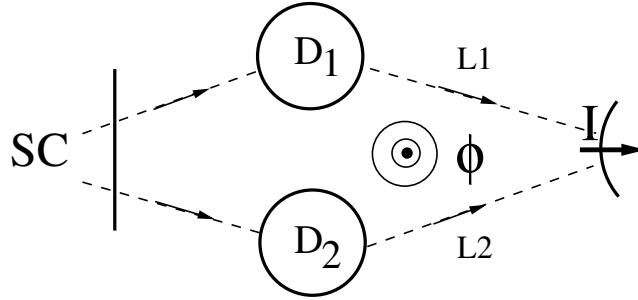


Figure 2.4: The setup where the two outgoing leads 1 (L1) and 2 (L2) are connected to a common lead so that the tunneling path of the electrons can form a loop. By applying a magnetic flux ϕ the current shows Aharonov-Bohm oscillations with periods h/e and $h/2e$ which can be used to identify different tunneling paths of the two electrons.

the presence of a magnetic flux, each tunneling amplitude obtains a phase factor, $T_{D_1L_1} \rightarrow T_{D_1L_1} e^{i\phi/2\phi_0}$, and $T_{D_2L_2} \rightarrow T_{D_2L_2} e^{-i\phi/2\phi_0}$, where $\phi_0 = h/e$ is the single-electron flux quantum. For simplicity of the discussion we assume that the entire phase is acquired when the electron hops from the dot into the leads, so that the process dot-lead-dot gives basically the full Aharonov-Bohm phase factor $e^{\pm i\phi/\phi_0}$ of the loop and only a negligible amount of phase is picked up along the path from the superconductor to the dots. We stress that there is no loss of generality in this assumption. The transition amplitude from the initial state to the final state has now the following structure $\langle f|T_0|i\rangle \sim T_{D_1L_1}T_{D_2L_2} + T_{D_1L_1}^2 e^{i\phi/\phi_0} + T_{D_2L_2}^2 e^{-i\phi/\phi_0}$. Here, the first term comes from the process via different leads (see Eq. (2.23)), where no Aharonov-Bohm phase is picked up. The Aharonov-Bohm phase appears in the remaining two terms, which come from processes via the same leads, either via lead 1 or lead 2 (see Eqs. (2.31) and (2.32)). The total current I is now obtained from $|\langle f|T_0|i\rangle|^2$ together with a summation over the final states, giving $I = I_1 + I_2 + I_{AB}$, and the flux-dependent Aharonov-Bohm current I_{AB} is given by

$$I_{AB} = \sqrt{8I_1I_2}F(\epsilon_l) \cos(\phi/\phi_0) + I_2 \cos(2\phi/\phi_0), \quad (2.38)$$

$$F(\epsilon_l) = \frac{\epsilon_l}{\sqrt{\epsilon_l^2 + (\gamma_L/2)^2}}, \quad (2.39)$$

where, for simplicity, we have assumed that $\epsilon_1 = \epsilon_2 = \epsilon_l$, and $\gamma_1 = \gamma_2 = \gamma_L$. Here, the first term (different leads) is periodic in ϕ_0 like for single-electron

Aharonov-Bohm interference effects, while the second one (same leads) is periodic in *half* the flux quantum $\phi_0/2$, describing thus the interference of two coherent electrons travelling the upper or the lower arm of the loop⁸. It is clear from Eq. (2.38) that the h/e oscillation comes from the interference between a contribution where the two electrons travel through different arms with contributions where the two electrons travel through the same arm. Both Aharonov-Bohm oscillations with period h/e , and $h/2e$, vanish with decreasing I_2 , i.e. with increasing on-site repulsion U and/or gap Δ . However, their relative weight is given by $\sqrt{I_1/I_2}$, implying that the $h/2e$ oscillations vanish faster than the h/e ones. This behavior is quite remarkable since it opens up the possibility to tune down the unwanted leakage process $\sim I_2 \cos(2\phi/\phi_0)$ where two electrons proceed via the same dot/lead by increasing U with a gate voltage applied to the dots. The dominant current contribution with period h/e comes then from the desired entangled electrons proceeding via different leads. On the other hand, if $\sqrt{I_1/I_2} < 1$, which could become the case e.g. for $k_F \delta r > \mathcal{E}/\gamma$, we are left with $h/2e$ oscillations only. Besides the fact that the Aharonov-Bohm oscillations are interesting in their own right, the Aharonov-Bohm oscillations further provide an experimental probe of the nonlocality of the two spin-entangled electrons. Note that dephasing processes which affect the orbital part suppress I_{AB} . Still, the flux-independent current $I_1 + I_2$ can remain finite and contain electrons which are entangled in spin-space, provided that there is only negligible spin-orbit coupling so that the spin is still a good quantum number.

We would like to mention another important feature of the Aharonov-Bohm effect under discussion, namely the relative phase shift between the amplitudes of tunneling to the same lead and to different leads, resulting in the additional prefactor $F(\epsilon_l)$ in the first term of the right-hand side of Eq. (2.38). This phase shift is due to the fact that there is a two-particle resonance in the amplitude Eq. (2.23), while there is only a single-particle resonance in the amplitudes Eqs. (2.31) and (2.32)⁹. Thus, when the chemical potential μ_S of the superconductor crosses the resonance, $|\epsilon_l| \lesssim \gamma_L$, the amplitude Eq. (2.23) acquires an extra phase factor $e^{i\phi_r}$, where $\phi_r = \arg[1/(\epsilon_l - i\gamma_L/2)]$. Then the interference of the two amplitudes leads to the prefactor $F(\epsilon_l) = \cos \phi_r$ in the first term on the right-hand side of Eq. (2.38).

⁸Similar single- and two-particle Aharonov-Bohm effects occur in the Josephson current through an Aharonov-Bohm loop [56]

⁹We recall that the second resonance is suppressed by the Coulomb blockade effect.

In particular, exactly at the middle of the resonance, $\epsilon_l = 0$, the phase shift is $\phi_r = \pi/2$, and thus the h/e oscillations vanish, since $F(0) = \cos(\pi/2) = 0$. Note however, that although $F = \pm 1$ away from the resonance ($|\epsilon_l| > \gamma_L$) the h/e oscillations vanish again, now because the current $I_1 \sim e\gamma_S^2\gamma_L/\epsilon_l^2$ vanishes. Thus, the optimal regime for the observation of the Aharonov-Bohm effect is $|\epsilon_l| \sim \gamma_L$.

Finally, the preceding discussion shows that even if the spins of two electrons are entangled their associated charge current does not reveal this spin-correlation in a simple Aharonov-Bohm interference experiment¹⁰. Only if we consider the current-current correlations (noise) in a beam splitter setup, can we detect also this spin-correlation in the transport current via its charge properties [47].

2.2.8 Conclusion

In this section, we proposed an entangler device that can create pairwise spin-entangled electrons and provide coherent injection by an Andreev process into different dots which are tunnel-coupled to leads. The unwanted process of both electrons tunneling into the same lead can be suppressed by increasing the Coulomb repulsion on the quantum dot. We have calculated the ratio of currents of these two competing processes and shown that there exists a regime of experimental interest where the entangled current shows a resonance and assumes a finite value with both partners of the singlet being in different leads but having the same orbital energy¹¹. This entangler then satisfies the necessary requirements needed to detect the spin-entanglement via transport and noise measurements. We also discussed the flux-dependent oscillations of the current in an Aharonov-Bohm loop.

¹⁰We note, however, that the Aharonov-Bohm current can be used as a probe to detect localized spin singlets in coupled double-dots [83].

¹¹More generally, the two electrons of a pair are injected into different leads within the lifetime broadenings γ_1 and γ_2 of the dot levels ϵ_1 and ϵ_2 , respectively. The resonance condition for the current is $2\mu_S = \epsilon_1 + \epsilon_2$ where $\mu_S \simeq \epsilon_1 \simeq \epsilon_2$ is a special case— interesting for measuring noise of spin-entangled electrons.

2.3 Andreev Entangler with Luttinger liquid leads

In this section, we propose to use Luttinger liquid correlations present in one-dimensional quantum wires to separate the two spin-entangled electrons which originate from an Andreev process. Such a setup could be implemented if a superconductor is brought into contact with metallic carbon nanotubes or semiconducting cleaved edge quantum wires which show evidence of Luttinger liquid physics.

2.3.1 About Fermi liquids and Luttinger liquids

In three dimensional metals, Fermi liquid theory [84] is based on the existence of quasiparticles evolving out of electrons (holes) of a Fermi gas upon adiabatically switching on interactions. These quasiparticles resemble essentially free electrons with *renormalized masses* and a *lifetime* which, however, diverges as $\tau \sim (\varepsilon - \varepsilon_F)^{-2}$ so that these states are very long-lived close to the Fermi energy ε_F . The existence of low-lying quasiparticle states is also visible in a finite step in the momentum distribution function at k_F with its height being directly proportional to the quasiparticle weight factor z_F of the spectral function at the Fermi energy. It is this one-to-one correspondence which makes the Fermi gas a reasonable description of a three dimensional interacting metal.

In one dimension the effects of electron-electron interactions are far more dramatic since it leads to the complete breakdown of the quasiparticle picture even for an arbitrarily weak interaction strength.

In this subsection, we will discuss some important features and predictions of the so-called Luttinger liquid model [85] which describes interacting electrons in one dimension and close to the Fermi energy. Here, we consider *spinless* electrons and will generalize to the case with spin in the main part of the section. The basic assumption of the model is that the underlying non-interacting theory has a linear energy dispersion relation $\varepsilon(p) = v_F(\pm p - p_F)$ counted from the chemical potential. This is a reasonable assumption if we are only concerned with properties around the Fermi energy. The second assumption is that this linear spectrum can be extended to negative infinity, see Fig. 2.5. This should not affect the low energy physics since all states

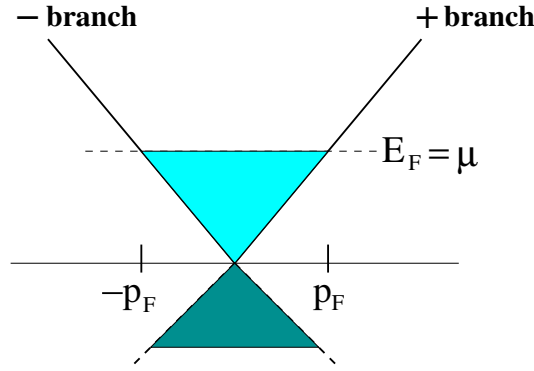


Figure 2.5: Energy dispersion relation of the Luttinger liquid model: There are two linear branches + and - which extend to negative infinity. The addition of extra states (dark grey) makes the model exactly solvable and should not influence the low energy physics. At zero temperature and without interaction, the states are filled up to the chemical potential μ .

well below the Fermi energy are filled. The free Hamiltonian is then given as

$$H_0 = v_F \sum_{p,r=\pm} (rp - p_F) : c_{rp}^\dagger c_{rp} : , \quad (2.40)$$

where c_{rp}^\dagger , and c_{rp} create and annihilate electrons with wave number p in the left ($r = -$) and the right ($r = +$) branches of the spectrum and are completely uncorrelated, i.e. $\{c_{rp}, c_{r'p'}^\dagger\} = \delta_{rr'}\delta_{pp'}$. The Fermi normal ordering $: :$ measures the quantity with respect to the ground state, i.e. $: c_{rp}^\dagger c_{rp} : := c_{rp}^\dagger c_{rp} - \langle c_{rp}^\dagger c_{rp} \rangle_0$. The subtraction of the ground state energy in Eq. (2.40) is necessary to compensate for the divergence due to the inclusion of negative energy states. It can be shown (see e.g. Ch. 4 in Ref. [76]) that in this model the exact commutation relation holds

$$[\rho_r(q), \rho_{r'}(q')] = -r\delta_{rr'}\delta_{qq'}\frac{qL}{2\pi}, \quad (2.41)$$

where we have introduced the density operator $\rho_r(q) = \sum_p : c_{rp+q}^\dagger c_{rp} : .$ It is then straightforward to prove the commutation relation

$$[H_0, \rho_r(q)] = rv_F q \rho_r(q), \quad (2.42)$$

by using Eq. (2.41) and the linearity of the spectrum. This shows that the electron hole pairs created by $\rho_r(q)$ correspond to eigenstates of the Hamiltonian H_0 with energies rv_Fq . This then leads to the bosonized form of the Hamiltonian

$$H_0 = \frac{\pi v_F}{L} \left[\sum_{q \neq 0, r = \pm} \rho_r(q) \rho_r(-q) + \sum_{r = \pm} N_r^2 \right]. \quad (2.43)$$

Here, $N_r = \rho_r(q = 0)$ is the number of particles added to the ground state into branch r . The Hamiltonian in the fermionic representation (Eq. (2.40)) and in the bosonic representation (Eq. (2.43)) are completely equivalent, since they have the same spectrum and degeneracy of the energy levels [86, 87]. To calculate Green's functions in the bosonic representation we have to write the electron operator in terms of the bosons. This is achieved via $\psi_r(x) \simeq e^{ip_F x} \psi_+(x) + e^{-ip_F x} \psi_-(x)$ with the slowly-varying components given by

$$\psi_r(x) \simeq e^{i[r\phi(x) - \theta(x)]}. \quad (2.44)$$

The phase fields ϕ and θ are linear combinations of the density operators $\rho_r(q)$ and satisfy the commutation relation $[\phi(x), \theta(x')] = -i(\pi/2) \text{sgn}(x - x')$. From Eq. (2.44), we see that $:\psi_+^\dagger(x)\psi_+(x): + :\psi_-^\dagger(x)\psi_-(x): = \partial_x \phi / \pi$ and $:\psi_+^\dagger(x)\psi_+(x): - :\psi_-^\dagger(x)\psi_-(x): = -\partial_x \theta / \pi$ which will be derived in more detail in Appendix C. We can then write the Hamiltonian also in the phase field representation

$$H_0 = \frac{v_F}{2\pi} \int dx [(\partial_x \theta)^2 + (\partial_x \phi)^2]. \quad (2.45)$$

Up to now we did not gain any advantage over the fermionic representation.

Now let's consider interactions. Whereas interaction terms are fourth order in the electron field operators $\psi(x)$, they are only quadratic in the phase fields. To show this we consider the interaction term

$$H_{int} = \frac{1}{2} \int dx \int dx' \rho(x) V(x - x') \rho(x'), \quad (2.46)$$

with $V(x - x')$ being the interaction potential. The density operator $\rho(x) \simeq :\psi_+^\dagger(x)\psi_+(x): + :\psi_-^\dagger(x)\psi_-(x): = \partial_x \phi / \pi$ where we neglect rapidly oscillating terms (on the scale of $1/2p_F$) coming from cross products like $\psi_+^\dagger(x)\psi_-(x)$. The inclusion of such terms would lead to backscattering terms

in H_{int} with large momentum transfers of order $2p_F$. If the Fourier transform $V(q)$ of the potential is small at $q \simeq 2p_F$ compared to $V(q \simeq 0)$ these rapidly oscillating terms can be neglected in H_{int} and we obtain $H_{int} = \frac{1}{2\pi^2} \int dx \int dx' \partial_x \phi(x) V(x-x') \partial_{x'} \phi(x')$. If we restrict ourselves to low energy excitations with wavelengths much larger than the range of the interaction potential, we can use a local potential $V(x) = V_0 \delta(x)$ with $V_0 = V(q \simeq 0)$. We then obtain the interaction term $H_{int} = \frac{1}{2\pi^2} V_0 \int dx (\partial_x \phi(x))^2$. In Fourier space this Hamiltonian describes forward scattering events where electrons stay in the same branch of left and right movers, see Fig. 2.6. With this

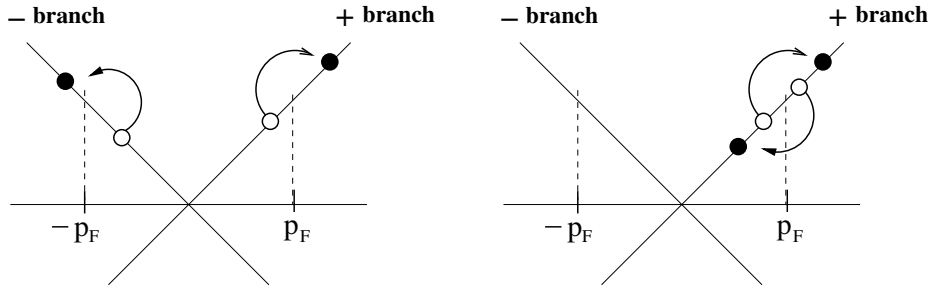


Figure 2.6: Forward scattering events included in the Luttinger model where electrons stay in the same branch of left (-) and right (+) movers.

interaction term we obtain the Luttinger liquid Hamiltonian

$$H = \frac{1}{2\pi} \int dx \left[K u (\partial_x \theta)^2 + \frac{u}{K} (\partial_x \phi)^2 \right]. \quad (2.47)$$

The velocity of the collective charge modes is given by $u = v_F/K$ where $K = (1 + \frac{V_0}{v_F \pi})^{-1/2} < 1$.

Next, we want to discuss briefly some very peculiar consequences of the Luttinger model for *spectral* properties. The tunneling into a Luttinger liquid at position x and energy E counted from the Fermi energy is given by the tunneling-DOS

$$\rho(E, x) = \frac{1}{\pi} \text{Re} \sum_{r=\pm} \int_0^{\infty} dt e^{iEt} \langle \psi_r(x, t) \psi_r^\dagger(x, 0) \rangle. \quad (2.48)$$

In an infinite system and at zero temperature the single-particle correlation function is approximately, see Subsection 2.3.6

$$\langle \psi_r(x, t) \psi_r^\dagger(0, 0) \rangle = \frac{1}{2\pi} \frac{e^{ip_F r x}}{\Lambda + i(ut - rx)} \left[\frac{\Lambda^2}{x^2 + (iut + \Lambda)^2} \right]^{\alpha/2}, \quad (2.49)$$

where $\alpha = (1/2)[K + K^{-1}] - 1$ depends on interaction and determines the power law decay of correlations at long times or distances, and Λ is a large momentum cut-off on the order of $1/p_F$. Evaluating the Fourier integral in Eq. (2.48) leads to

$$\rho(E) \propto \Theta(E) \left(\frac{E}{\varepsilon_0} \right)^\alpha, \quad (2.50)$$

with $\varepsilon_0 = \Lambda/u$. This result is in stark contrast to Fermi liquid theory which predicts a finite density of states at the Fermi energy $E = 0$. The tunneling into a Luttinger liquid is therefore strongly suppressed at low energies since the absorption of an electron requires the rearrangement of all the electrons in the bulk of the Luttinger liquid system. As a further example we examine the momentum distribution function $n_p = \langle c_p^\dagger c_p \rangle$. Going over to position space we can write the momentum distribution function as

$$n_p = \sum_{r=\pm} \int dx e^{i(p-rp_F)x} \langle \psi_r^\dagger(x) \psi_r(0) \rangle, \quad (2.51)$$

with the result

$$n_p \simeq \frac{1}{2} - C_1 \text{sgn}(p - p_F) |p - p_F|^\alpha - C_2 (p - p_F), \quad (2.52)$$

which is valid for p near p_F . This result shows that there is *no jump* in the momentum distribution function at p_F , but rather a continuous power-law variation. This again is in contrast to the higher dimensional Fermi liquid case where there is a finite jump at p_F due to a nonvanishing quasiparticle weight factor z_F . The absence of (low-lying) quasiparticles in a Luttinger liquid is therefore evident in view of Eq. (2.52).

Experimentally accessible systems that show strong evidence of Luttinger liquid properties are, e.g., carbon nanotubes in the metallic regime [88] or cleaved edge GaAs quantum wires [89].

2.3.2 Setup of entangler

We have shown above that the low energy excitations of Luttinger liquids are collective modes rather than quasiparticles which resemble free electrons like they exist in a Fermi liquid. As a consequence, the single-electron tunneling into a Luttinger liquid is suppressed by strong correlations. The question then arises quite naturally whether these strong correlations can even further suppress the coherent tunneling of *two* electrons into the same Luttinger liquid, as provided by a correlated two-particle tunneling event (Andreev tunneling), so that the two electrons preferably separate and tunnel into different Luttinger liquid leads. We show in the following that the answer is positive.

To address this question we introduce a setup consisting of an s-wave superconductor which is weakly tunnel-coupled to the center (bulk) of two spatially separated one-dimensional wires 1,2 described as Luttinger liquids, see Figs. 2.7 and 2.8. In this model we calculate the stationary current generated by the tunneling of a singlet, transferred from the superconductor into two separate leads (nonlocal process) or into the same lead (local process), 1 or 2. We show that there exists a regime of experimental interest where the desired injection of the two electrons into two separate leads is favored. We remark again that in this case the two spins, forming a singlet, are entangled in spin space while separated in orbital space and therefore represent an electronic EPR pair. In addition to the familiar suppression of single-electron tunneling into a Luttinger liquid, we find now that the subsequent tunneling of a second electron into the same Luttinger liquid is further suppressed, again in a characteristic interaction dependent power law, provided the applied voltage bias between the superconductor and the Luttinger liquid is much smaller than the energy gap Δ in the superconductor so that single-electron tunneling is suppressed. The two-particle tunneling event is strongly correlated within the uncertainty time \hbar/Δ , characterizing the time-delay between subsequent tunneling events of the two electrons of the same Cooper pair. In other words, the second electron of a Cooper pair is influenced by the existence of its preceding partner electron already present in the Luttinger liquid. This effect can also be interpreted as a Coulomb blockade effect, in analogy to what occurs in quantum dots attached to a superconductor as discussed in Section 2.2. Similar Coulomb blockade effects were also found in a mesoscopic chiral Luttinger liquid within a quantum dot coupled to macroscopic chiral Luttinger liquid edge-states in the fractional quantum

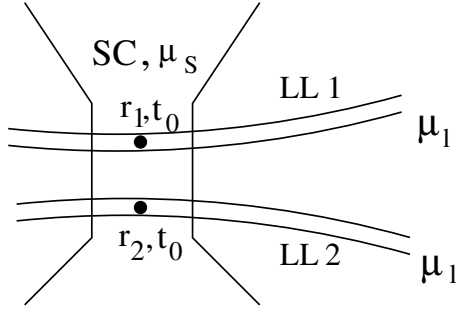


Figure 2.7: A possible implementation of the entangler setup: Two quantum wires 1,2 with chemical potential μ_l , described as infinitely long Luttinger liquids (LL), are deposited on top of an s-wave superconductor (SC) with chemical potential μ_S . The electrons of a Cooper pair can tunnel by means of an Andreev process from two points \mathbf{r}_1 and \mathbf{r}_2 on the superconductor to the center (bulk) of the two quantum wires 1 and 2, respectively with tunneling amplitude t_0 . The interaction between the wires 1,2 is assumed to be negligible.

Hall regime [90]. There, the Coulomb blockade-like energy gap is quantized in units of the non-interacting energy level spacing of the quantum dot and its existence is therefore a finite size effect, whereas in the present case, we will see that the suppression comes from strong correlations in a two-particle tunneling event which is present even in an infinitely long Luttinger liquid as considered here. On the other hand, if the two electrons of a Cooper pair tunnel to different leads, they will preferably do this from different points \mathbf{r}_1 and \mathbf{r}_2 from the superconductor, with distance $\delta r = |\mathbf{r}_1 - \mathbf{r}_2|$ due to the spatial separation of the leads, see Figs. 2.7 and 2.8. We again find, in complete analogy to Section 2.2, that the current is exponentially suppressed if the distance δr exceeds the coherence length ξ of a Cooper pair in the superconductor. This limitation poses no severe experimental restriction since ξ is on the order of micrometers for usual s-wave materials and δr can be assumed to be on the order of nanometers. Still, a power law suppression $\propto 1/(k_F \delta r)^{d-1}$, with k_F being the Fermi wavenumber of the superconductor and d its effective dimension, remains and is more relevant. Next, we discuss the decay in time of an electronic spin singlet injected into two Luttinger liquids, one electron into each lead, due to the interaction present in the Luttinger liquid and find a characteristic power law decay in time at zero

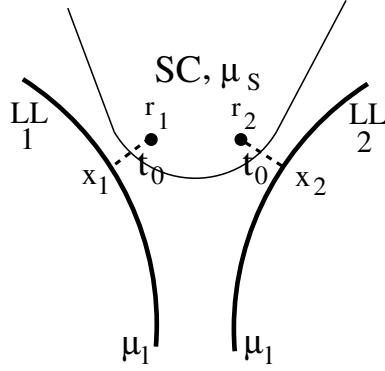


Figure 2.8: An alternative implementation of the proposed entangler setup: The two quantum wires 1,2 with chemical potential μ_l , described as infinitely long Luttinger liquids (LL), are tunnel-coupled with amplitude t_0 from two points x_1 and x_2 to two points r_1 and r_2 of a superconducting (SC) tip with chemical potential μ_S .

temperature. Despite this decay of the singlet state, the spin information can still be transported through the Luttinger liquid wires via the spin-density fluctuations (collective spin modes) created by the injected electrons. These collective excitations are shown to be well localized in space and therefore locally accessible for measurements.

2.3.3 Hamiltonian

The Hamiltonian of this system is represented as $H = H_0 + H_T$ with $H_0 = H_S + \sum_{n=1,2} H_{Ln}$ describing the isolated superconductor and Luttinger liquid leads 1,2, respectively. Tunneling between the superconductor and the leads is governed by the tunneling Hamiltonian H_T [76]. Each part of the system will be described in the following.

The s-wave superconductor with chemical potential μ_S is described by the BCS-Hamiltonian [59]

$$H_S - \mu_S N_S = \sum_{\mathbf{k}, s} E_{\mathbf{k}} \gamma_{\mathbf{k}s}^\dagger \gamma_{\mathbf{k}s}, \quad (2.53)$$

where $s = (\uparrow, \downarrow)$ and $N_S = \sum_{\mathbf{k}s} c_{\mathbf{k}s}^\dagger c_{\mathbf{k}s}$ is the number operator for electrons in the superconductor. The quasiparticle operators $\gamma_{\mathbf{k}s}$ describe excitations

out of the BCS-ground state $|0\rangle_S$ defined by $\gamma_{\mathbf{k}s}|0\rangle_S = 0$. They are related to the electron annihilation and creation operators $c_{\mathbf{k}s}$ and $c_{\mathbf{k}s}^\dagger$ through the Bogoliubov transformation

$$\begin{aligned} c_{\mathbf{k}\uparrow} &= u_{\mathbf{k}}\gamma_{\mathbf{k}\uparrow} + v_{\mathbf{k}}\gamma_{-\mathbf{k}\downarrow}^\dagger \\ c_{-\mathbf{k}\downarrow} &= u_{\mathbf{k}}\gamma_{-\mathbf{k}\downarrow} - v_{\mathbf{k}}\gamma_{\mathbf{k}\uparrow}^\dagger, \end{aligned} \quad (2.54)$$

where $u_{\mathbf{k}} = (1/\sqrt{2})(1 + \xi_{\mathbf{k}}/E_{\mathbf{k}})^{1/2}$ and $v_{\mathbf{k}} = (1/\sqrt{2})(1 - \xi_{\mathbf{k}}/E_{\mathbf{k}})^{1/2}$ are the standard BCS coherence factors [59], and $\xi_{\mathbf{k}} = \epsilon_{\mathbf{k}} - \mu_S$ is the normal state single-electron energy counted from the Fermi level μ_S , and $E_{\mathbf{k}} = \sqrt{\xi_{\mathbf{k}}^2 + \Delta^2}$ is the quasiparticle energy. The field operator for an electron with spin s is $\Psi_s(\mathbf{r}) = V^{-1/2} \sum_{\mathbf{k}} e^{i\mathbf{k}\mathbf{r}} c_{\mathbf{k}s}$, where V is the volume of the superconductor.

The two leads 1, 2 are supposed to be infinite one dimensional interacting electron systems described by Luttinger liquid theory as discussed briefly in Subsection 2.3.1. To treat the Luttinger liquid *with spin* we introduce phase fields θ and ϕ for each spin projection separately, and then perform the transformation to charge and spin bosons via $\theta_{\rho,\sigma} = (\theta_\uparrow \pm \theta_\downarrow)/\sqrt{2}$ and $\phi_{\rho,\sigma} = (\phi_\uparrow \pm \phi_\downarrow)/\sqrt{2}$. We only include forward scattering processes which describe scattering events in which electrons stay in the same branch of left and right movers, see Fig. 2.6. We neglect backscattering interactions which involve large momentum transfers of order $2p_F$ with p_F the Fermi wavenumber in the Luttinger liquid (see also Subsection 2.3.1). In context with carbon nanotubes we remark that it was pointed out in Refs. [91, 92] that for the (metallic) armchair nanotubes (N, N) with $N \gtrsim 10$ it is appropriate to use a Luttinger liquid model where backscattering and umklapp scattering can be neglected. This is so because for large N , the probability for two electrons to be near each other is small ($\sim 1/N$) and therefore one can neglect the short range part $r \sim a$, with a the lattice spacing, of the Coulomb potential which corresponds to large momentum transfers $\sim 2p_F$ at which backscattering and Umklapp scattering takes place.

The Hamiltonian for the low energy excitations of lead $n = 1, 2$ can then be written in a bosonized form as [93]

$$H_{Ln} - \mu_l N_n = \sum_{\nu=\rho,\sigma} \frac{u_\nu}{2\pi} \int_{-L/2}^{+L/2} dx (K_\nu (\partial_x \theta_{n\nu})^2 + K_\nu^{-1} (\partial_x \phi_{n\nu})^2), \quad (2.55)$$

where the phase fields $\theta_n(x)$ and $\phi_n(x)$ satisfy bosonic commutation relations $[\phi_{n\nu}(x), \theta_{m\mu}(x')] = -i(\pi/2)\delta_{nm}\delta_{\nu\mu}\text{sgn}(x - x')$, and μ_l is the chemi-

cal potential of the leads (assumed to be identical for both leads), and $N_n = \sum_s \int dx \psi_{ns}^\dagger(x) \psi_{ns}(x)$ is the number operator for electrons in lead n . The Hamiltonian Eq. (2.55) describes long-wavelength charge ($\nu = \rho$) and spin ($\nu = \sigma$) density oscillations propagating with velocities u_ρ and u_σ , respectively. The velocities u_ν and the stiffness parameters K_ν depend on the interactions between the electrons in the Luttinger liquid. In the limit of vanishing backscattering, we have $u_\sigma = v_F$ and $K_\sigma = 1$, and the Luttinger liquid is described by only two parameters $K_\rho < 1$ and u_ρ . In a system with full translational invariance we have further $u_\rho = v_F/K_\rho$. We decompose the field operator describing electrons with spin s into a right and left moving part, $\psi_{ns}(x) = e^{ip_F x} \psi_{ns+}(x) + e^{-ip_F x} \psi_{ns-}(x)$. The right (left) moving field operator $\psi_{ns+}(x)$ ($\psi_{ns-}(x)$) is then expressed as an exponential of bosonic fields as [86, 87]

$$\psi_{ns\pm}(x) = \lim_{\alpha \rightarrow 0} \frac{\eta_{\pm,ns}}{\sqrt{2\pi\alpha}} \exp \left\{ \pm \frac{i}{\sqrt{2}} \left(\phi_{n\rho}(x) + s\phi_{n\sigma}(x) \mp (\theta_{n\rho}(x) + s\theta_{n\sigma}(x)) \right) \right\}. \quad (2.56)$$

The operators $\eta_{\pm,ns}$ are needed to ensure the correct fermionic anticommutation relations. In the thermodynamic limit ($L \rightarrow \infty$), $\eta_{\pm,ns}$ can be presented by Hermitian operators satisfying the anticommutation relation $\{\eta_r, \eta_{r'}\} = 2\delta_{rr'}$, with $r = \pm, ns$ [93]. We adopt the convention throughout this section that $s = +1$ for $s = \uparrow$, and $s = -1$ for $s = \downarrow$, if s has not the meaning of an operator index.

Transfer of electrons from the superconductor to the leads is described by the tunneling Hamiltonian $H_T = \sum_n H_{Tn} + \text{h.c.}$, where H_{Tn} is defined as

$$H_{Tn} = t_0 \sum_s \psi_{ns}^\dagger \Psi_s(\mathbf{r}_n). \quad (2.57)$$

The field operator $\Psi_s(\mathbf{r}_n)$ annihilates an electron with spin s at point \mathbf{r}_n on the superconductor, and ψ_{ns}^\dagger creates it again with amplitude t_0 at point x_n in the Luttinger liquid n which is nearest to \mathbf{r}_n , see Figs. 2.7 and 2.8. We assume that the spin is conserved during the tunneling process, and thus the tunneling amplitudes t_0 do not depend on spin, and, for simplicity, are the same for both leads $n = 1, 2$. We remark that our point-contact approach for describing the electron transfer from the superconductor to the leads is the simplest possible description but it captures presumably the relevant features of a real device. The scheme shown in Fig. 2.8 has a geometry which suggests that electrons tunnel from point $\mathbf{r}_n \rightarrow x_n$ which are closest

to each other, due to the fact that t_0 depends exponentially on the tunneling distance. In the setup shown in Fig. 2.7, a point-like tunnel contact between the superconductor and the Luttinger liquids might be induced by slightly bending the quantum wires (e.g. nanotubes). If the contact area has a finite extension, we note that the two electrons preferably tunnel from the same point on the superconductor, when they tunnel into the same lead, since the two-particle tunneling event is coherent and shows a suppression in the probability already on a length scale given by $1/k_F$, as we discuss in more detail below.

2.3.4 Stationary current

We now calculate the current of singlets, i.e. pairwise spin-entangled electrons (Cooper pairs), from the superconductor to the Luttinger liquid leads due to Andreev tunneling [60,94] in first non-vanishing order, starting from a general T-matrix approach [77]. We thereby distinguish two transport channels. First we calculate the current when two electrons tunnel from different points \mathbf{r}_1 and \mathbf{r}_2 of the superconductor into *different* interacting Luttinger liquid leads which are separated in space such that there is no inter-lead interaction. In this case the only correlation in the tunneling process is due to the superconducting pairing of electrons which results in a coherent two-electron tunneling process of opposite spins from different points \mathbf{r}_1 and \mathbf{r}_2 of the superconductor, and with a delay time $\sim \hbar/\Delta$ between the two tunneling events. Since the total spin is a conserved quantity $[H, \mathbf{S}^2] = 0$, the spin entanglement of a Cooper pair is transported to *different* leads, thus leading to nonlocal spin-entanglement. On the other hand, if two electrons tunnel from the same point of the superconductor into the *same* lead there is an additional correlation in the Luttinger liquid itself due to the intra-lead interaction. It is the goal of this section to investigate how the transport current for tunneling of two electrons from the superconductor into the *same* Luttinger liquid lead is affected by this additional correlation.

2.3.5 T-matrix

We again apply a T-matrix (transmission matrix) approach [77] to calculate the current which we have introduced already in Subsection 2.2.3. For completeness, we also explain this approach here in detail. The stationary current of *two* electrons passing from the superconductor to the leads is then

given by

$$I = 2e \sum_{f,i} W_{fi} \rho_i, \quad (2.58)$$

where W_{fi} is the transition rate from the superconductor to the leads, given by

$$W_{fi} = 2\pi |\langle f | T(\varepsilon_i) | i \rangle|^2 \delta(\varepsilon_f - \varepsilon_i). \quad (2.59)$$

Here, $T(\varepsilon_i) = H_T \frac{1}{\varepsilon_i + i\eta - H} (\varepsilon_i - H_0)$ is the on-shell transmission or T-matrix, with η being a positive infinitesimal which we set to zero at the end of the calculation. The T-matrix can be expanded in a power series in the tunneling Hamiltonian H_T ,

$$T(\varepsilon_i) = H_T + H_T \sum_{n=1}^{\infty} \left[\frac{1}{\varepsilon_i + i\eta - H_0} H_T \right]^n, \quad (2.60)$$

where ε_i is the energy of the initial state $|i\rangle$, which, in our case, is the energy of a Cooper pair at the Fermi surface of the superconductor, $\varepsilon_i = 2\mu_S$. Finally, $\rho_i = \langle i | \rho | i \rangle$ is the stationary occupation probability for the entire system to be in the state $|i\rangle$. We work in the regime $\Delta > \delta\mu > k_B T$, where $\delta\mu = \mu_S - \mu_l$ is the applied voltage bias between the superconductor and the leads, and T the temperature with k_B the Boltzmann constant. The regime $\Delta > \delta\mu$ ensures that single electron tunneling from the superconductor to the leads is excluded and only tunneling of *two* coherent electrons of opposite spins is allowed. In the regime $\delta\mu > k_B T$ we only have transport from the superconductor to the leads, and not in the opposite direction. Since temperature is assumed to be the smallest energy scale in the system, we assume $k_B T = 0$ in the calculation.

The set of initial states $|i\rangle$, virtual states $|v\rangle$ and final states $|f\rangle$ consists of the BCS ground state $|0\rangle_S$ and excitations $\gamma_{\mathbf{k}s}^\dagger |0\rangle_S$ for the superconductor and a complete set [86,87] of energy eigenstates $|N_{nr\nu}, \{b_{n\nu}\}\rangle$ of the Luttinger liquid Hamiltonian H_{Ln} given in Eq. (2.55). $N_{nr\nu}$ is the number of excess spin ($\nu = \sigma$) and charge ($\nu = \rho$) in branch r relative to the ground state. The Bose operators $b_{n\nu}$ form a continuous spectrum describing collective spin and charge modes and will be introduced in Eqs. (2.64) and (2.65). The ground state of the Luttinger liquid is then $|0, 0\rangle$, which means that we have no integral excess charge and spin and no bosonic excitations. The energy contribution of the excess charge and spin is included in the so-called zero mode ($p = 0$) terms in the diagonalized Hamiltonian K_{Ln} [Eq. (2.66)] and

are of no importance in the thermodynamic limit ($L \rightarrow \infty$) considered here, since the contribution of these terms due to an additional electron on top of the ground state is $\mathcal{O}(1/L)$ and is neglected in Eq. (2.66). For a detailed description of the Luttinger liquid Hamiltonian Eq. (2.55) including the zero-modes we refer to Appendix C. Since we want to calculate the transition rate for transport of a Cooper pair to the leads, the final states $|f\rangle$ of interest contain two additional electrons of opposite spins in the leads compared to the initial state $|i\rangle$.

2.3.6 Current for tunneling into different leads

We first calculate the current for tunneling of two spin-entangled electrons into different leads. Here, we are not facing a resonance as appeared in the last section with quantum dots. We therefore are allowed to treat tunneling to lowest possible order in the tunneling Hamiltonian H_T . We expand the T-matrix to second order in H_T [the term with $n = 1$ in Eq. (2.60)] and go over to the interaction representation by using $\delta(\epsilon) = (1/2\pi) \int_{-\infty}^{+\infty} dt e^{i\epsilon t}$, and $\langle v | (\epsilon_i - H_0 + i\eta)^{-1} | v \rangle = -i \int_0^\infty dt e^{i(\epsilon_i - \epsilon_v + i\eta)t}$. By transforming the time dependent phases into a time dependence of the tunneling Hamiltonian we can integrate out all final and virtual states. The forward current I_1 for tunneling of two electrons into different leads can then be written as

$$I_1 = 2e \lim_{\eta \rightarrow 0^+} \sum_{\substack{n \neq n' \\ m \neq m'}} \int_{-\infty}^{\infty} dt \int_0^{\infty} dt' \int_0^{\infty} dt'' e^{-\eta(t'+t'')} e^{i(2t-t'-t'')\delta\mu} \\ \times \langle H_{Tm}^\dagger(t-t'') H_{Tm'}^\dagger(t) H_{Tn}(t') H_{Tn'}(0) \rangle, \quad (2.61)$$

where $\langle \dots \rangle$ denotes $\text{Tr} \rho \{ \dots \}$. The bias has been introduced in a standard way [76], and the time dependence of the operators in Eq. (2.61) is then governed by $H_{Tn}(t) = e^{i(K_{Ln}+K_S)t} H_{Tn} e^{-i(K_{Ln}+K_S)t}$ with $K_{Ln} + K_S = H_{Ln} + H_S - \mu_L N_n - \mu_S N_S$. The interaction representation Eq. (2.61) has the advantage that we only have to calculate statistical averages of (time-dependent) correlation functions. No explicit summation over final states is needed here which would be particularly tedious for the Luttinger liquid part. The transport process involves two electrons with *different* spins which suggests that the average in Eq. (2.61) is of the form (suppressing time variables), $\langle \dots \rangle = \sum_{ss'} \langle H_{Tm-s}^\dagger H_{Tm's'}^\dagger H_{Tn-s} H_{Tn's} \rangle$, where H_{Tns} describes tunneling of

spin s governed by H_{Tn} . The time sequence in Eq. (2.61) contains the dynamics of the hopping of a Cooper pair from the superconductor to the Luttinger liquid leads (one electron per lead) and back. The times t' and t'' are delay times between subsequent hoppings of two electrons from the *same* Cooper pair, whereas t is the time between injecting and taking out a Cooper pair. We evaluate the thermal average in Eq. (2.61) at zero temperature where the expectation value is to be taken in the ground state of $K_0 = \sum_n K_{Ln} + K_S$ which is the BCS ground state of the superconductor and the bosonic vacuum of the Luttinger liquid leads. We remark that since the interaction between the different subsystems (SC, L_1, L_2) is included in the tunneling-perturbation, the expectation value factorizes into a superconductor part times a Luttinger liquid part. In addition, the Luttinger liquid correlation function factorizes into two single-particle correlation functions due to the negligible interaction between the leads 1, 2 (this will be not the case if two electrons tunnel into the *same* lead). Note that in the thermodynamic limit the time dynamics of all Luttinger liquid correlation functions is governed by a Hamiltonian that depends only on Bose operators [see Eq. (2.66)]. The operators $\eta_{\pm,rs}$ commute with all Bose operators, and as a consequence $\eta_{\pm,rs}$ are time independent. Therefore, interaction terms of the form $\psi_\alpha \psi_\beta \psi_\gamma^\dagger \psi_\delta^\dagger$ can be written as $\eta_\alpha \eta_\beta \eta_\gamma \eta_\delta \times (\text{Bose operators})$, where $\alpha, \beta, \gamma, \delta$ are composite indices containing $r = \pm, ns$. The correlation function in Eq. (2.61) is then of the form

$$\begin{aligned}
& \sum_{\substack{n \neq n' \\ m \neq m'}} \langle H_{Tm}^\dagger(t-t'') H_{Tm'}^\dagger(t) H_{Tn}(t') H_{Tn'}(0) \rangle \\
&= |t_0|^4 \sum_s \langle \psi_{ns}(t-t'') \psi_{ns}^\dagger(0) \rangle \langle \psi_{m-s}(t-t') \psi_{m-s}^\dagger(0) \rangle \\
&\quad \times \langle \Psi_s^\dagger(\mathbf{r}_n, t-t'') \Psi_{-s}^\dagger(\mathbf{r}_m, t) \Psi_{-s}(\mathbf{r}_m, t') \Psi_s(\mathbf{r}_n, 0) \rangle \\
&- |t_0|^4 \sum_{\substack{s \\ n \neq m}} \langle \psi_{m-s}(t-t'-t'') \psi_{m-s}^\dagger(0) \rangle \langle \psi_{ns}(t) \psi_{ns}^\dagger(0) \rangle \\
&\quad \times \langle \Psi_{-s}^\dagger(\mathbf{r}_m, t-t'') \Psi_s^\dagger(\mathbf{r}_n, t) \Psi_{-s}(\mathbf{r}_m, t') \Psi_s(\mathbf{r}_n, 0) \rangle. \quad (2.62)
\end{aligned}$$

The four-point correlation functions of the superconductor are calculated by Fourier decomposing $\Psi_s(\mathbf{r}_n, t) = V^{-1/2} \sum_{\mathbf{k}} (u_{\mathbf{k}s} \gamma_{\mathbf{k}s} e^{-iE_{\mathbf{k}}t} + v_{\mathbf{k}s} \gamma_{-\mathbf{k}-s}^\dagger e^{iE_{\mathbf{k}}t}) e^{i\mathbf{k}\mathbf{r}_n}$,

with $u_{\mathbf{k}s} = u_{\mathbf{k}}$, and $v_{\mathbf{k}\uparrow} = -v_{\mathbf{k}\downarrow} = v_{\mathbf{k}}$. For the first correlation function in Eq. (2.62) we then obtain

$$\begin{aligned}
& V^2 \langle \Psi_s^\dagger(\mathbf{r}_n, t - t'') \Psi_{-s}^\dagger(\mathbf{r}_m, t) \Psi_{-s}(\mathbf{r}_m, t') \Psi_s(\mathbf{r}_n, 0) \rangle \\
&= \sum_{\mathbf{k}\mathbf{k}'} u_{\mathbf{k}} v_{\mathbf{k}} u_{\mathbf{k}'} v_{\mathbf{k}'} e^{-i(E_{\mathbf{k}}t' - E_{\mathbf{k}'}t'' - (\mathbf{k} + \mathbf{k}')\delta\mathbf{r})} \\
&+ \sum_{\mathbf{k}\mathbf{k}'} (v_{\mathbf{k}} v_{\mathbf{k}'})^2 e^{-i(E_{\mathbf{k}}(t - t'') + E_{\mathbf{k}'}(t - t'))}, \tag{2.63}
\end{aligned}$$

where $\delta\mathbf{r} = \mathbf{r}_1 - \mathbf{r}_2$ is the distance vector between the two tunneling points in the superconductor. The first sum in Eq. (2.63) describes the (time-dependent) correlation of creating and annihilating a quasiparticle (with same spin), whereas the second term in Eq. (2.63) describes correlation of creating *two* quasiparticles (with different spin). It is obvious that the second term describes processes which involve final states $|f\rangle$ in the T-matrix element $\langle f|T(\varepsilon_i)|i\rangle$ that contain two excitations in the superconductor and, therefore, does not describe an Andreev process. In the regime $\Delta > \delta\mu$ such a process is not allowed by energy conservation. We will see this explicitly by calculating the integral over t which originates from the Fourier representation of the δ -function present in the rate W_{fi} . Similarly, for the correlator $\langle \Psi_{-s}^\dagger(\mathbf{r}_m, t - t'') \Psi_s^\dagger(\mathbf{r}_n, t) \Psi_{-s}(\mathbf{r}_m, t') \Psi_s(\mathbf{r}_n, 0) \rangle$ in Eq. (2.62) we obtain Eq. (2.63) with a minus sign, and we have to replace $t - t''$ by $t - t' - t''$, and $t - t'$ by t , in the second term of Eq. (2.63).

To evaluate the Luttinger liquid correlation functions in Eq. (2.62), we decompose the phase fields $\phi_{n\nu}(x, t)$ and $\theta_{n\nu}(x, t)$ into a sum over the spin and charge bosons (see also Appendix C),

$$\begin{aligned}
\theta_{n\nu}(x, t) &= - \sum_p \text{sgn}(p) \sqrt{\frac{\pi}{2LK_\nu|p|}} e^{ipx} e^{-\alpha|p|/2} \\
&\times (b_{n\nu p} e^{-iu_\nu|p|t} - b_{n\nu-p}^\dagger e^{iu_\nu|p|t}), \tag{2.64}
\end{aligned}$$

and

$$\begin{aligned}
\phi_{n\nu}(x, t) &= \sum_p \sqrt{\frac{\pi K_\nu}{2L|p|}} e^{ipx} e^{-\alpha|p|/2} \\
&\times (b_{n\nu p} e^{-iu_\nu|p|t} + b_{n\nu-p}^\dagger e^{iu_\nu|p|t}). \tag{2.65}
\end{aligned}$$

The spin and charge bosons satisfy Bose commutation relations, in particular $[b_{n\nu p}, b_{n'\nu'p'}^\dagger] = \delta_{rr'}$, where $r \equiv n\nu p$, and the ground state of the Luttinger liquid is defined as $b_{n\nu p}|0\rangle_{LL} = 0$. The Hamiltonian Eq. (2.55) can then be written in terms of the b -operators as (see Appendix C)

$$K_{Ln} = \sum_{\nu p} u_\nu |p| b_{n\nu p}^\dagger b_{n\nu p}, \quad (2.66)$$

where we have subtracted the zero-point energy coming from the filled Dirac sea of negative-energy particle states. In all p -sums we will explicitly exclude $p = 0$ as discussed in Subsection 2.3.5 and explained in more detail in Appendix C. To account for the p -dependence of the interaction, we apply a high momentum-transfer cut-off Λ on the order of $1/p_F$ so that $K_\nu(p) = K_\nu$, $u_\nu(p) = u_\nu$ for $|p| < 1/\Lambda$, and $K_\nu(p) = 1$, $u_\nu(p) = v_F$ for $|p| > 1/\Lambda$. By writing $\psi_{n sr}(x, t) = (2\pi\alpha)^{-1/2} \eta_{r, ns} e^{i\Phi_{n sr}(x, t)}$ with $r = \pm$ and $\Phi_{n sr}$ defined according to Eq. (2.56), we can represent the single-particle Luttinger liquid correlation function as $\langle \psi_{n sr}(x, t) \psi_{n sr}^\dagger(0, 0) \rangle \equiv G_{n rs}^1(x, t)$ with

$$G_{n rs}^1(x, t) = (2\pi\alpha)^{-1} e^{(\Phi_{n sr}(x, t)\Phi_{n sr}(0, 0) - (\Phi_{n sr}^2(x, t) + \Phi_{n rs}^2(0, 0))/2)}. \quad (2.67)$$

This follows from the fact that $\Phi_{n sr}(x, t)$ is a linear combination of creation and annihilation operators $b_{n\nu p}^\dagger$ and $b_{n\nu p}$, respectively¹². By evaluating the averages in the exponent as outlined in Appendix D we obtain [95–98]

$$G_{n rs}^1(x, t) = \frac{1}{2\pi} \lim_{\alpha \rightarrow 0} \frac{\Lambda + i(v_F t - rx)}{\alpha + i(v_F t - rx)} \times \prod_{\nu=\rho, \sigma} \frac{1}{\sqrt{\Lambda + i(u_\nu t - rx)}} \left[\frac{\Lambda^2}{(\Lambda + iu_\nu t)^2 + x^2} \right]^{\gamma_\nu/2}, \quad (2.68)$$

where $\gamma_\nu = (K_\nu + K_\nu^{-1})/4 - 1/2 > 0$ is an interaction dependent parameter which describes the power law decay of the long time and long distance correlations. The factor containing the Fermi velocity v_F in Eq. (2.68) is only important if one is interested in x, t satisfying $|v_F t - rx| < \Lambda$ and is a result of including the p -dependence of the interaction parameters K_ν and u_ν (see Appendix D). The Luttinger liquid correlation function Eq. (2.68) has singular points as a function of time in the upper complex plane. It is now clear

¹²Eq. (2.67) is obtained by using the identities $e^A e^B = e^{A+B} e^{[A, B]/2}$ and $\langle e^A \rangle = e^{\langle A^2 \rangle/2}$ for A and B linear in Bose creation and annihilation operators.

that the integration over t is only nonzero if the phase of $e^{i\omega t}$ in Eq. (2.61) is positive, i.e. $\omega > 0$. Since the phases of the terms containing $(v_{\mathbf{k}})^2$ in Eq. (2.63) depend also on t , the requirement for a nonzero contribution to the current from these terms requires $2\delta\mu - E_{\mathbf{k}} - E_{\mathbf{k}'} > 0$. This, however, is excluded in our regime of interest, since $E_{\mathbf{k}} + E_{\mathbf{k}'} \geq 2\Delta$, and therefore, we will not consider these terms any further in what follows¹³. In our model the electrons tunnel into the same point x_n in Luttinger liquid n , i.e. $x = 0$ in Eq. (2.68). In addition, Luttinger liquid 1 and 2 are assumed to be similar. In this case the single-particle correlation function does not depend on n and r , i.e. $G_{nrs}^1(x = 0, t) \equiv G^1(t)$, and the current I_1 can then be written as

$$\begin{aligned}
I_1 &= (32e |t_0|^4 / V^2) \\
&\times \lim_{\eta \rightarrow 0^+} \int_{-\infty}^{\infty} dt \int_0^{\infty} dt' \int_0^{\infty} dt'' e^{-\eta(t'+t'')+i(2t-t'-t'')\delta\mu} \\
&\times \sum_{\mathbf{k}\mathbf{k}'} u_{\mathbf{k}} v_{\mathbf{k}} u_{\mathbf{k}'} v_{\mathbf{k}'} e^{-i(E_{\mathbf{k}}t' - E_{\mathbf{k}'}t'' - (\mathbf{k}+\mathbf{k}')\delta\mathbf{r})} \\
&\times \{G^1(t-t'')G^1(t-t') + G^1(t-t'-t'')G^1(t)\}. \quad (2.69)
\end{aligned}$$

We evaluate Eq. (2.69) in leading order in the small parameter $\delta\mu/\Delta$, and remark that the delay times t' and t'' are restricted to $t', t'' \lesssim 1/\Delta$. This becomes clear if we set $\delta\mathbf{r} = 0$ and express the contribution in Eq. (2.69) containing the dynamics of the superconductor as

$$\begin{aligned}
&\sum_{\mathbf{k}\mathbf{k}'} u_{\mathbf{k}} v_{\mathbf{k}} u_{\mathbf{k}'} v_{\mathbf{k}'} e^{-i(E_{\mathbf{k}}t' - E_{\mathbf{k}'}t'')} \\
&= (\pi\nu_S\Delta/2)^2 H_0^{(1)}(t''\Delta) H_0^{(2)}(t'\Delta), \quad (2.70)
\end{aligned}$$

where $H_0^{(1)}$ and $H_0^{(2)}$ are Hankel functions of the first and second kind, and ν_S is the energy DOS per spin in the superconductor at μ_S . For times $t', t'' > 1/\Delta$, the Hankel functions are rapidly oscillating, since for large x we have $H_0^{(1/2)}(x) \sim \sqrt{2/\pi x} \exp(\pm(ix - (\pi/4)))$. In contrast, the time-dependent phase in Eq. (2.69) containing the bias $\delta\mu$ suppresses the integrand in Eq. (2.69) only for times $|2t - t' - t''| > 1/\delta\mu > 1/\Delta$. Being interested only

¹³We remark that for $r \neq r'$, the correlation function $\langle \psi_{n,sr}(x, t) \psi_{n,sr'}^\dagger(0, 0) \rangle$ gives a negligible contribution in the thermodynamic limit. This statement is also true for a finite size Luttinger liquid as long as the interaction preserves the total number of right- and left-movers.

in the leading order in $\delta\mu/\Delta$, we can assume that $|t| > t', t''$ in the current formula Eq. (2.69), since the Luttinger liquid correlation functions are slowly decaying in time with the main contribution (in the integral) coming from large times $|t|$. In addition, since $1/\delta\mu > \Lambda/v_F$, we can neglect the term containing the Fermi velocity v_F in Eq. (2.68).

To test the validity of our approximations we first consider the non-interacting limit with $K_\nu = 1$ and $u_\nu = v_F$, for which an analytic expression is also available for higher order terms in $\delta\mu/\Delta$.

Noninteracting limit for current I_1

Let us first consider a one-dimensional (1D) Fermi gas (i.e. $K_\nu = 1$ and $u_\nu = v_F$), and evaluate the integral over t in Eq. (2.69) in the non-interacting limit. The Luttinger liquid-correlation functions simplify to $G^1(t) = (1/2\pi) \lim_{\alpha \rightarrow 0} 1/(\alpha + iv_F t)$, and we are left with the integral

$$\begin{aligned} & \int_{-\infty}^{\infty} dt e^{i2\delta\mu t} \{G^1(t-t'')G^1(t-t') + G^1(t-t'-t'')G^1(t)\} \\ &= \left(\frac{1}{2\pi}\right)^2 \int_{-\infty}^{\infty} dt e^{i2\delta\mu t} \left\{ \frac{1}{(\alpha + iv_F(t-t''))(\alpha + iv_F(t-t'))} \right. \\ & \quad \left. + \frac{1}{(\alpha + iv_F(t-t'-t''))(\alpha + iv_F t)} \right\} \Big|_{\alpha \rightarrow 0} \end{aligned} \quad (2.71)$$

which can be evaluated by closing the integration contour in the upper complex plane. Inserting then the result into Eq. (2.69) we obtain for the non-interacting limit I_1^0

$$\begin{aligned} I_1^0 &= (32e|t_0|^4/V^2) \lim_{\eta \rightarrow 0^+} \int_0^{\infty} dt' \int_0^{\infty} dt'' e^{-\eta(t'+t'')} \\ & \times \sum_{\mathbf{k}\mathbf{k}'} u_{\mathbf{k}} v_{\mathbf{k}} u_{\mathbf{k}'} v_{\mathbf{k}'} e^{-i(E_{\mathbf{k}} t' - E_{\mathbf{k}'} t'' - (\mathbf{k} + \mathbf{k}') \delta \mathbf{r})} \\ & \times \frac{1}{\pi v_F^2} \left\{ \frac{\sin[(t'' - t')\delta\mu]}{t'' - t'} + \frac{\sin[(t' + t'')\delta\mu]}{t' + t''} \right\}. \end{aligned} \quad (2.72)$$

The sine-functions in Eq. (2.72) can be expanded in powers of $\delta\mu$, and for $\delta\mu < \Delta$ it is sufficient to keep just the leading order term in $\delta\mu$ since the integrals over t', t'' have the form

$$\int_0^{\infty} dt e^{-(\eta \pm iE_{\mathbf{k}})t} t^n = \frac{n!}{(\eta \pm iE_{\mathbf{k}})^{n+1}}, \quad (2.73)$$

where $n = 1, 2, 3 \dots$. Since $E_{\mathbf{k}} \geq \Delta$, higher powers in t', t'' produce higher powers in $\delta\mu/\Delta$, and, as expected, we can therefore ignore the dependence on t', t'' in the Luttinger liquid-correlation functions. In contrast to this, when we consider the current for tunneling of two electrons into the same (interacting) Luttinger liquid-lead, we will see that the two-particle correlation function will not allow for such a simplification. In leading order in $\delta\mu/\Delta$, the integrals over t', t'' are evaluated according to Eq. (2.73) with $n = 0$, and we get an (effective) momentum-sum for the superconductor-correlations $(\sum_{\mathbf{k}} (u_{\mathbf{k}}v_{\mathbf{k}}/E_{\mathbf{k}}) \cos(\mathbf{k} \cdot \delta\mathbf{r}))^2$, which we also found in the quantum dot entangler setup. There we found (see Eq. (2.16))

$$\sum_{\mathbf{k}} \frac{u_{\mathbf{k}}v_{\mathbf{k}}}{E_{\mathbf{k}}} \cos(\mathbf{k} \cdot \delta\mathbf{r}) = \frac{\pi}{2} \nu_S \frac{\sin(k_F \delta r)}{k_F \delta r} e^{-(\delta r/\pi\xi)}. \quad (2.74)$$

In Eq. (2.74) we have introduced the coherence length of a Cooper pair in the superconductor, $\xi = v_F/\pi\Delta$ and $\delta r = |\delta\mathbf{r}|$. We finally obtain I_1^0 , the current I_1 in the non-interacting limit,

$$I_1^0 = e\pi\gamma^2\delta\mu \left[\frac{\sin(k_F\delta r)}{k_F\delta r} \right]^2 \exp\left(-\frac{2\delta r}{\pi\xi}\right). \quad (2.75)$$

Here, we have defined $\gamma = 4\pi\nu_S\nu_l|t_0|^2/LV$, which is the dimensionless conductance per spin in a tunneling event from the superconductor to the Luttinger liquid leads. The non-interacting DOS of the Luttinger liquid per spin ν_l is given by $\nu_l = L/\pi v_F$. We remark in passing that the result Eq. (2.75) agrees with a T-matrix calculation in the energy domain [99]. In this case we sum explicitly over the final states, given by a singlet $|f\rangle = (1/\sqrt{2})(a_{1p\uparrow}^\dagger a_{2q\downarrow}^\dagger - a_{1p\downarrow}^\dagger a_{2q\uparrow}^\dagger)|i\rangle$, where the a -operators describe electrons in a (non-interacting) 1D Fermi gas. Note that triplet states are excluded as final states since our Hamiltonian H does not change the total spin which can be checked explicitly in analogy to Section 2.2. We see that the current I_1^0 gets exponentially suppressed on the scale of ξ , if the tunneling of the two (coherent) electrons takes place from different points \mathbf{r}_1 and \mathbf{r}_2 of the superconductor. For conventional s-wave superconductors the coherence length ξ

is typically on the order of micrometers (see e.g. Ref. [78]) and therefore this poses not severe experimental restrictions. This suppression of I_1^0 caused by the superconductor correlations is the same as appears in the entangler with quantum dots, see formula Eq. (2.24). We therefore refer to Subsection 2.2.6 for further details and remark here only that the power-law suppression in $k_F \delta r$ is crucially dependent on the effective dimension of the superconductor with smoother powers in lower dimensions. Approximately we obtain that $I_1^0 \propto (1/k_F \delta r)^{d-1}$ for large $k_F \delta r$ where d is the effective dimension of the superconductor, see Eqs. (2.35) and (2.36).

Current I_1 including interaction

We now are ready to treat the interacting case. Having obtained confidence in our approximation schemes from the non-interacting case above, we can neglect now the t', t'' dependence of the Luttinger liquid correlation function appearing in Eq. (2.69), valid in leading order in $\delta\mu/\Delta$. In this limit the t -integral considerably simplifies to

$$\begin{aligned} & (2\pi)^2 \int_{-\infty}^{\infty} dt e^{i(2t-t'-t'')\delta\mu} \{G^1(t-t'')G^1(t-t') \\ & \quad + G^1(t-t'-t'')G^1(t)\} \\ & \simeq \frac{2\Lambda^{2(\gamma_\rho+\gamma_\sigma)}}{\prod_{\nu=\rho,\sigma} u_\nu^{2\gamma_\nu+1}} \int_{-\infty}^{\infty} dt \frac{e^{i2\delta\mu t}}{\prod_{\nu=\rho,\sigma} ((\Lambda/u_\nu) + it)^{2\gamma_\nu+1}}. \end{aligned} \quad (2.76)$$

An analytical expression for this integral is available [100], and given in Appendix E. The treatment of the remaining integrals over t', t'' and the calculation of the Andreev contribution is the same as in the non-interacting case and we obtain for the current I_1 , in leading order in $\delta\mu/\Delta$ and in the small parameters $2\Lambda\delta\mu/u_\nu$,

$$I_1 = \frac{I_1^0}{\Gamma(2\gamma_\rho + 2)} \frac{v_F}{u_\rho} \left[\frac{2\delta\mu}{u_\rho/\Lambda} \right]^{2\gamma_\rho}. \quad (2.77)$$

In Eq. (2.77) we used $K_\sigma = 1$ and $u_\sigma = v_F$. The interaction suppresses the current considerably and the bias dependence has its characteristic nonlinear form, $I_1 \propto (\delta\mu)^{2\gamma_\rho+1}$, with an interaction dependent exponent $2\gamma_\rho + 1$. The

parameter γ_ρ is the exponent for tunneling into the bulk of a single Luttinger liquid [93], i.e. $\rho(\varepsilon) \simeq \varepsilon^{\gamma_\rho}$, where $\rho(\varepsilon)$ is the single-particle tunneling-DOS, defined in Subsection 2.3.1. Note that the current I_1 does not show a dependence on the correlation time $1/\Delta$, which is a measure for the time separation between the two electron tunneling-events. This is so since the two partners of a Cooper pair tunnel to *different* Luttinger liquid leads with no interaction-induced correlations between the leads.

2.3.7 Current for tunneling into the same lead

The main new feature for the case where two electrons, originating from an Andreev process, tunnel into the same lead, is that now the four-point correlation function of the Luttinger liquid no longer factorizes as was the case before when the two electrons tunnel into different leads [see Eq. (2.62)]. In addition, the two electrons will tunnel into the lead preferably from the same spatial point on the superconductor, i.e. $\delta r = 0$. We denote by I_2 the current for coherent transport of two electrons into the *same* lead, either lead 1 *or* lead 2. It can be written in a similar way as I_1 given in Eq. (2.61) with the difference that now we consider final states with two additional electrons (of opposite spin) in the same lead (either 1 or 2) compared to the initial state. We then obtain for I_2 ,

$$I_2 = 4e \lim_{\eta \rightarrow 0^+} \sum_{s,s'} \int_{-\infty}^{\infty} dt \int_0^{\infty} dt' \int_0^{\infty} dt'' e^{-\eta(t'+t'')+i(2t-t'-t'')\delta\mu} \times \langle H_{Tn-s'}^\dagger(t-t'') H_{Tns'}^\dagger(t) H_{Tn-s}(t') H_{Tns}(0) \rangle, \quad (2.78)$$

where we have used that the leads 1 and 2 are identical which results in an additional factor of two. Again, the thermal average is to be taken at $T = 0$, and this ground state expectation value factorizes into a superconductor part times a Luttinger liquid part. However, the Luttinger liquid part does not factorize anymore due to strong correlations between the two tunneling

electrons. In this case we obtain

$$\begin{aligned}
& \sum_{s,s'} \langle H_{Tn-s'}^\dagger(t-t'')H_{Tns'}^\dagger(t)H_{Tn-s}(t')H_{Tns}(0) \rangle \\
&= |t_0|^4 \sum_s \langle \psi_{ns}(t-t'')\psi_{n-s}(t)\psi_{n-s}^\dagger(t')\psi_{ns}^\dagger(0) \rangle \\
&\quad \times \langle \Psi_s^\dagger(\mathbf{r}_n, t-t'')\Psi_{-s}^\dagger(\mathbf{r}_n, t)\Psi_{-s}(\mathbf{r}_n, t')\Psi_s(\mathbf{r}_n, 0) \rangle \\
&+ |t_0|^4 \sum_s \langle \psi_{n-s}(t-t'')\psi_{ns}(t)\psi_{n-s}^\dagger(t')\psi_{ns}^\dagger(0) \rangle \\
&\quad \times \langle \Psi_{-s}^\dagger(\mathbf{r}_n, t-t'')\Psi_s^\dagger(\mathbf{r}_n, t)\Psi_{-s}(\mathbf{r}_n, t')\Psi_s(\mathbf{r}_n, 0) \rangle. \tag{2.79}
\end{aligned}$$

The four-point correlation functions for the superconductor in Eq. (2.79) are the same as in Eq. (2.62) for the case when the two electrons tunnel into different leads, except that now $\delta\mathbf{r} = 0$. The four-point correlation functions in Eq. (2.79) for the Luttinger liquid, normalized to the product of two single-particle correlation functions (given in Eq. (2.68)), are

$$\begin{aligned}
G_{rr'1}^2(t, t', t'') &\equiv \langle \psi_{nrs}(t-t'')\psi_{nr'-s}(t)\psi_{nr'-s}^\dagger(t')\psi_{nrs}^\dagger(0) \rangle / \\
&\quad \langle \psi_{nrs}(t-t'')\psi_{nrs}^\dagger(0) \rangle \langle \psi_{nr'-s}(t-t')\psi_{nr'-s}^\dagger(0) \rangle, \tag{2.80}
\end{aligned}$$

which can be calculated using similar methods as described above for the single-particle correlation function. After some calculation outlined in Appendix D we obtain

$$\begin{aligned}
& G_{rr'1}^2(t, t', t'') = \\
& \prod_{\nu=\rho,\sigma} \left(\frac{\Lambda - iu_\nu t''}{\Lambda + iu_\nu(t-t'-t'')} \right)^{\lambda_{\nu rr'}} \left(\frac{\Lambda + iu_\nu t'}{\Lambda + iu_\nu t} \right)^{\lambda_{\nu rr'}}. \tag{2.81}
\end{aligned}$$

where $\lambda_{\nu rr'} = \xi_\nu(rr'K_\nu + (1/K_\nu))/4$ with $\xi_{\rho/\sigma} = \pm 1$. For the other sequence

$$\begin{aligned}
G_{rr'2}^2 &\equiv \langle \psi_{nr'-s}(t-t'')\psi_{nrs}(t)\psi_{nr'-s}^\dagger(t')\psi_{nrs}^\dagger(0) \rangle / \\
&\quad \langle \psi_{nr'-s}(t-t'-t'')\psi_{nr'-s}^\dagger(0) \rangle \langle \psi_{nrs}(t)\psi_{nrs}^\dagger(0) \rangle, \tag{2.82}
\end{aligned}$$

we obtain

$$G_{rr'2}^2(t, t', t'') = - \prod_{\nu=\rho, \sigma} \left(\frac{\Lambda - iu_\nu t''}{\Lambda + iu_\nu(t - t'')} \right)^{\lambda_{\nu rr'}} \left(\frac{\Lambda + iu_\nu t'}{\Lambda + iu_\nu(t - t')} \right)^{\lambda_{\nu rr'}}. \quad (2.83)$$

We remark that contributions from other combinations of left- and right-movers, as indicated in Eqs. (2.81) and (2.83), are negligible. A contribution like $\langle \psi_{nr's}(t - t'') \psi_{nr-s}(t) \psi_{nr'-s}^\dagger(t') \psi_{nr's}^\dagger(0) \rangle_{r \neq r'}$ is only non-zero if spin exchange between right- and left-movers is possible, but this is a backscattering process which we explicitly exclude. Using Eqs. (2.78)-(2.83), together with Eq. (2.70) we obtain a formal expression for I_2 (with $\delta r = 0$):

$$\begin{aligned} I_2 &= 4e \left(\frac{\pi \nu_S \Delta |t_0|^2}{V} \right)^2 \lim_{\eta \rightarrow 0^+} \sum_{b=\pm 1} \int_{-\infty}^{\infty} dt \int_0^{\infty} dt' \int_0^{\infty} dt'' e^{-\eta(t'+t'')} \\ &\times e^{i(2t-t'-t'')\delta\mu} H_0^{(1)}(t''\Delta) H_0^{(2)}(t'\Delta) \\ &\times [G_{b1}^2(t, t', t'') G^1(t - t'') G^1(t - t') - G_{b2}^2(t, t', t'') G^1(t - t' - t'') G^1(t)]. \end{aligned} \quad (2.84)$$

In Eq. (2.84) the meaning of the summation index is $b \equiv +1$ for $rr' = +1$, and $b \equiv -1$ for $rr' = -1$. We proceed to evaluate the current I_2 with $K_\sigma = 1$ and $u_\sigma = v_F$. To calculate the current I_2 we assume that the time scales Λ/u_ρ and Λ/v_F are the smallest ones in the problem. These time scales are both on the order of the inverse Fermi energy in the Luttinger liquid, which is larger than the energy gap Δ and the bias $\delta\mu$. By applying the same arguments as in Subsection 2.3.6 for the current I_1 , we approximate the current I_2 , assuming $|t| > t', t'' > \Lambda/v_F, \Lambda/u_\rho$, which is accurate in leading order in the small parameters $\delta\mu/\Delta$, $\Lambda\Delta/u_\nu$ and $\Lambda\delta\mu/u_\nu$. In this limit we obtain for the two-particle correlation functions

$$G_{rr'1}^2 = -G_{rr'2}^2 = \frac{(t't'')^{\gamma_{\rho rr'}}}{((\Lambda/u_\rho) + it)^{2\lambda_{\rho rr'}} ((\Lambda/v_F) + it)^{-(1+rr')/2}}, \quad (2.85)$$

where $\gamma_{\rho rr'} = ((1/K_\rho) + rr'K_\rho - (1+rr'))/4 > 0$. The exponent $\gamma_{\rho rr'}$ is related to γ_ρ , introduced in the single-particle correlation function [Eq. (2.68)] via

$\gamma_{\rho r r'} = \gamma_\rho$ for $r = r'$, and $\gamma_{\rho r r'} = \gamma_\rho + (1 - K_\rho)/2$ for $r \neq r'$. The current I_2 for tunneling of two electrons into the *same* lead 1 or 2 then becomes (with $\delta r = 0$)

$$\begin{aligned}
I_2 &= 2e \left(\frac{2\pi\nu_S\Delta|t_0|^2}{V} \right)^2 \frac{\Lambda^{2\gamma_\rho}}{u_\rho^{2\gamma_\rho+1}v_F} \\
&\times \lim_{\eta \rightarrow 0^+} \sum_{b=\pm 1} \int_0^\infty dt' \int_0^\infty dt'' e^{-\eta(t'+t'')} (t't'')^{\gamma_{\rho b}} \\
&\times H_0^{(1)}(t''\Delta) H_0^{(2)}(t'\Delta) \frac{1}{(2\pi)^2} \int_{-\infty}^\infty dt \\
&\times \frac{e^{i2\delta\mu t}}{\left(\frac{\Lambda}{u_\rho} + it\right)^{2\lambda_{\rho b}+2\gamma_\rho+1} \left(\frac{\Lambda}{v_F} + it\right)^{(1-b)/2}}.
\end{aligned} \tag{2.86}$$

Again, the integrals appearing in Eq. (2.86) can be evaluated analytically [100] with the results given in Appendix E.

Note that according to the two-particle Luttinger liquid-correlation functions [Eqs. (2.81) and (2.83)], we find that the dynamics coming from the delay times t' and t'' cannot be neglected anymore, as was done e.g. in Ref. [94].

We evaluate Eq. (2.86) in leading order in $2\delta\mu\Lambda/u_\nu$ and finally obtain for the current I_2

$$I_2 = I_1 \sum_{b=\pm 1} A_b \left(\frac{2\delta\mu}{\Delta} \right)^{2\gamma_{\rho b}}. \tag{2.87}$$

The interaction dependent constant A_b in Eq. (2.87) is given by

$$A_b = \frac{2^{2\gamma_{\rho b}-1}}{\pi^2} \frac{\Gamma(2\gamma_\rho + 2)}{\Gamma(2\gamma_{\rho b} + 2\gamma_\rho + 2)} \Gamma^4 \left(\frac{\gamma_{\rho b} + 1}{2} \right), \tag{2.88}$$

which is decreasing when interactions in the leads are increased, see Fig. 2.9. The function $\Gamma(x)$ is the Gamma function. We remark that in Eq. (2.87) the current I_1 is given by Eq. (2.77) with $\delta r = 0$. The non-interacting limit, $I_2 = I_1 = I_1^0$, is recovered by putting $\gamma_\rho = \gamma_{\rho b} = 0$, and $u_\rho = v_F$. The result for I_2 shows that the unwanted injection of two electrons into the same lead is suppressed compared to I_1 by a factor of $A_+(2\delta\mu/\Delta)^{2\gamma_{\rho+}}$ if both electrons

are injected into the same branch (left or right movers), or by $A_-(2\delta\mu/\Delta)^{2\gamma_{\rho-}}$ if the two electrons travel in different directions. Since it holds that $\gamma_{\rho-} = \gamma_{\rho+} + (1 - K_\rho)/2 > \gamma_{\rho+}$, it is more favorable that two electrons travel in the same direction than in opposite directions. The suppression of the current I_2

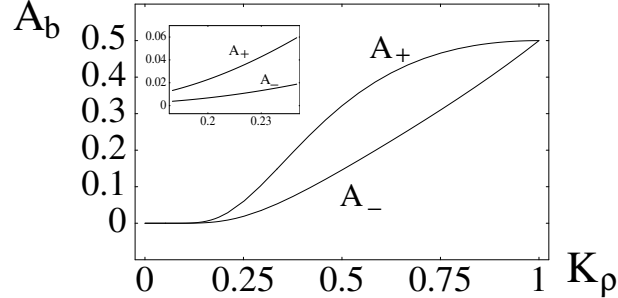


Figure 2.9: The interaction dependent constants A_+ and A_- as given in Eq. (2.88) plotted against the interaction strength K_ρ . For a strong interaction parameter $K_\rho \ll 1$ we obtain a sizable suppression of I_2 also due to this prefactor A_\pm . Note that $A_+ > A_-$.

by $1/\Delta$ shows very nicely the two-particle correlation effect for the coherent tunneling of two electrons into the same lead. The larger Δ is, the shorter the delay time between the arrivals of the two partner electrons of a given Cooper pair, and, in turn, the more the second electron will be influenced by the presence of the first one already in the Luttinger liquid. By increasing the bias $\delta\mu$ the electrons can tunnel faster through the barrier due to more channels becoming available into which the electron can tunnel, and therefore the suppression effect of Δ is less pronounced. Also note that this correlation effect disappears when interactions are absent in the Luttinger liquid ($\gamma_\rho = \gamma_{\rho b} = 0$).

2.3.8 Efficiency and discussion

We have established that there indeed exists a suppression for tunneling of two spin-entangled electrons into the same Luttinger liquid lead compared to the desired process where the two electrons tunnel into different leads. However, we have to take into account that the process into different leads suffers a suppression due to a finite distance separation δr between the two tunneling points on the superconductor. As already discussed earlier in this

This (see Subsection 2.2.6) this suppression can be considerably reduced if one uses effectively low-dimensional superconductors. To estimate the efficiency of the entangler we form the ratio I_1/I_2 and demand that it is larger than one. This requirement is fulfilled if approximately

$$A_+ \left(\frac{2\delta\mu}{\Delta} \right)^{2\gamma_{\rho+}} < 1/(k_F\delta r)^{d-1}, \quad (2.89)$$

where d is the dimension of the superconductor, and it is assumed that the coherence length ξ of the superconductor is large compared to δr . The leading term of I_2 is proportional to $(2\delta\mu/\Delta)^{2\gamma_{\rho+}}$ describing the power-law suppression, with exponent $2\gamma_{\rho+} = 2\gamma_{\rho}$, of the process where two electrons, entering the same lead, will propagate in the same direction. The exponent $\gamma_{\rho+}$ is the exponent for the single-particle tunneling-DOS from a metal into the center (bulk) of a Luttinger liquid.

Experimentally accessible systems which exhibit Luttinger liquid-behavior are e.g. metallic carbon nanotubes. It was pointed out in Refs. [91, 92] that the long range part of the Coulomb interaction, which is dominated by forward scattering events with small momentum transfer, can lead to Luttinger liquid behavior in carbon nanotubes with very small values of $K_{\rho} \simeq 0.2 - 0.3$, as measured experimentally in Refs. [88, 101] and predicted theoretically in Ref. [92]. This would correspond to an exponent $2\gamma_{\rho} \simeq 0.8 - 1.6$, which seems very promising. We also remark that in this scenario of small K_{ρ} the interaction dependent constants A_b also become much smaller than unity, see Fig. 2.9. For $K_{\rho} = 0.3$ we obtain from Eq. (2.88) that $A_+ \simeq 0.11$ and for $K_{\rho} = 0.2$ we get $A_+ \simeq 0.02$ (note that $A_- < A_+$).

In addition, single-wall carbon nanotubes show similar tunneling exponents as derived here. The tunneling-DOS for a single-wall carbon nanotube is predicted [91, 92] to be $\rho(\varepsilon) \propto \varepsilon^{\eta}$ with $\eta = (K_{\rho}^{-1} + K_{\rho} - 2)/8$, which is half of γ_{ρ} , and was measured [88, 101] to be $\simeq 0.3 - 0.4$. Similar values were found also in multiwall carbon nanotubes [102]. More recently, Luttinger liquid behavior was found also in GaAs quantum wires [89] with Luttinger liquid parameter $K_{\rho} \simeq 0.66 - 0.82$.

The results presented in this section show again that the delay time between the two electrons of the same pair $\sim \hbar/\Delta$ is much shorter than the average time between subsequent pairs $\sim 2e/I_1$. The correlation time τ_c of a pair (introduced in Subsection 2.2.6) which is important for current-current correlation measurements to detect entanglement, is given here by

$\hbar/\delta\mu$, since the bias voltage determines the energy range within the electrons are injected into the Luttinger liquids. The requirement $2e/I_1 > \tau_c$ is therefore also satisfied here due to weak tunneling and strong correlations, see Eq. (2.77).

2.3.9 Decay of the electron-singlet due to interactions

We have shown in the preceding subsections that interaction in a Luttinger liquid lead can help to separate two spin-entangled electrons so that the two electrons enter *different* leads. A natural question then arises: what is the lifetime of a (nonlocal) spin-singlet state formed of two electrons which are injected into different Luttinger liquid leads, one electron per lead? To address this issue we introduce the following correlation function

$$P(\mathbf{r}, t) = |\langle S(\mathbf{r}, t) | S(0, 0) \rangle|^2. \quad (2.90)$$

This function is the probability density that an electronic singlet state, injected at point $\mathbf{r} \equiv (x_1, x_2) = 0$ and at time $t = 0$, is found at some later time t and at point \mathbf{r} . Therefore, $P(\mathbf{r}, t)$ is a measure of how much of the initial singlet state remains after the two injected electrons have interacted with all the other electrons in the Luttinger liquid during the time interval t . Here,

$$|S(\mathbf{r}, t)\rangle = \sqrt{\pi\alpha} (\psi_{1\uparrow}^\dagger(x_1, t)\psi_{2\downarrow}^\dagger(x_2, t) - \psi_{1\downarrow}^\dagger(x_1, t)\psi_{2\uparrow}^\dagger(x_2, t))|0\rangle \quad (2.91)$$

is the electron singlet state created on top of the Luttinger liquid ground states. The extra normalization factor $\sqrt{2\pi\alpha}$ is introduced to guarantee $\int d\mathbf{r} P(\mathbf{r}, t) = 1$ in the non-interacting limit and corresponds to the replacement of ψ_{ns} by $(2\pi\alpha)^{1/4}\psi_{ns}$. The singlet-singlet correlation function factorizes into two single-particle Green's functions due to negligible interaction between the leads 1 and 2. Therefore, we have $P(\mathbf{r}, t) = (2\pi\alpha)^2 \prod_n |\langle \psi_{ns}(x_n, t) \times \psi_{ns}^\dagger(0, 0) \rangle|^2$, with $\langle \psi_{ns}(x_n, t)\psi_{ns}^\dagger(0, 0) \rangle = \sum_{r=\pm} e^{ik_F r x_n} G_{nr}^1(x_n, t)$. For simplicity we just study the slow spatial variations of $|\langle \psi_{ns}(x_n, t)\psi_{ns}^\dagger(0, 0) \rangle|^2$. Using Eq. (2.68) together with $\pi\delta(x) = \lim_{\alpha \rightarrow 0} \alpha/(\alpha^2 + x^2)$ we can then write the remaining probability of the singlet as

$$P(\mathbf{r}, t) = \prod_n \frac{1}{2} \sum_{r=\pm} F(t) \delta(x_n - rv_F t) \quad (2.92)$$

with a time decaying weight factor of the δ -function

$$F(t) = \prod_{\nu=\rho,\sigma} \sqrt{\frac{\Lambda^2}{\Lambda^2 + (v_F - u_\nu)^2 t^2}} \times \left(\frac{\Lambda^4}{(\Lambda^2 + (v_F^2 - u_\nu^2) t^2)^2 + (2\Lambda u_\nu t)^2} \right)^{\gamma_\nu/2}. \quad (2.93)$$

From Eqs. (2.92) and (2.93) we see that charge and spin of an electron propagate with velocity v_F , whereas charge (spin) excitations of the Luttinger liquid propagate with u_ρ (u_σ). Without interaction, i.e. $u_\nu = v_F$ and $K_\nu = 1$, we have $F(t) = 1$ which means that there is no decay of the singlet state. Using again $u_\sigma = v_F$, $K_\sigma = 1$ and $u_\rho = v_F/K_\rho$ we see from Eq. (2.93) that as interactions are turned on, the singlet state starts to decay on a time scale given by Λ/u_ρ . For long times t and for $u_\sigma = v_F$, $K_\sigma = 1$ and $u_\rho = v_F/K_\rho$, we find the asymptotic behavior $F(t) \simeq \frac{\Lambda}{u_\rho(1-K_\rho)} \left[\frac{\Lambda^2}{u_\rho^2(1-K_\rho^2)} \right]^{\gamma_\rho} \left[\frac{1}{t} \right]^{2\gamma_\rho+1}$ which for very strong interactions in the Luttinger liquid leads, i.e. K_ρ much smaller than one, becomes

$$F(t) \simeq \left(\frac{\Lambda}{u_\rho t} \right)^{2\gamma_\rho+1}. \quad (2.94)$$

We will show in the next section that although the probability to recover the electron singlet decays in time due to interactions, we still can observe charge and spin of the initial singlet via the spin and charge density fluctuations of the Luttinger liquid, since the spin of the injected electron cannot be destroyed by Coulomb interaction.

2.3.10 Propagation of charge and spin

The propagation of charge and spin in a state $|\Psi\rangle$ as a function of time can be described by the correlation function $\langle \Psi | \rho(x, t) | \Psi \rangle$ for the charge, and $\langle \Psi | \sigma_z(x, t) | \Psi \rangle$ for the spin. The normal-ordered charge density operator for Luttinger liquid n is $\rho_n(x_n) = \sum_s : \psi_{ns}^\dagger(x_n) \psi_{ns}(x_n) := \sum_{sr} : \psi_{nsr}^\dagger(x_n) \psi_{nsr}(x_n) :$, if we only consider the slow spatial variations of the density operator. Similarly, the normal-ordered spin density operator in z -direction is $\sigma_n^z(x_n) = \sum_{sr} s : \psi_{nsr}^\dagger(x_n) \psi_{nsr}(x_n) :$. These density fluctuations

can be expressed in a bosonic form (see Appendix C) as

$$\rho_n(x_n) = \frac{\sqrt{2}}{\pi} \partial_x \phi_{n\rho}(x_n), \quad (2.95)$$

and for the spin

$$\sigma_n^z(x_n) = \frac{\sqrt{2}}{\pi} \partial_x \phi_{n\sigma}(x_n). \quad (2.96)$$

We now consider a state $|\Psi\rangle = \psi_{nsr}^\dagger(x_n)|0\rangle$ where we inject an electron with spin s at time $t = 0$ into branch r on top of the Luttinger liquid ground state in lead n ¹⁴ and calculate the time dependent charge and spin density fluctuations according to $\langle 0|\psi_{nsr}(x_n)\rho_n(x'_n, t)\psi_{nsr}^\dagger(x_n)|0\rangle$ for the charge and similar for the spin $\langle 0|\psi_{nsr}(x_n)\sigma_n^z(x'_n, t)\psi_{nsr}^\dagger(x_n)|0\rangle$. If we express the bosonic phase fields $\phi_{n\nu}$ and $\theta_{n\nu}$ in terms of the Boson modes shown in Eqs. (2.64) and (2.65) and the Fermi operators according to the bosonization dictionary [Eq. (2.56)] we obtain for the charge fluctuations

$$\begin{aligned} & (2\pi\alpha) \langle 0|\psi_{nsr}(x_n)\rho_n(x'_n, t)\psi_{nsr}^\dagger(x_n)|0\rangle \\ &= \frac{1}{2}(1 + rK_\rho)\delta(x'_n - x_n - u_\rho t) \\ & \quad + \frac{1}{2}(1 - rK_\rho)\delta(x'_n - x_n + u_\rho t), \end{aligned} \quad (2.97)$$

and for the spin fluctuations

$$\begin{aligned} & (2\pi\alpha) \langle 0|\psi_{nsr}(x_n)\sigma_n^z(x'_n, t)\psi_{nsr}^\dagger(x_n)|0\rangle \\ &= \frac{s}{2}(1 + rK_\sigma)\delta(x'_n - x_n - u_\sigma t) \\ & \quad + \frac{s}{2}(1 - rK_\sigma)\delta(x'_n - x_n + u_\sigma t). \end{aligned} \quad (2.98)$$

The results Eqs. (2.97) and (2.98) are obtained by sending $\Lambda \rightarrow 0$. We see that in contrast to the singlet, the charge and spin density fluctuations in the Luttinger liquid created by the injected electron do not decay and show a pulse shape (δ -function) with no dispersion in time. This is due to the linear energy dispersion relation of the Luttinger liquid model. In carbon nanotubes

¹⁴This describes the interesting case where the two electrons of a Cooper pair tunnel to different leads.

such a highly linear dispersion relation is indeed realized, and, therefore, nanotubes should be well suited for spin transport¹⁵. Another interesting effect that shows up in Eq. (2.97) and Eq. (2.98) is the different velocities of spin and charge, which is known as spin-charge separation. It would be interesting to test Bell inequalities [42] via spin-spin correlation measurements between the two Luttinger liquid leads and see if the initial entanglement of the spin singlet is still observable in the spin density-fluctuations which are well localized in space according to Eqs. (2.97) and (2.98). Although detection of spin-densities with magnitudes on the order of a single electron spin has still not been achieved, magnetic resonance force microscopy (MFRM) seems to be very promising in doing so [103].

Another scenario is to use the Luttinger liquid just as an intermediate medium which is needed to first separate the two electrons of a Cooper pair and then to take them (in general other electrons) out again (via another tunnel junction) into two (spatially separated) Fermi liquid leads where the (possibly reduced) spin entanglement could be measured via the current noise in a beamsplitter experiment [47]. Similarly, to test Bell inequalities one can make then use of measuring spin via the charge of the electron [12, 48, 104, 105], see Section 3.8 in this Thesis. In this context we remark that in order to have exclusively singlet states as an input for the beamsplitter setup or the quantum dot spin filters, it is important that the Luttinger liquid leads return to their spin ground state after the injected electrons have tunneled out again into the Fermi liquid leads in which the detection of spin-entanglement takes place. For an infinite Luttinger liquid, the spin-excitations are gapless and therefore an arbitrary small bias voltage $\delta\mu$ between the superconductor and the Fermi liquids would allow for spin-excitations in the Luttinger liquids. However, if we consider a finite size Luttinger liquid (e.g. a nanotube), spin excitations are gapped on an energy scale $\sim \hbar v_F/L$ where L is the length of the Luttinger liquid, see Appendix C. Therefore, if $k_B T, \delta\mu < \hbar v_F/L$, only singlets can leave the Luttinger liquid again to the Fermi leads since the total spin of the system has to be conserved. For the metallic carbon nanotubes L is on the order of micrometers and the Fermi velocity is $\sim 10^6$ m/s which gives an excitation gap on the order of a few meV which is large enough for our regime of interest. We finally note that the decay of the singlet state given by Eq. (2.92) sets in almost immediately after the injection into the

¹⁵We also note that if $K_\sigma = 1$, the spin of the injected electron is detectable locally since then only one peak is present in Eq. (2.98).

Luttinger liquids (the time scale is approximately the inverse of the Fermi energy), but at least at zero temperature, the suppression is only polynomial in time, which suggests that some fraction of the electron singlet state can still be recovered, but, as discussed above, this does not mean that the spin-entanglement is destroyed by interactions.

2.3.11 Conclusion and outlook

We proposed an s-wave superconductor, coupled to two spatially separated Luttinger liquid leads, as an entangler for electron spins. We showed that the strong correlations present in the Luttinger liquid can be used to separate two electrons, forming a spin singlet state, which originate from an Andreev tunneling process of a Cooper pair from the superconductor to the leads. We have calculated that the coherent tunneling of two electrons into the same lead is suppressed by a characteristic power law in the small parameter $\delta\mu/\Delta$, where $\delta\mu$ is the applied bias between the superconductor and the Luttinger liquid leads, and Δ is the gap of the superconductor. On the other hand, when the two electrons tunnel into different leads, the current is suppressed by the initial separation of the two electrons. This suppression, however, can be considerably reduced by going over to effective lower-dimensional superconductors. We also addressed the question of how much of the electron singlet initially injected into the Luttinger liquid can be recovered at some later time, and we found that the probability decreases with time, again with a power-law at zero temperature. Nevertheless, the spin information can still be transported through the wires by means of the (proper) spin excitations of the Luttinger liquid which show a pulse shape in space with no dispersion. Therefore, the spin information is locally accessible in an experiment.

There still remain interesting open questions which could be investigated in future works. One obvious extension of this work is to consider tunneling into the *end* of a Luttinger liquid (instead of the bulk). It is known that the power-law suppression of the single-particle DOS is larger if one considers tunneling into the *end* of a Luttinger liquid. For single-wall carbon nanotubes one finds [91,92] $\eta_{end} = (K_\rho^{-1} - 1)/4 > \eta$, or for conventional Luttinger liquid-theory again an enhancement by a factor of two [106]. We therefore expect to get an even stronger suppression if the Cooper pairs tunnel into the end of the Luttinger liquids. This scenario of end-tunneling was investigated in Ref. [63] also in the context of entanglement creation with the help of a superconductor weakly coupled to two semi-infinite metallic carbon nanotubes, but within a

different theoretical model where the time delay between the tunneling events of the two electrons of the same Cooper pair is neglected, as in Ref. [94]. As a consequence, the entangler efficiency $I_2/I_1 \propto (2\delta\mu/\varepsilon_0)^{2\eta_{end}}$ where $\varepsilon_0 \sim 1$ eV is the bandwidth in the nanotube [63], and not, as in our result Eq. (2.87), the energy gap Δ of the superconductor. With a ratio $\Delta/\varepsilon_0 \sim 10^{-3}$ this difference is sizable.

We remark that the nonlocality of the two electrons could be probed via the Aharonov-Bohm oscillations in the current, when the leads 1,2 are formed into a loop enclosing a magnetic flux. We have discussed such a setup in detail for the entangler with quantum dots in Subsection 2.2.7. Here, we expect that the h/e oscillation contribution should be $\propto (I_1 I_2)^\alpha$, and the $h/2e$ oscillation contribution should be $\propto I_2^{2\alpha}$, with an exponent α that has to be determined by explicit calculations. In the non-interacting limit α should be $1/2$, as found in Subsection 2.2.7. The different periods then allow for an experimental test of how successful the separation of the two electrons is. For instance, if the two electrons only can tunnel into the same lead, e.g. if $k_F \delta r$ is too large or the interaction in the leads too weak, then $I_1 \sim 0$ and we would only see the $h/2e$ oscillations in the current. The determination of the precise value of the exponent α requires a separate calculation including finite size properties of the Luttinger liquid along the lines discussed in Ref. [107].

2.4 Andreev Entangler with high-resistance leads

Here, we investigate a dynamical Coulomb blockade effect caused by leads with a finite resistance. In contrast to the proposal with quantum dots, the Coulomb blockade effect here is caused by non-ballistic motion in the leads with the consequence that the charge fluctuations at the tunnel-junctions induced by the tunneling electrons cannot relax sufficiently fast due to the resistance of the leads. We describe this dynamical Coulomb blockade effect phenomenologically in terms of an electromagnetic environment and show that it can lead to currents of nonlocal and pairwise spin-entangled electrons when the leads are coupled to a superconductor.

2.4.1 Introduction

The Coulomb blockade effect in transport through a quantum dot attached to leads and possibly to a gate voltage, see Chapter 3, is based on a gapped energy spectrum of the quantum dot as a function of the number of electrons added to it. By sweeping the gate voltage, one is able to change the number of electrons on the dot one by one.

In a single tunnel-junction, charging effects can also show up as we will explain here in terms of qualitative arguments which will be confirmed in subsequent subsections. A tunnel-junction that couples two conductors possesses a capacitance C with an associated charging energy $Q^2/2C$ where the continuous influence charge $Q = VC$ is determined by the voltage V across the junction. If an electron succeeds in tunneling from the conductor with higher electrostatic potential (chemical potential) to the side with the lower potential, the charging energy is changed from $Q^2/2C$ to $(Q - e)^2/2C$ since the tunneled charge $-e$ is the charge of an electron. At zero temperature this process can occur only if we can lower the charging energy due to this tunneling process. This is possible only for a voltage $V > e/2C$. So we conclude that there is a Coulomb gap in the current voltage characteristic for $V < e/2C$. This effect is based mainly on the fact that the tunneling charge $-e$ is discrete, whereas the junction charge Q is continuous. Usually, this Coulomb blockade effect is not seen in a transport experiment since the tunnel junction is biased by a voltage source so that the *non-equilibrium* situation after the tunneling event is immediately removed. This relaxation time, however, depends on the environment which surrounds the tunnel-junction. If the conductors have a resistance R , then the relaxation time of a classical circuit is given by $\tau_{cl} = RC$. If this time is short, quantum fluctuations will wash out the charging effects due to the energy-time uncertainty relation $\Delta E \Delta t \simeq \hbar$. Therefore, we can expect to see charging effects only if $e^2/2C > \hbar/RC$, which is equivalent to

$$R > R_Q, \tag{2.99}$$

where $R_Q = h/e^2$ is the quantum resistance.

We show in this section that these dynamical Coulomb blockade effects can produce nonlocal and mobile spin-entangled electrons in two spatially separated leads if they are weakly coupled to an s-wave superconductor. Indeed, if the normal leads are resistive the second electron of a pair tunneling event into the same lead still experiences the presence of the first one which

has not yet diffused away from the tunnel-junction due to the resistance. The advantage of this proposal is that it only requires existing technologies. No quantum dots nor strong correlations are necessary. Natural existing candidates with long spin decoherence lengths ($\gtrsim 100 \mu\text{m}$ [7]) for such a setup are e.g. semiconductor systems tunnel-coupled to a superconductor, as experimentally implemented in InAs [71, 108], InGaAs [72] or GaAs/AlGaAs [109]. Recently, two dimensional electron gases (2DEGs) with a resistance per square approaching the quantum resistance $R_Q = h/e^2 \sim 25.8 \text{ k}\Omega$ could be achieved by depleting the 2DEG with a voltage applied between a back gate and the 2DEG [110]. In metallic normal NiCr leads of width $\simeq 100 \text{ nm}$ and length $\simeq 10 \mu\text{m}$, resistances of $R = 22 - 24 \text{ k}\Omega$ have been produced at low temperatures. Even larger resistances $R = 200 - 250 \text{ k}\Omega$ have been measured in Cr leads [111].

We use a phenomenological approach to describe charge dynamics in the electromagnetic circuit which is described in terms of normal-lead impedances and junction capacitances, see Fig. 2.10. The subgap transport of a single SN-junction under the influence of an electromagnetic environment has been studied in detail [112, 113]. In order to create nonlocal entangled states in the leads we have to go beyond previous work to investigate the physics of *two* tunnel junctions in parallel with two distinct transport channels for singlets. A Cooper pair can tunnel as a whole into one lead, or the pair can split and the two electrons tunnel to separate leads, leading to a nonlocal entangled spin-pair in the leads. In the case where the pair splits we find that the Coulomb blockade effect provided by the electromagnetic environment is uncorrelated for the two electron charges. In contrast, if the two electrons tunnel into the same lead we find a dynamical Coulomb blockade consistent with a charge $q = 2e$. Thus, the Coulomb blockade effect is twice as large for the unsplit process which enhances the probability for a nonlocal (pair-split) process. Again we have to compare the effect of the Coulomb blockade to the suppression for tunneling into different leads due to the spatial correlation of a Cooper pair.

2.4.2 Setup and formalism

The setup is sketched in Fig. 2.10. The superconductor is held at the (electro-)chemical potential μ_S by a voltage source V . The two electrons of a Cooper pair can tunnel via two junctions placed at points \mathbf{r}_1 and \mathbf{r}_2 on the superconductor to two separate normal leads 1 and 2 which have resistances

R_1 and R_2 , respectively. They are kept at the same chemical potential μ_l so that a bias voltage $\delta\mu \equiv \mu_S - \mu_l$ is applied between superconductor and leads. The system Hamiltonian decomposes into three parts

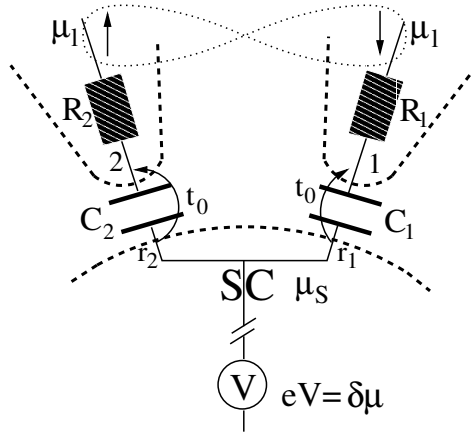


Figure 2.10: Entangler setup: A bulk superconductor (SC) with chemical potential μ_S is tunnel-coupled (amplitude t_0) via two points \mathbf{r}_1 and \mathbf{r}_2 of the superconductor to two Fermi liquid leads 1,2 with resistance $R_{1,2}$. The two leads are held at the same chemical potential μ_l such that a bias voltage $\delta\mu = \mu_S - \mu_l$ is applied between the superconductor and the two leads. The tunnel-junctions 1,2 have capacitances $C_{1,2}$.

$$H = H^e + H_{env} + H_T. \quad (2.100)$$

Here, $H^e = H_S + \sum_{n=1,2} H_{ln}$ describes the electronic parts of the isolated subsystems consisting of the superconductor and Fermi liquid leads $n = 1, 2$, with

$$H_{ln} = \sum_{\mathbf{p}\sigma} \epsilon_{\mathbf{p}} c_{n\mathbf{p}\sigma}^\dagger c_{n\mathbf{p}\sigma}, \quad (2.101)$$

where $\sigma = (\uparrow, \downarrow)$. The s-wave bulk superconductor is described by the BCS-Hamiltonian [59]

$$H_S - \mu_S N_S = \sum_{\mathbf{k}\sigma} E_{\mathbf{k}} \gamma_{\mathbf{k}\sigma}^\dagger \gamma_{\mathbf{k}\sigma} \quad (2.102)$$

with the quasiparticle spectrum $E_{\mathbf{k}} = (\xi_{\mathbf{k}}^2 + \Delta^2)^{1/2}$ where $\xi_{\mathbf{k}} = \epsilon_{\mathbf{k}} - \mu_S$. The electron creation ($c_{\mathbf{k}\sigma}^\dagger$) and annihilation ($c_{\mathbf{k}\sigma}$) operators are related to the quasiparticle operators by the Bogoliubov transformation

$c_{\mathbf{k}(\uparrow/\downarrow)} = u_{\mathbf{k}}\gamma_{\mathbf{k}(\uparrow/\downarrow)} \pm v_{\mathbf{k}}\gamma_{-\mathbf{k}(\downarrow/\uparrow)}^\dagger$, where $u_{\mathbf{k}}$ and $v_{\mathbf{k}}$ are the usual BCS coherence factors [59].

To describe resistance and dissipation in the normal leads we use a phenomenological approach [114], where the electromagnetic fluctuations in the circuit (being bosonic excitations) due to electron-electron interaction and the lead resistances are modeled by a bath of harmonic oscillators which is linearly coupled to the charge fluctuation Q_n of the junction capacitor n (induced by the tunneling electron). This physics is described by [114,115]

$$H_{env,n} = \frac{Q_n^2}{2C_n} + \sum_{j=1}^N \left[\frac{q_{nj}^2}{2C_{nj}} + \frac{(\phi_n - \varphi_{nj})^2}{2e^2 L_{nj}} \right]. \quad (2.103)$$

The phase ϕ_n of junction n is the conjugate variable to the charge satisfying $[\phi_n, Q_m] = ie\delta_{n,m}$. As a consequence $e^{-i\phi_n}$ reduces Q_n by one elementary charge e . Any lead impedance $Z_n(\omega)$ can be modeled with Eq. (2.103) via $Z_n^{-1}(\omega) = \int_{-\infty}^{+\infty} dt \exp(-i\omega t) Y_n(t)$ where the admittance is given as $Y_n(t) = \sum_{j=1}^N (\Theta(t)/L_{nj}) \cos(t/\sqrt{L_{nj}C_{nj}})$. For a more detailed investigation of the Hamiltonian Eq. (2.103) we refer to Appendix F. We remark that in our setup the superconductor is held at the constant chemical potential μ_S by the voltage source, see Fig. 2.10. Therefore, the charge relaxation of a non-equilibrium charge on one of the capacitors described by Eq. (2.103) does not influence the charge dynamics of the other junction and, as a consequence, $H_{env} = \sum_{n=1,2} H_{env,n}$. A correction to this decoupling assumption is determined by the cross-capacitance $C_{12} \ll C_n$, $n = 1, 2$ between the leads 1,2 and is therefore of no significance.

Electron tunneling through junctions 1,2 located at points $\mathbf{r}_1, \mathbf{r}_2$ of the superconductor nearest to the leads 1,2 is described by the tunneling Hamiltonian $H_T = \sum_{n=1,2} H_{Tn} + \text{h.c.}$ where

$$H_{Tn} = t_0 \sum_{\sigma} \psi_{n\sigma}^\dagger \Psi_{\sigma}(\mathbf{r}_n) e^{-i\phi_n}. \quad (2.104)$$

Here, t_0 is the bare electron tunneling amplitude which we assume to be spin-independent and the same for both leads. Since H_T conserves spin we have $[H, \mathbf{S}_{tot}^2] = 0$, and thus the two electrons from a given Cooper pair singlet which have tunneled to the lead(s) remain in the singlet state. We assume that tunneling is weak such that the relaxation processes described by H_{env} are faster than the appearance of pair-tunneling events. It is then allowed to calculate the tunneling currents to lowest possible order in H_T .

2.4.3 Current for tunneling into different leads

We again use a T-matrix approach [77] to calculate tunneling currents. At zero temperature the current I_1 for tunneling of two electrons coming from the same Cooper pair into *different* leads is given to lowest order in t_0 by

$$I_1 = 2e \sum_{\substack{n \neq n' \\ m \neq m'}} \int_{-\infty}^{\infty} dt \int_0^{\infty} dt' \int_0^{\infty} dt'' e^{-\eta(t'+t'')+i(2t-t'-t'')\delta\mu} \\ \times \langle H_{Tm}^\dagger(t-t'') H_{Tm'}^\dagger(t) H_{Tn}(t') H_{Tn'}(0) \rangle, \quad (2.105)$$

where $\eta \rightarrow 0^+$, and the expectation value is to be taken in the ground state of the unperturbed system. The physical interpretation of Eq. (2.105) is a hopping process of two electrons with opposite spins from two spatial points \mathbf{r}_1 and \mathbf{r}_2 of the superconductor to the two leads 1,2, thereby removing a Cooper pair in the superconductor, and back again. The delay times between the two tunneling processes of the electrons within a pair is given by t' and t'' , *resp.*, whereas the time between destroying and creating a Cooper pair is given by t . This process is contained in the correlation function

$$\sum_{\substack{n \neq n' \\ m \neq m'}} \langle H_{Tm}^\dagger(t-t'') H_{Tm'}^\dagger(t) H_{Tn}(t') H_{Tn'}(0) \rangle \\ = |t_0|^4 \sum_{\sigma, n \neq m} \{ G_{n\sigma}(t-t'') G_{m,-\sigma}(t-t') \mathcal{F}_{nm\sigma}(t') \mathcal{F}_{nm\sigma}^*(t'') \\ \times \langle e^{i\phi_n(t-t'')} e^{-i\phi_n(0)} \rangle \langle e^{i\phi_m(t-t')} e^{-i\phi_m(0)} \rangle \\ - G_{m,-\sigma}(t-t'-t'') G_{n\sigma}(t) \mathcal{F}_{nm\sigma}(t') \mathcal{F}_{mn,-\sigma}^*(t'') \\ \times \langle e^{i\phi_m(t-t'-t'')} e^{-i\phi_m(0)} \rangle \langle e^{i\phi_n(t)} e^{-i\phi_n(0)} \rangle \}. \quad (2.106)$$

The lead Green's functions are $G_{n\sigma}(t) \equiv \langle \psi_{n\sigma}(t) \psi_{n\sigma}^\dagger(0) \rangle \simeq (\nu_l/2)/it$, with ν_l being the DOS per volume at the Fermi level μ_l of the leads. The anomalous Green's function of the superconductor is $\mathcal{F}_{nm\sigma}(t) \equiv \langle \Psi_{-\sigma}(\mathbf{r}_m, t) \Psi_\sigma(\mathbf{r}_n, 0) \rangle = (\text{sgn}(\sigma)/V_S) \sum_{\mathbf{k}} u_{\mathbf{k}} v_{\mathbf{k}} \exp(-iE_{\mathbf{k}}t + i\mathbf{k} \cdot \delta\mathbf{r})$ with $\delta\mathbf{r} = \mathbf{r}_1 - \mathbf{r}_2$, and V_S is the volume of the superconductor. The bath correlator can be expressed as

$$\langle \exp(i\phi_n(t)) \exp(-i\phi_n(0)) \rangle = \exp \{ \langle [\phi_n(t) - \phi_n(0)] \phi_n(0) \rangle \}. \quad (2.107)$$

The relation in Eq. (2.107) holds since the Hamiltonian Eq. (2.103) can in principle be diagonalized in new Bose operators and the junction charge Q_n and ϕ_n are then linear combinations of them. The thermal average in the exponent on the right hand side of Eq. (2.107), $J(t) \equiv \langle [\phi_n(t) - \phi_n(0)]\phi_n(0) \rangle$, can be calculated via the susceptibility $\chi_{\phi_n\phi_n}(\omega)$. Its explicit calculation we defer to Appendix F. Then using the fluctuation dissipation theorem we obtain

$$J(t) = 2 \int_0^\infty \frac{d\omega}{\omega} \frac{\text{Re } Z_T(\omega)}{R_Q} (\exp(-i\omega t) - 1). \quad (2.108)$$

Here, we introduced the total impedance $Z_T = (i\omega C + R^{-1})^{-1}$, with a purely Ohmic lead impedance $Z_n(\omega) = R$, which we assume to be the same for both tunnel-junctions and leads. The bath correlation function can be evaluated analytically in terms of exponential integrals. For small times, $\omega_R|t| < 1$, we can approximate $J(t) \simeq -iE_c t$ where $E_c = e^2/2C$ is the charging energy and $\omega_R = 1/RC$ is the bath frequency cut-off which is the inverse classical charge relaxation time τ_{cl} of an RC-circuit. For the long-time behavior, $\omega_R|t| > 1$, we get $J(t) \simeq -(2/g)[\ln(i\omega_R t) + \gamma]$ with $\gamma = 0.5772$ the Euler number and $g = R_Q/R$ is the dimensionless lead conductance which determines the power-law decay of the bath correlator at long times, since $\exp[J(t)] \propto (1/t)^{2/g}$.

We first consider the low bias regime $\delta\mu < \Delta, \omega_R$. In this limit the delay times t' and $t'' \lesssim 1/\Delta$ can be neglected compared to $t \lesssim 1/\delta\mu$ in all correlators in Eq. (2.106) and the bath correlators are dominated by the long-time behavior of $J(t)$. To calculate I_1 we come across similar integrals as discussed in detail in Section 2.3. We then obtain for the current

$$I_1 = e\pi\delta\mu\Gamma^2 F_d^2(\delta r) \frac{e^{-4\gamma/g}}{\Gamma(2 + 4/g)} \left(\frac{2\delta\mu}{\omega_R} \right)^{4/g}. \quad (2.109)$$

The geometrical factor coming from the spatial correlation of a Cooper pair is $F_{d=3}(\delta r) = [\sin(k_F\delta r)/k_F\delta r] \exp(-\delta r/\pi\xi)$ with $\delta r = |\delta\mathbf{r}|$. The exponential decay of the correlation sets in on the length scale of the coherence length ξ . It is on the order of micrometers for usual s-wave materials (see e.g. Ref. [78]) and can be assumed to be larger than δr which is assumed to be in the range of nanometers. More severe is the power-law decay $\propto 1/(k_F\delta r)^2$ with k_F the Fermi wavenumber in the superconductor. This power-law is sensitive to the effective dimensionality d of the superconductor with weaker decay in lower dimensions as we have shown already in Subsection 2.2.6. For completeness, we again summarize the findings: In two dimensions and for

$k_F \delta r > 1$, but still $\delta r < \xi$, we get $F_{d=2}^2 \propto 1/(k_F \delta r)$ and in one dimension there is no power-law decay as a function of $k_F \delta r$. In Eq. (2.109) we introduced the Gamma function $\Gamma(x)$ and the dimensionless tunnel-conductance $\Gamma = \pi \nu_S \nu_l |t_0|^2$ with ν_S being the DOS per volume of the superconductor at the Fermi level μ_S . The result shows the well known power-law decay at low bias $\delta\mu$ characteristic of dynamical CB [114]. The exponent $4/g$ in Eq. (2.109) is two times the power for single electron tunneling via one junction. This is so, because the two tunneling events are not correlated since each electron tunnels to a different lead and the charge relaxation process for each circuit is independent.

We consider now the large bias regime $\Delta, \delta\mu > \omega_R$. In the regime $\Delta, |\delta\mu - E_c| > \omega_R$ we can use the short time expansion for $J(t)$ in Eq. (2.106). As long as $|\delta\mu - E_c| < \Delta$ we can again neglect the delay times t' and t'' compared to t in all correlation functions in Eq. (2.106) and obtain the current I_1 in the large bias limit and up to small contributions $\simeq e\pi\Gamma^2 F_d^2(\delta r)\omega_R[\mathcal{O}(\omega_R/\delta\mu) + \mathcal{O}(\omega_R/|\delta\mu - E_c|)]$

$$I_1 = e\pi\Gamma^2 F_d^2(\delta r)\Theta(\delta\mu - E_c)(\delta\mu - E_c). \quad (2.110)$$

This shows the development of a gap in I_1 for $\delta\mu < E_c$ and $R \rightarrow \infty$ which is the hallmark of dynamical CB.

2.4.4 Current for tunneling into the same lead

We turn now to the calculation of the current I_2 carried by spin-entangled electrons that tunnel both into the *same* lead either 1 or 2. The current formula for I_2 is given by Eq. (2.105) but with $n = n'$ and $m = m' = n$, and we assume that the two electrons tunnel off the superconductor from the same point and therefore $\delta r = 0$ here. Since both electrons tunnel into the same lead the bath correlation functions do not separate anymore as was the case in Eq. (2.106). Instead we have to look at the full four-point correlator

$$\begin{aligned} & \langle e^{i\phi_n(t-t'')} e^{i\phi_n(t)} e^{-i\phi_n(t')} e^{-i\phi_n(0)} \rangle \\ &= \frac{e^{J(t-t'-t'')+J(t-t')+J(t-t'')+J(t)}}{e^{J(t')+J(-t')}}. \end{aligned} \quad (2.111)$$

The lead correlators again factorize into a product of two single-particle Green's functions since they are assumed to be Fermi liquids and in ad-

dition there appear no spin correlations due to tunneling of two electrons with opposite spins.

We first consider the low bias regime $\delta\mu < \omega_R, \Delta$. Here again, we can assume that $|t|$ is large compared to the delay times t' and t'' , but it turns out to be crucial to distinguish carefully between $\Delta > \omega_R$ and $\Delta < \omega_R$. We first treat the case $\Delta > \omega_R$ and approximate $\exp[-(J(t') + J(-t''))] \simeq \exp[-iE_c(t'' - t')]$ in Eq. (2.111). In this limit, and for $\Delta - E_c > 0$, the current I_2 becomes

$$I_2 = e\pi\delta\mu\Gamma^2 \frac{(4\Delta/\pi)^2}{\Delta^2 - E_c^2} \arctan^2 \left\{ \sqrt{\frac{\Delta + E_c}{\Delta - E_c}} \right\} \frac{e^{-8\gamma/g}}{\Gamma(2 + 8/g)} \left(\frac{2\delta\mu}{\omega_R} \right)^{8/g}. \quad (2.112)$$

The exponent $8/g$ in Eq. (2.112) we would also obtain in a *first-order* tunneling event if the operator $e^{-i\phi_n}$ is replaced by $e^{-i2\phi_n}$ in Eq. (2.104) which changes the charge of the tunnel junction capacitor n by $2e$. In addition to this *double* charging effect we see from Eq. (2.112) that an enhancement of E_c gives not only rise to a suppression of I_2 via the term $(2\delta\mu/\omega_R)^{8/g} = (2\pi\delta\mu/gE_c)^{8/g}$ but also to an increase due to the Δ -dependent prefactor. This enhancement can be interpreted as a relaxation of the charge imbalance created by the first tunneling event for times much smaller than the classical relaxation time τ_{cl} . The result Eq. (2.112) is valid if $\sqrt{(\Delta - E_c)/(\Delta + E_c)} > \sqrt{\omega_R/\Delta}$. In the interesting case $\Delta > E_c$, we expand Eq. (2.112) to leading order in the parameter E_c/Δ with the result

$$I_2 = e\pi\delta\mu\Gamma^2 \frac{e^{-8\gamma/g}}{\Gamma(2 + 8/g)} \left(\frac{2\delta\mu}{\omega_R} \right)^{8/g}. \quad (2.113)$$

In the other limit where $\Delta < \omega_R$, e.g. for small R , we can assume that $\omega_R t'$ and $\omega_R t'' > 1$ and therefore we approximate $\exp[-(J(t') + J(-t''))] \simeq \exp(4\gamma/g) \omega_R^{4/g} (t' t'')^{2/g}$. In this limit, the four-point correlator Eq. (2.111) has the same form as the corresponding two-particle correlation function of a Luttinger liquid, see Eq. (2.85). In this regime we obtain for the current

$$I_2 = e\pi\delta\mu\Gamma^2 A(g) \left(\frac{2\delta\mu}{\omega_R} \right)^{4/g} \left(\frac{2\delta\mu}{\Delta} \right)^{4/g}, \quad (2.114)$$

with $A(g) = (2e^{-\gamma})^{4/g} \Gamma^4(1/g + 1/2)/\pi^2 \Gamma(2 + 8/g)$. Here, the relative suppression of the current I_2 compared to I_1 is given essentially by $(2\delta\mu/\Delta)^{4/g}$

and not by $(2\delta\mu/\omega_R)^{4/g}$ as in the case of an *infinite* Δ . This is because the virtual state with a quasiparticle in the superconductor can last much longer than the classical relaxation time τ_d , and, as a consequence, the power law suppression of the current is weakened since $\Delta < \omega_R$ here. To our knowledge, the result Eq. (2.114) was not discussed in the literature so far¹⁶, but a similar result is obtained when a superconductor is coupled to a Luttinger liquid, see Subsection 2.3.7. It is important to note that a large gap Δ is therefore crucial to suppress I_2 .

In the large voltage regime $\Delta, \delta\mu > \omega_R$ we expect a Coulomb gap due to a charge $q = 2e$. Indeed, in the parameter range $|\delta\mu - 2E_c| > \omega_R$ and $\Delta > |\delta\mu - E_c|$ we obtain I_2 again up to small contributions $\simeq e\pi\Gamma^2\omega_R[\mathcal{O}(\omega_R/\delta\mu) + \mathcal{O}(\omega_R/|\delta\mu - 2E_c|)]$

$$I_2 = e\pi\Gamma^2\Theta(\delta\mu - 2E_c)(\delta\mu - 2E_c). \quad (2.115)$$

This shows that I_2 is small ($\propto \omega_R^2/|\delta\mu - 2E_c|$) in the regime $E_c < \delta\mu < 2E_c$, whereas I_1 is finite ($\propto F_d^2(\delta r)(\delta\mu - E_c)$).

2.4.5 Discussion and conclusion

We now provide numerical values for the current magnitudes and efficiencies of the entangler. We first discuss the low bias regime $\delta\mu < \Delta, \omega_R$. In Fig. 2.11 we show the ratio I_2/I_1 (efficiency of entangler) and I_1 for $\Delta > E_c, \omega_R$ [Eq. (2.113)] as a function of $4/g$ for realistic system parameters (see figure caption). The plots show that a very efficient entangler can be expected for lead resistances $R \lesssim R_Q$. The total current is then on the order of $I_1 \gtrsim 10$ fA. In the large bias regime $\delta\mu > \omega_R$ and for $E_c < \delta\mu < 2E_c$ we obtain

$$I_2/I_1 \propto (k_F\delta r)^{d-1}\omega_R^2/(2E_c - \delta\mu)(\delta\mu - E_c), \quad (2.116)$$

where we assume that $2E_c - \delta\mu$ and $\delta\mu - E_c > \omega_R$. For $\delta\mu \simeq 1.5E_c$ and using $\omega_R = gE_c/\pi$ we obtain approximately $I_2/I_1 \propto (k_F\delta r)^{d-1}g^2$. To have $I_2/I_1 < 1$ we require $g^2 < 0.01$ for $d = 3$, and $g^2 < 0.1$ for $d = 2$. Such small values of g have been produced approximately in Cr leads [111]. For I_1 we obtain $I_1 \simeq e(k_F\delta r)^{1-d}(\delta\mu - E_c)\Gamma^2 \simeq e(k_F\delta r)^{1-d}E_c\Gamma^2 \simeq 2.5$ pA for $d = 3$ and for the same parameters as used in Fig. 2.11. This shows that here I_1 is much larger than for low bias voltages, but to have an efficient entangler very

¹⁶The result Eq. (2.114) is in contrast to predictions made in Ref. [112].

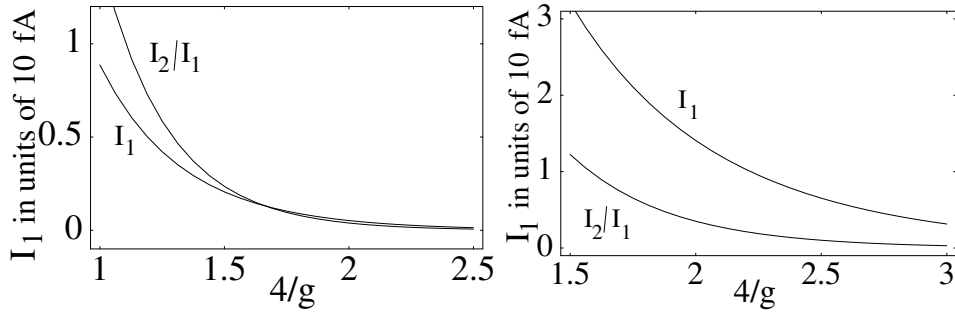


Figure 2.11: Current ratio I_2/I_1 (entangler efficiency) and current I_1 in the low bias regime, $\delta\mu < \Delta, \omega_R$ and for $\Delta > E_c, \omega_R$, as a function of $4/g = 4R/R_Q$. We have chosen realistic parameters: $E_c = 0.1$ meV, $k_F\delta r = 10$, $\Gamma = 0.1$. The left plot is for $\delta\mu = 5$ μeV and the right one for $\delta\mu = 15$ μeV . In the case of a 2D superconductor, I_1 and I_1/I_2 can be multiplied by 10.

high lead resistances $R \gtrsim 10R_Q$ should be used. Our discussion shows that it should be possible to implement the proposed device within state-of-the-art techniques.

We finally remark that the resistance in the leads is caused by elastic and/or inelastic scatterings of electrons by impurities. As long as only momentum scattering is present, the spin is unaffected and the spin-entanglement between the two electrons of the pair is still present.

Chapter 3

Quantum dot as spin filter and spin memory

3.1 Introduction

An increasing number of spin-related experiments [4, 7–9, 116–119] show that the spin of the electron offers unique possibilities to find novel mechanisms for information processing—most notably in quantum-confined semiconductors with unusually long spin dephasing times approaching microseconds [7], and where spins can be transported coherently over distances of up to 100 micrometers [7]. Besides the intrinsic interest in spin-related phenomena, spin-based devices hold promise for future applications in conventional [4] as well as in quantum computer hardware [12]. A few examples were mentioned in Section 1.1. One of the challenging problems for such applications is to obtain sufficient control over the spin dynamics in nanostructures. In the following we address this issue and propose a quantum-dot setup which can be either operated as a spin filter (spin diode) to produce spin polarized currents or as a device to detect (“read-out”) and manipulate single-spin states (single-spin memory). Both effects occur at the single spin level and thus represent the ultimate quantum limit of a spin filter and spin memory¹.

Quantum dots are structures where charge carriers are confined in all three spatial dimensions, usually achieved by electrical gating of a two-dimensional electron gas (2DEG), possibly combined with etching techniques.

¹For a review of earlier spin filter/memory devices operating on a many-spin level we refer to the articles in [4].

Semiconductor quantum dots are typically sized between 10 nm and 1 μm [3], which is on the order of the Fermi wavelength in the host material, leading to a discrete energy spectrum. Such small dots have a charging energy in the meV-range, resulting in quantization of charge on the dot (Coulomb blockade) for temperatures in the sub-Kelvin range. This allows precise control of the number of electrons on the dot, which has been achieved in GaAs heterostructures—starting from zero electrons [82,120]. Quantum dots open up many possibilities in spintronics by providing a versatile system for manipulation of electronic degrees of freedom, in particular the spin, with many tunable parameters such as geometry, energy spectrum, coupling to leads, etc. Electronic properties prominent for atoms like a shell structure or Hund’s rule² have been observed in quantum dots via transport experiments [82,121]. Consequently, quantum dots are sometimes referred to as *artificial atoms*.

In both operation regimes of the proposed device, we will work in the Coulomb blockade regime [3] and consider sequential and cotunneling processes. A new feature of our proposal is that the spin-degeneracy is lifted³ with *different* Zeeman splittings in the dot and in the leads which then results in Coulomb blockade peaks which are uniquely associated with a definite spin state on the dot. The effectiveness of such a spin filter has been demonstrated experimentally in a GaAs lateral quantum dot subjected to an in-plane magnetic field containing just a few electrons (from 0-2) [122]. The resulting spin-filter efficiency was measured to be nearly 100%.

The creation of spin-polarized currents in semiconductor structures have been considered also in tunable ZnSe/Zn_{1-x}Mn_xSe heterostructures where the s-d exchange in the paramagnetic layer gives rise to a spin-dependent potential [123], in ballistic mesoscopic ring systems in the presence of an inhomogeneous magnetic field [124], in a chaotic open quantum dot in the presence of an in-plane magnetic field within a pumping configuration [125] and in tunneling devices where Rashba spin-orbit coupling produces a spin-polarized current [126,127]. A spin filter consisting of an open quantum dot in an in-plane magnetic field has been implemented experimentally. The in-plane magnetic field gives the two spin directions different Fermi wavelengths which results in a spin-dependent interference of transport channels through the dot. Polarization of up to 70 % have been achieved [128].

²Hund’s rule describes the successive filling of an atomic shell with respect to the spin of the added electrons, see e.g. Ref. [78].

³We remark that by breaking the spin-degeneracy Kondo effects are excluded.

The outline of this chapter is as follows. We first describe the proposed setup in terms of detailed calculations and show that a quantum dot in a magnetic field and attached to Fermi liquid leads can work as an efficient spin filter, or when the leads are spin-polarized, as a single spin memory with read-in and read-out capabilities. In single-wall carbon nanotubes quantum dots, the dependence on a magnetic field is mainly given by Zeeman energy, and orbital effects are suppressed since the tube diameter is much smaller than the magnetic length $l_B = (\hbar c/eB)^{1/2}$ for usual laboratory magnetic field strengths $B \sim 1 - 2$ T. This allows for interesting applications in terms of a switchable spin filter with high control. We further discuss how we could use in principle the quantum dot spin filter for spin correlation measurements as needed to measure Bell inequalities.

3.2 Hamiltonian and formalism

Our system consists of a quantum dot (QD) connected to two Fermi-liquid leads which are in equilibrium with reservoirs kept at the chemical potentials μ_l , $l = 1, 2$, where outgoing currents can be measured, see Fig. 3.1. Using a standard tunneling Hamiltonian approach [76], we write the full Hamiltonian as $H_0 + H_T$, where $H_0 = H_L + H_D$ describes the leads and the dot, with H_D including the charging and interaction energies of the dot electrons as well as the Zeeman energy $g\mu_B B$ of their spins in the presence of an external magnetic field $\mathbf{B} = (0, 0, B)$, where g is the effective g-factor. We concentrate first on unpolarized leads and assume that its Zeeman splitting Δ_z^l is negligibly small compared to the one in the quantum dot. This can be achieved e.g. by using InAs for the dot ($g = 15$) attached to GaAs 2DEG leads ($g = -0.44$), or by implanting a magnetic impurity (say Mn) inside a GaAs dot (again attached to GaAs 2DEG leads) with a strongly enhanced electron g-factor due to exchange splitting with the magnetic impurity [129].

In Section 3.6, we will consider the opposite situation with a fully spin polarized lead current, and a much smaller Zeeman splitting on the dot. The tunneling between leads and the quantum dot is described by the perturbation

$$H_T = \sum_{l,k,p,\sigma} t_{lp} c_{lk\sigma}^\dagger d_{p\sigma} + \text{h.c.}, \quad (3.1)$$

where $d_{p\sigma}$ and $c_{lk\sigma}$ annihilate electrons with spin σ in the dot and in the

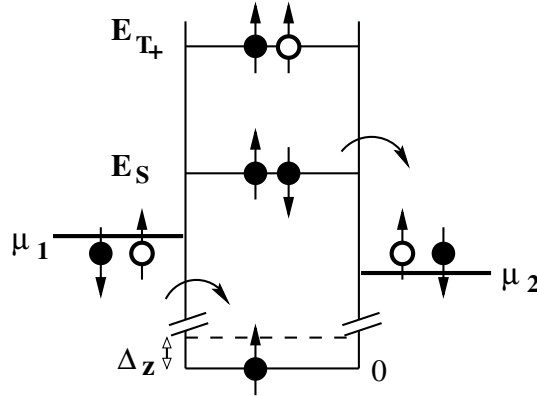


Figure 3.1: The energy diagram of a quantum dot (QD) attached to two leads is shown in the regime where the quantum dot contains an odd number N of electrons with a top-most single electron in the ground state (\uparrow filled circle, and $E_{\uparrow} = 0$). A cotunneling process is depicted (arrows) where two possible virtual states, singlet E_S and triplet E_{T+} , are shown. The parameter $E_S - \mu_1$ can be tuned by the gate voltage to get into the sequential tunneling regime, defined by $\mu_1 \geq E_S \geq \mu_2$, where N on the QD fluctuates between odd and even. For N even, the ground state contains a top-most singlet state with $E_S < \mu_1, \mu_2$.

l th lead, respectively. While the orbital k -dependence of the tunneling amplitude t_{lp} can be safely neglected, this is not the case in general for the quantum dot orbital states p . From now on we concentrate on the Coulomb blockade (CB) regime [3], where the charge in the quantum dot, $\hat{N} = \sum_{p,\sigma} d_{p\sigma}^\dagger d_{p\sigma}$, is quantized, i.e. $\langle \hat{N} \rangle = N$. Next, turning to the dynamics induced by H_T , we introduce the reduced density matrix for the dot, $\rho_D = \text{Tr}_L \rho$, where ρ is the full stationary density matrix, and Tr_L is the trace over the leads. To describe the stationary limit, we use a master equation approach [130] formulated in terms of the dot eigenstates and eigenenergies, $H_D |n\rangle = E_n |n\rangle$, where $n = (\mathbf{n}, N)$. Denoting with $\rho(n) = \langle n | \rho_D | n \rangle$ the stationary probability for the dot to be in the state $|n\rangle$, and with $W(n', n)$ the transition rates between n and n' , the stationary master equation to be solved reads $\sum_n [W(n', n)\rho(n) - W(n, n')\rho(n')] = 0$.

The rates W can be calculated in a standard “golden rule” approach [131] where we go up to 2nd order in H_T , i.e. $W = \sum_l W_l + \sum_{l',l} W_{l'l}$, where $W_l \propto t^2$ is the rate for a tunneling process of an electron from the l th lead

to the dot and vice versa and given as

$$W_l(n', n) = 2\pi \sum_{i_l, f_l} \rho_l(i_l) |\langle f_l, n' | H_T^l | i_l, n \rangle|^2 \delta(\varepsilon_i - \varepsilon_f) \delta_{N', N \pm 1}, \quad (3.2)$$

while $W_{l'l} \propto t^4$ describes the simultaneous tunneling of two electrons from the lead l to the dot and from the dot to the lead l' . The rate for such a higher-order process is given by

$$W_{l',l}(n', n) = 2\pi \sum_{i_{l'}, f_{l'}} \rho_{l'}(i_{l'}) \times \left| \langle f_{l'}, n' \left| H_T \frac{1}{\varepsilon_i - H_0} H_T \right| i_{l'}, n \right|^2 \delta(\varepsilon_i - \varepsilon_f) \delta_{N, N'}.$$

We have introduced the equilibrium density matrix for the leads, $\rho_l(i_l) = \langle i_l | \rho_l | i_l \rangle$, and the eigenstates $|i_l, n\rangle$ and $|f_l, n\rangle$ of H_0 in the initial and final states which are just product states of the leads and the quantum dot. Consequently, $|i_{l'}, n\rangle = |i_l, i_{l'}, n\rangle$, $|f_{l'}, n\rangle = |f_l, f_{l'}, n\rangle$ and $\rho_{i_{l'}}(i_{l'}) = \rho_l(i_l) \rho_{l'}(i_{l'})$. So two regimes of transport through the quantum dot can be distinguished: Sequential tunneling (ST) and cotunneling (CT) [3, 132]. The ST regime is at the degeneracy point, where \hat{N} fluctuates between N and $N' = N \pm 1$, and 1st order transitions are allowed by energy conservation. By using $\text{Tr}_L(\rho_l c_{lk}^\dagger c_{lk}) = f_l(\varepsilon_k) = (1 + \exp[(\varepsilon_k - \mu_l)/k_B T])^{-1}$, and $\sum_{\mathbf{k}} \rightarrow \nu \int d\varepsilon$ we obtain explicit ST rates

$$W_l(n', n) = 2\pi\nu [f_l(\Delta_{n'n}) |A_{lnn'}^\sigma|^2 \delta_{N', N+1} + [1 - f_l(\Delta_{nn'})] |A_{ln'n}^\sigma|^2 \delta_{N', N-1}], \quad (3.3)$$

where $\nu = \sum_k \delta(\varepsilon_F - \varepsilon_k)$ is the lead density-of-states per spin at the Fermi energy ε_F , $\Delta_{n'n} = E_{n'} - E_n$ is the level distance, and we have introduced the matrix elements $A_{ln'n}^\sigma = \sum_p t_{lp} \langle n' | d_{p\sigma} | n \rangle$ (note that n and n' in Eq. (3.3) fix the spin index σ). We remark that the role of the leads is revealed mainly through the lead density-of-states ν at the Fermi energy ε_F . Therefore, the effect of the lead Zeeman energy Δ_z^l on the tunneling rates is small as long as $\Delta_z^l \ll \varepsilon_F$. In the ST regime the current through the quantum dot can be written as

$$I_s = \pm e \sum_{n, n'} W_2(n', n) \rho(n), \quad (3.4)$$

where \pm stands for $N' = N \mp 1$. We emphasize that the rates $W(n, n')$ and thus the current depend on the spin state of the dot electrons via n, n' . The ST current takes a particularly simple form if the voltage bias $\delta\mu = \mu_1 - \mu_2 > 0$ and the temperature T are small compared to the level distance on the dot (the case of interest here), $\delta\mu, k_B T < |\Delta_{mn}|, \forall m, n$, and, thus only the lowest energy levels n, n' participate in the transport [3]. We consider first the case where $N' = N + 1$ with the ST current $I_s = e [W_2(n, n')\rho_{n'} - W_2(n', n)\rho_n]$. The master equation then becomes

$$\begin{aligned} W(n', n)\rho_n &= W(n, n')\rho_{n'} \\ \rho_n + \rho_{n'} &= 1, \end{aligned} \quad (3.5)$$

with rates $W(n, n') = \sum_l W_l(n, n')$, since in the ST regime the solution of the master equation is dominated by the ST rates only, and CT rates can be neglected. In the regime of interest, $\delta\mu, k_B T < |\Delta_{mn}|, \forall m, n$, the omission of the CT processes in the master equation is even exact since the state of the quantum dot can not be changed by these processes (see below). We then obtain for the occupation probability $\rho_n = W(n, n')/[W(n', n) + W(n, n')]$ and $\rho_{n'} = W(n', n)/[W(n', n) + W(n, n')]$. By using $W_l(n, n') = \gamma_l - W_l(n', n)$ we obtain the ST current

$$I_s = \frac{e\gamma_1\gamma_2}{\gamma_1 + \gamma_2} [f_1(\Delta_{n'n}) - f_2(\Delta_{n'n})], \quad N' = N + 1. \quad (3.6)$$

We have defined $\gamma_l = 2\pi\nu |A_{l'n'n'}^\sigma|^2$ which is the tunneling rate through the l th barrier. For $N' = N - 1$, we get again Eq. (3.6) but with $n \leftrightarrow n'$.

In the CT regime the only allowed processes are 2nd order transitions with initial and final electron number on the quantum dot being equal, i.e. $N = N'$, and with the rate

$$\begin{aligned} W_{l'l}(n', n) &= 2\pi\nu^2 \int d\varepsilon f_l(\varepsilon) [1 - f_{l'}(\varepsilon - \Delta_{n'n})] G_{n'n}(\varepsilon) \\ G_{n'n}(\varepsilon) &= \sum_{\sigma, \sigma'} \left| \sum_{n_1} \frac{A_{l'n'n_1}^{\sigma'} A_{l'n n_1}^{\sigma*}}{\varepsilon + \Delta_{n n_1}} + \sum_{n_2} \frac{A_{l'n_2 n}^{\sigma'} A_{l'n_2 n'}^{\sigma*}}{\varepsilon - \Delta_{n' n_2}} \right|^2, \end{aligned} \quad (3.7)$$

where $N_1 = N + 1$, and $N_2 = N - 1$, and thus the two terms in Eq. (3.7) differ by the sequence of tunneling. Our regime of interest here is *elastic* CT where $E_{n'} = E_n$, which holds for $|\Delta_{mn}| > \delta\mu, k_B T, \forall m \neq n$. That means the

system is always in the ground state with $\rho(n) = 1$, and thus the CT current is given by

$$\begin{aligned} I_c &= eW_{21}(n, n) - eW_{12}(n, n) \\ &= e2\pi\nu^2 \int d\varepsilon G_{nn}(\varepsilon)[f_1(\varepsilon) - f_2(\varepsilon)]. \end{aligned} \quad (3.8)$$

We proceed by expanding G_{nn} around $\mu = (\mu_1 + \mu_2)/2$ as $G(\varepsilon) = G(\mu) + (\varepsilon - \mu)G^{(1)}(\mu) + \frac{1}{2}(\varepsilon - \mu)^2G^{(2)}(\mu) + \dots$ where we have dropped the state index n and introduced $G^{(j)}(\varepsilon) \equiv \partial^j G(\varepsilon)/\partial\varepsilon^j$. This expansion is valid as long as we are in the CT regime, i.e. $|\mu \pm \Delta_{nn_i}| > \delta\mu, k_B T$, since $f_1 - f_2$ is only finite for energies ε within a region where $|\varepsilon - \mu| \lesssim \delta\mu, k_B T$. Integrating by parts and using $\varepsilon^m f^{(n)} = 0$ at infinity for $n \geq 1$, and $\int d\varepsilon f^{(n)}(\varepsilon) = -1$ for $n = 1$ and 0 for $n \geq 2$, we only have to retain terms up to $f^{(3)}$ in an expansion of $f_1 - f_2$ around μ . We then obtain the CT current

$$I_c = 2\pi e\nu^2 \delta\mu \left[G_{nn}(\mu) + \frac{1}{6} \left(\pi^2 (k_B T)^2 + \frac{1}{4} (\delta\mu)^2 \right) G_{nn}^{(2)}(\mu) \right]. \quad (3.9)$$

In particular, close to a ST resonance (but still in the CT regime) only one virtual state n_i in $G_{nn}(\mu)$ contributes and for $\delta\mu, k_B T < |\mu \pm \Delta_{nn_i}|$, we only keep the leading order term in Eq. (3.9) and obtain

$$I_c = \frac{e}{2\pi} \frac{\gamma_1 \gamma_2 \delta\mu}{(\mu \pm \Delta_{nn_i})^2}, \quad (3.10)$$

where $+$ stands for $i = 1$, and $-$ for $i = 2$. From Eqs. (3.6) and (3.10) it follows that $I_s \sim \gamma_i$, while $I_c \sim \gamma_i^2$, and therefore $I_c \ll I_s$. Thus, in the CB regime the current as a function of μ (or gate voltage) consists of resonant ST peaks, where \hat{N} on the quantum dot fluctuates between N and $N \pm 1$. The peaks are separated by plateaus, where N is fixed, and where the (residual) current is due to CT.

We note that the tunneling rates γ_l depend on the tunneling path through the matrix elements A_{lmn}^σ . In general, this can lead to a spin-dependence of the current, which, however, is difficult to measure [133]. In contrast to this, we will show now that a much stronger spin dependence can come from the resonance character of the currents I_s and I_c , when the position of a resonance (as function of gate voltage) depends on the spin orientation of the tunneling electron. To proceed we first specify the energy spectrum of the quantum dot

more precisely. In general, the determination of the spectrum of a quantum dot is a complicated many-electron problem [38]. However, it is known from experiment [82, 121, 134] that especially away from orbital degeneracy points (which can be easily achieved by applying magnetic fields [82, 121, 134]) the spectrum is formed mainly by single-particle levels, possibly slightly renormalized by exchange interaction. When exchange interactions become dominant (e.g. for N very small), our analysis of course still applies, since all we require is a sufficiently large energy splitting $\Delta_{n'n}$ between singlet and triplet.

For a quantum dot with N odd there is one unpaired electron in one of the two lowest energy states, $|\uparrow\rangle$ and $|\downarrow\rangle$, with energies E_\uparrow and E_\downarrow , which become Zeeman split due to a magnetic field B , $\Delta_z = |E_\uparrow - E_\downarrow| = \mu_B |gB|$. Let us assume that $|\uparrow\rangle$ is the ground state, and set $E_\uparrow = 0$ for convenience. For N even, the two topmost electrons (with the same orbital wave function), form a spin singlet, $(|\uparrow\downarrow\rangle - |\downarrow\uparrow\rangle)/\sqrt{2}$, with energy E_S . This is the ground state, while the other states, such as three triplets $|T_+\rangle = |\uparrow\uparrow\rangle$, $|T_-\rangle = |\downarrow\downarrow\rangle$, and $|T_0\rangle = (|\uparrow\downarrow\rangle + |\downarrow\uparrow\rangle)/\sqrt{2}$ with energies E_{T_\pm} and E_{T_0} are excited states, because of higher (mostly) single-particle orbital energy.

3.3 Spin filter in the ST regime

First, we consider the ST peak, which separates two plateaus with N and $N + 1$ electrons on the dot, where N is odd (odd-to-even transition). In the regime $E_{T_+} - E_S, \Delta_z > \delta\mu, k_B T$, only ground-state transitions are allowed by energy conservation. The tunneling of spin-up electrons is blocked by energy conservation, i.e. $I_s(\uparrow) = 0$, because it involves excited states $|T_+\rangle$ and $|\downarrow\rangle$. The only possible process is tunneling of spin-down electrons as shown in Fig. 3.2, which leads to a *spin-polarized* ST current, $I_s(\downarrow)$, given by Eq. (3.6), where $\Delta_{n'n} = E_S > 0$ (since $E_\uparrow = 0$). Thus, we have

$$I_s(\downarrow)/I_0 = \Theta(\mu_1 - E_S) - \Theta(\mu_2 - E_S), \quad k_B T < \delta\mu, \quad (3.11)$$

$$I_s(\downarrow)/I_0 = \frac{\delta\mu}{4k_B T} \cosh^{-2} \left[\frac{E_S - \mu}{2k_B T} \right], \quad k_B T > \delta\mu, \quad (3.12)$$

where $I_0 = e\gamma_1\gamma_2/(\gamma_1 + \gamma_2)$. Hence, in the specified regime the dot acts as spin filter through which only spin-down electrons can pass. We mention that “spin-blockade” effects based on spin-selection rules have been considered before [135]. However, these effects are different from the ones found here, in

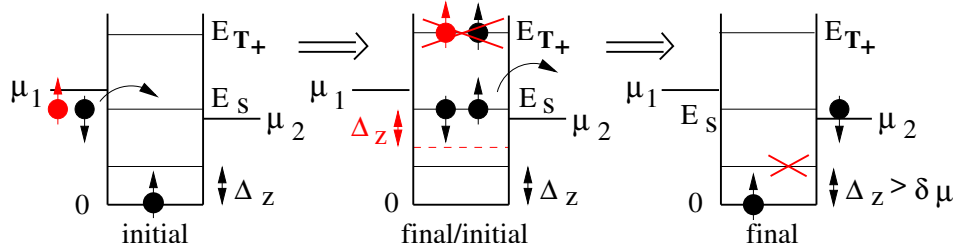


Figure 3.2: The only allowed processes for charge transport through the dot in the ST regime at the odd-to-even transition. A spin-down electron tunnels from lead 1 to the dot forming a singlet and tunnels out again into lead 2. Tunneling of spin-up electrons into (and out-off) the dot is forbidden by energy conservation since this process involves excited states. The resulting current, $I_s(\downarrow)$, is spin-polarized.

particular, they do not lead to spin-polarized currents, they appear only in the non-linear voltage regime for $\Delta S = 1/2$, and they vanish with increasing magnetic field [135]—all in contrast to the case considered here.

Now we consider the ST peak at the transition from even to odd, i.e. when N is even. Then the current is given by Eq. (3.6) with $\Delta_{n'n} = -E_S > 0$. The spin-down current is now blocked, $I_s(\downarrow) = 0$, while spin-up electrons can pass through the dot, with the current $I_s(\uparrow)$ given by (3.11) and (3.12), where E_S has to be replaced by $-E_S$. Because this case is very similar to the previous one with \downarrow replaced by \uparrow , we shall concentrate on the odd-to-even transition only.

Next, we will demonstrate that although CT processes can in general lead to a leakage of unwanted current, this turns out to be a minor effect, and spin filtering works also in the CT regime.

3.4 Spin filter in the CT regime

Above or below a ST resonance, i.e. when $E_S > \mu_{1,2}$ or $E_S < \mu_{1,2}$, the system is in the CT regime. Close to this peak the main contribution to the transport is due to two processes (a) and (c), see Fig. 3.3, where the energy cost of the virtual states, $|\mu - E_S|$, is minimal. According to Eq. (3.10) we have

$$I_c(\downarrow) = \frac{e}{2\pi} \frac{\gamma_1 \gamma_2 \delta \mu}{(\mu - E_S)^2}. \quad (3.13)$$

Thus, we expect the spin filtering of down electrons to work even in the CT regime close to the resonance. However, there are additional CT processes,

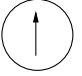
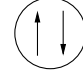
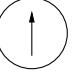
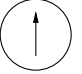
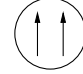
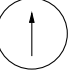
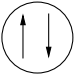
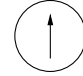
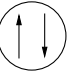
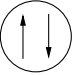
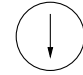
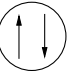
	initial	virtual	final
a	\downarrow 		 \downarrow
b	\uparrow 		 \uparrow
c	\downarrow 	\downarrow  \downarrow	 \downarrow
d	\uparrow 	\uparrow  \uparrow	 \uparrow

Figure 3.3: (a) and (b) are the main processes in the cotunneling regime with N odd if inelastic processes and processes where the dot is not in the ground state are suppressed by the Zeeman energy Δ_z . Only the leading virtual transitions are shown. (c) and (d) visualize the leading cotunneling processes for N even. Here, other processes are suppressed by the energy difference between singlet and triplet, $E_{T_+} - E_S$.

(b) and (d), which involve tunneling of spin-up electrons and lead to a leakage of up-spin. If N is odd (below the resonance), the dot is initially in its ground state (\uparrow), and an incoming spin-up electron can only form a virtual triplet state $|T_+\rangle$ (process (b) in Fig. 3.3). This process contributes to the rate (3.7) with an energy deficit $E_{T_+} - \mu$, so that for the efficiency of spin filtering [defined as $I(\downarrow)/I(\uparrow)$] we obtain in this regime,

$$I_c(\downarrow)/I_c(\uparrow) \simeq \left(1 + \frac{E_{T_+} - E_S}{E_S - \mu}\right)^2, \quad N \text{ odd.} \quad (3.14)$$

Above the resonance, i.e. when N is even and the ground state is the spin-singlet $|S\rangle$, the tunneling of spin-up electrons occurs via the virtual spin-down state (process (d) in Fig. 3.3) with an energy deficit $\Delta_z + \mu - E_S$, which has to be compared to the energy deficit $\mu - E_S$ of the main process (c). Thus, we obtain for the efficiency of the spin filtering in the CT regime

$$I_c(\downarrow)/I_c(\uparrow) \simeq \left(1 + \frac{\Delta_z}{\mu - E_S}\right)^2, \quad N \text{ even.} \quad (3.15)$$

We see that in both cases, above and below the resonance, the efficiency can be made large by tuning the gate voltage to the resonance, i.e. $|\mu - E_S| \rightarrow 0$. Eventually, the system goes to the ST regime, $|\mu - E_S| \lesssim k_B T, \delta\mu$.

3.5 Efficiency of spin filter in the ST regime

As we have seen in Section 3.3, the ST current is completely spin-polarized in the parameter range of interest, thus the leakage of spin filtering in the ST regime is due to CT processes via the excited states triplet $|T_+\rangle$ (if N is odd) and $|\downarrow\rangle$ (if N is even). Using Eqs. (3.10), (3.11), and (3.12) we can estimate this efficiency of spin filtering in the ST regime,

$$I_s(\downarrow)/I_c(\uparrow) \simeq \frac{\min\{\Delta_z^2, (E_{T_+} - E_S)^2\}}{\gamma \max\{k_B T, \delta\mu\}}, \quad (3.16)$$

where we assumed $\gamma_1 \sim \gamma_2 \sim \gamma$ for simplicity. In the ST regime considered here we have $\gamma_i < k_B T, \delta\mu$ [3]. Therefore, if the requirement $k_B T, \delta\mu < \Delta_z, E_{T_+} - E_S$ is satisfied, filtering of spin-down electrons in the ST regime is very efficient, i.e. $I_s(\downarrow)/I_c(\uparrow) \gg 1$. In the quantum regime, $\gamma_i > k_B T, \delta\mu$, tunneling occurs as a Breit-Wigner resonance [3], and $\max\{k_B T, \delta\mu\}$ in Eq. (3.16) has to be replaced by γ_i . Finally, we note that the spin polarization of the transmitted current oscillates between up and down as we change the number of dot electrons N one by one.

The functionality of the spin filter can be tested e.g. with the use of a p-i-n diode [8, 9] which is placed in the outgoing lead 2. Via excitonic photoluminescence, the diode transforms the spin polarized electrons (entering lead 2) into correspondingly circularly polarized photons which can then be detected.

3.6 Spin read-out and spin memory

We consider now the opposite case where the current in the leads is fully spin polarized. Recent experiments have demonstrated that fully spin-polarized carriers can be tunnel-injected from a spin-polarized magnetic semiconductor (III-V or II-VI materials) with large effective g-factor into an unpolarized GaAs system [8, 9]. Another possibility would be to work in the quantum Hall regime where spin-polarized edge states are coupled to a quantum dot [120].

To be specific, we consider the case where $E_{T_+} - E_S + \Delta_z > \delta\mu, k_B T$ with $E_{T_+} > E_S$ ($\Delta_z > k_B T$ is not necessary as long as the spin relaxation time is longer than the measurement time, see below). We assume that the spin polarization of both leads is, say, up and N is odd, see Fig. 3.4. To have only one spin component available in the leads we require that $\Delta_z^l > \varepsilon_F > \Delta_z$.

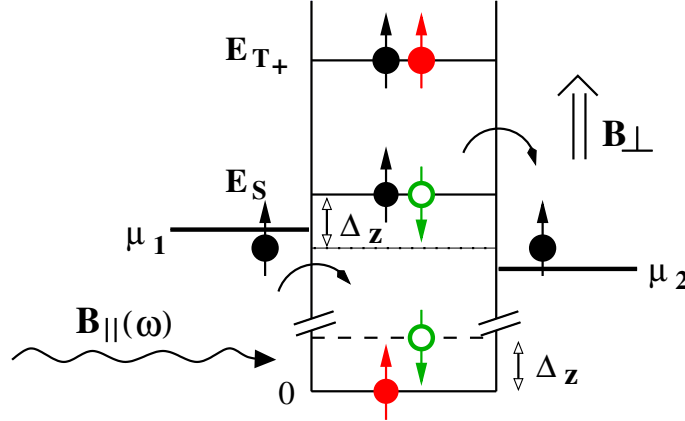


Figure 3.4: The quantum dot as a single-spin memory: The dot is attached to spin-polarized leads where only one spin direction is available at the Fermi energy, say $|\uparrow\rangle$. The quantum dot in its ground state, $|\uparrow\rangle$ and $E_{\uparrow} = 0$, cannot transport a ST current, i.e. $I_s^{\uparrow} = 0$, since the triplet energy $E_{T_+} > \mu \simeq E_S - \Delta_z$ and only small CT processes are allowed. By applying a transverse magnetic field $B_{\parallel}(\omega = \Delta_z)$ we can flip the spin from $|\uparrow\rangle$ to $|\downarrow\rangle$ thereby allowing a finite ST current $I_s^{\downarrow} > 0$ to flow via the singlet. Therefore, the spin state of the dot is detected by the magnitude of the charge current flowing through the dot.

There are now two cases for the current, I^{\uparrow} or I^{\downarrow} , corresponding to a spin up or down on the quantum dot. First, we assume the dot to be in the ground state with its topmost electron-spin pointing up. According to previous analysis [see paragraph before Eqs. (3.11,3.12)], the ST current vanishes, i.e. $I_s^{\uparrow} = 0$, since the tunneling into the level E_{T_+} (and higher levels) is blocked by energy conservation, while the tunneling into E_S is blocked by spin conservation because the leads can provide and take up only electrons with spin up. However, there is again a small CT current, I_c^{\uparrow} , which is given by Eq. (3.13) if E_S is replaced by E_{T_+} . Now we compare this to the second case where the topmost dot-spin is down with additional Zeeman energy $\Delta_z > 0$. Here, the ST current I_s^{\downarrow} is finite, and given by Eqs. (3.11) and (3.12)

with E_S replaced by $E_S - \Delta_z$. Therefore, the ratio $I_s^\downarrow/I_c^\uparrow$ is given by Eq. (3.16) but with the numerator replaced by $(E_{T_+} - E_S + \Delta_z)^2$ since here only the CT-process with an intermediate triplet state is possible. Hence, we see that the dot with its spin up transmits a much smaller current than the dot with spin down. This fact allows the read-out of the spin-state of the (topmost) dot-electron by comparing the measured currents. Furthermore, the spin state of the quantum dot can be changed (“read-in”) by electron spin resonance (ESR) techniques, i.e. by applying a pulse of an ac magnetic field (perpendicular to \mathbf{B}) with resonance frequency $\omega = \Delta_z$ [39]⁴. Thus, the proposed setup functions as a single-spin memory with read-in and read-out capabilities. The relaxation time of the memory is given by the spin relaxation time τ_S on the quantum dot. This time can be expected to exceed 100’s of nanoseconds [7]. We note that this τ_s can be easily measured since it is the time during which I_s^\downarrow is finite before it strongly reduces to I_c^\uparrow . Finally, this scheme can be upscaled: In an array of such quantum dots where each dot separately is attached to in- and outgoing leads (for read-out) we can switch the spin-state of each dot individually by locally controlling the Zeeman splitting Δ_z . This can be done [12] e.g. by applying a gate voltage on a particular dot that pushes the wave function of the dot-electrons into a region of, say, higher effective g-factor⁵.

A detailed analysis of the read-out procedure allows to quantify the measurement efficiency [104]. If the spin on the dot is $|\downarrow\rangle$, then the probability for no electron being transmitted after time t is $P_\downarrow(t) = \exp(-Wt)(1 + Wt)$, where $W = 2I/e$ is the rate of tunneling from one of the leads to the dot. For example, after time $2e/I$ the spin state can be determined with more than 90% probability. For a typical sequential tunneling current on the order of 0.1 – 1 nA [3], this measuring time is 0.3 – 3 ns. This is well below the expected relaxation time of the dot spin [7].

⁴Recently it was demonstrated that the same effect can be achieved via a voltage controlled time-dependent g-factor in a GaAs/Al_xGa_{1-x}As parabolic quantum well [118], which does not need local oscillating magnetic fields.

⁵The induced level shift in the dot can be compensated for by tuning the chemical potentials accordingly.

3.7 Switchable spin filter in carbon nanotubes

Recently, transport measurements on single-wall carbon nanotubes (SWNT) quantum dots [73, 74, 136], multiwall carbon nanotubes quantum dots [75] and in ropes of SWNT quantum dots [137] have demonstrated Coulomb blockade behavior [74, 75, 136, 137], level quantization [73–75, 136, 137] and spin-pairing [74, 75] leading to shell-structure—all very similar to conventional quantum dots in quantum confined 2DEG structures [3, 120, 121].

However, in the two dimensional quantum dots the magnetic length $l_B = (\hbar c/eB)^{1/2}$ can be on the order of the dot diameter for usual laboratory magnetic fields $B \sim 1 - 2$ T. Therefore, the dot orbitals are affected quite sensibly by a B -field, in particular the singlet-triplet splitting $J = E_{T_+} - E_S$ [121, 134]. In a SWNT quantum dot a magnetic field along the tube axis has almost no influence on the electronic orbitals since the diameter d_t of a tube is typically 1-3 nm [101] and therefore $d_t \ll l_B$. As a consequence, the level distance $E_{T_+} - E_S$ is determined solely by the Zeeman energy $\Delta_z = g\mu_B B$ (for given $J(B=0) \equiv J_0 > 0$)⁶ and therefore is a linear function of B . We work around the degeneracy point $B = B_c$ with $B_c = J_0/g\mu_B$ where we have $E_{T_+} = E_S$. The SWNT quantum dot then can act as a switchable spin filter since the degree of spin polarization can be tuned by the B -field very sensitively or can even be reversed completely when we change the two-particle ground state from the singlet $|S\rangle$ ($B < B_c$) where spin down is filtered to the triplet $|T_+\rangle$ ($B > B_c$) where spin up is filtered. The resulting change in the chemical potential of the dot can be compensated for by changing the gate voltage so that the dot is always in the ST-regime $\mu_1 > E^0(2) > \mu_2$. Here, $\mu_{1,2}$ are the chemical potentials of the contacts and $E^0(2)$ denotes the ground state energy for an even number of electrons on the dot (either E_S or E_{T_+}) counted from $E(\uparrow)$. The ideal working regime for the switchable spin filter is

$$J_0 - g\mu_B\Delta B/2, g\mu_B\Delta B/2 > \delta\mu, k_B T. \quad (3.17)$$

This inequality defines the “switching field” ΔB needed to switch from the \downarrow -filter to the \uparrow -filter regime. This requirement guarantees that only ground states can participate in the transport which leads to effective spin filtering,

⁶In SWNT the two-fold subband degeneracy is usually broken [74] with the result that the singlet state is the ground state for an even number of electrons in the SWNT quantum dot [74]. This is also the case for multiwall carbon nanotubes [75] and most probably in ropes of SWNT [137].

see Eq. (3.16). To estimate ΔB we use $\delta\mu \approx k_B T = 10 \mu\text{eV}$ and $g = 2$ [101] and therefore demand $\Delta B > 0.2 \text{ T}$ in view of Eq. (3.17). It was found experimentally [101] that $J_0 \approx 0.1 \text{ meV}$ which corresponds to $B_c \approx 1 \text{ T}$. This is compatible with the requirement $2B_c - \Delta B > 0.2 \text{ T}$.

3.8 Using the spin filter to measure Bell inequalities

One way to detect entanglement is to perform an experiment in which the so-called Bell inequality [42] is violated. The Bell inequality describes corre-

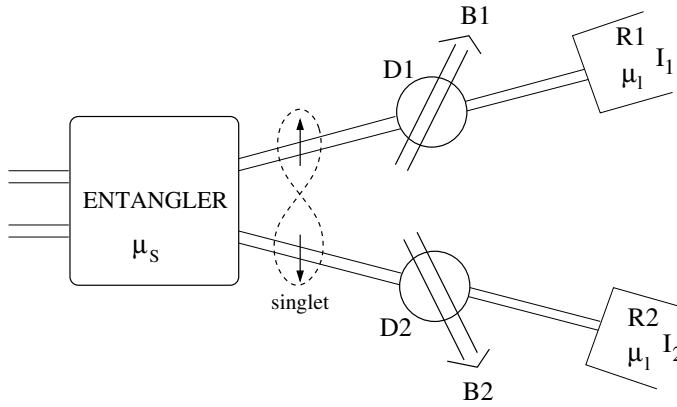


Figure 3.5: The setup for measuring Bell inequalities: The entangler delivers a current of nonlocal singlet spin-pairs due to a bias voltage $\delta\mu = \mu_s - \mu_l$. Subsequently, the two electrons in leads 1 and 2 pass two quantum dots D1 and D2, respectively, which only allow one spin direction, e.g. spin down, to pass the dots. The quantization axes for the spins are defined by the magnetic fields applied to the dots, which are in general different for D1 and D2. Since the quantum dot spin filters act as a spin-to-charge converter, spin correlation measurements as required for measuring Bell inequalities can be reduced to measure current-current fluctuation correlators $\langle \delta I_2(t) \delta I_1(0) \rangle$ in reservoirs R1 and R2 [49, 50].

lations between spin-measurements of pairs of particles within the framework of a *local* theory. The Bell inequality measurement requires that a nonlocal singlet pair, e.g., produced by the spin-entangler, can be measured along three different, not mutually orthogonal, axes defined by unit vectors $\hat{\mathbf{a}}$, $\hat{\mathbf{b}}$ and $\hat{\mathbf{c}}$. We present now briefly the derivation and the philosophy of the Bell

inequality for spin-1/2 particles following Sakurai [131] and will then show how, in qualitative arguments, the quantum dot spin filter combined with noise measurements could be used to measure the Bell inequality.

We consider a large number of particle pairs. In a classical *local* theory we can associate a state with every particle, e.g. of the kind $|\hat{\mathbf{a}}+, \hat{\mathbf{b}}-, \hat{\mathbf{c}}+\rangle$. This particle has the property that the measurement of the observable $\mathbf{S} \cdot \hat{\mathbf{a}}$ yields the result spin up with certainty and similar results for the other axes $\hat{\mathbf{b}}$ and $\hat{\mathbf{c}}$. Note that we do not demand that the spin in the $\hat{\mathbf{a}}$ direction and, let's say, in the $\hat{\mathbf{b}}$ direction can be measured simultaneously with definite values, which would violate quantum mechanics even on a local basis. If we measure $\mathbf{S} \cdot \hat{\mathbf{a}}$, we do not measure $\mathbf{S} \cdot \hat{\mathbf{b}}$ and vice versa. The second particle of the pair must be chosen so that the total spin is always zero as in a singlet. Therefore, we describe the pair by the state $|\hat{\mathbf{a}}+, \hat{\mathbf{b}}-, \hat{\mathbf{c}}+\rangle$ for particle one and $|\hat{\mathbf{a}}-, \hat{\mathbf{b}}+, \hat{\mathbf{c}}-\rangle$ for particle two. An important point to note is that locality is explicitly included in the sense that a measurement of particle one does not influence the measurement of particle two. This statement indeed makes sense if particles one and two are far apart, e.g. separated by the distance between the two leads 1 and 2 in our setup, see Fig. 3.5. The measurement outcome of $\mathbf{S} \cdot \hat{\mathbf{b}}$ of particle two (located in lead 2) is not influenced by whether particle one (located in lead 1) is measured along axes $\hat{\mathbf{a}}$, $\hat{\mathbf{b}}$ or $\hat{\mathbf{c}}$. This is in stark contrast to the singlet state. It can be shown straightforwardly [131] that such a classical local theory leads to the following inequality—known as the Bell inequality

$$P(\hat{\mathbf{a}}+, \hat{\mathbf{b}}+) \leq P(\hat{\mathbf{a}}+, \hat{\mathbf{c}}+) + P(\hat{\mathbf{c}}+, \hat{\mathbf{b}}+). \quad (3.18)$$

Here, $P(i, j)$ is the probability that under a random selection of a pair, particle one has property i and particle two has property j .

In quantum mechanics we describe all pairs by the same singlet state $|S\rangle = (1/\sqrt{2})(|\uparrow\rangle_1 |\downarrow\rangle_2 - |\downarrow\rangle_1 |\uparrow\rangle_2)$ which is entangled. The states $|\uparrow\rangle$ and $|\downarrow\rangle$ can be chosen to be eigenstates of \mathbf{S} in any direction ($|S\rangle$ is isotropic). For the singlet state, the probability $P(\hat{\mathbf{a}}+, \hat{\mathbf{b}}+)$ becomes $P(\hat{\mathbf{a}}+, \hat{\mathbf{b}}+) = (1/2) \sin^2(\theta_{ab}/2)$, where $1/2$ is just the probability to find particle one in the $\hat{\mathbf{a}}, +$ state, and θ_{ab} denotes the angle between axis $\hat{\mathbf{a}}$ and $\hat{\mathbf{b}}$. Therefore, the Bell inequality for the singlet (quantum state) reads

$$\sin^2\left(\frac{\theta_{ab}}{2}\right) \leq \sin^2\left(\frac{\theta_{ac}}{2}\right) + \sin^2\left(\frac{\theta_{cb}}{2}\right). \quad (3.19)$$

For a suitable choice of axes $\hat{\mathbf{a}}$, $\hat{\mathbf{b}}$ and $\hat{\mathbf{c}}$ and range of angles θ_{ij} , this inequality is violated. For simplicity, we choose $\hat{\mathbf{a}}$, $\hat{\mathbf{b}}$ and $\hat{\mathbf{c}}$ to lie in a plane such that $\hat{\mathbf{c}}$ bisects the two directions defined by $\hat{\mathbf{a}}$ and $\hat{\mathbf{b}}$:

$$\theta_{ab} = 2\theta, \quad \theta_{ac} = \theta_{cb} \equiv \theta. \quad (3.20)$$

The Bell inequality Eq. (3.19) is then violated for

$$0 < \theta < \frac{\pi}{2}. \quad (3.21)$$

The violation of the Bell inequality constitutes the most direct proof of a *nonlocal* quantum characteristic, namely entanglement.

We now show that, in principle, the quantum dot spin filters can be used for the necessary spin measurements. We have seen that all we require are the probabilities $P(i, j)$. Again, e.g. $P(\hat{\mathbf{a}}+, \hat{\mathbf{b}}+)$ is the probability that a measurement of $\mathbf{S} \cdot \hat{\mathbf{a}}$ of the particle in lead 1 yields spin up and the measurement of the particle in lead 2 yields also spin up when measured along $\mathbf{S} \cdot \hat{\mathbf{b}}$. The directions $\hat{\mathbf{a}}$, $\hat{\mathbf{b}}$ and $\hat{\mathbf{c}}$ are defined with a magnetic field along these axes⁷ applied to the dots 1 and 2, see Fig. 3.5. The principle of spin-measurement can be formulated in the following way.

Let us suppose we inject electrons into Fermi liquid leads via the entangler. We have shown in Section 2.2 that quantum dots can be used to resonantly inject electrons within some level width γ_e around the energies $\varepsilon_{1,2}$ for leads 1,2. Therefore, the energies of electrons injected into leads 1,2 are well defined. In the case where the entangler is based on the Luttinger liquid or the finite resistance setup, the injection is not resonant and therefore not peaked in energy around some level ε_i above the Fermi energy. In this case, the quantum dot spin filters in the leads themselves produce a resonance with width γ_D , where γ_D is the level broadening of the dot levels due to the coupling to the leads.

The quantum dot in lead $i = 1, 2$ is in the CT regime $(E_S - \mu_l) > k_B T, \gamma_D$. Note that no voltage bias is applied to the quantum dot filters, see Fig. 3.6. The quantum dot contains an odd number of electrons with a spin up ground state⁸. The injected electron has energy ε_i that coincides with the singlet

⁷In our case, see Fig. 3.6, spin down is filtered by the quantum dots. Therefore, if we want to measure the spin e.g. along $\hat{\mathbf{a}}+$, we should apply the magnetic field in $-\hat{\mathbf{a}}$ direction.

⁸According to Section 3.3, an even number of electrons could also be considered for the spin filter.

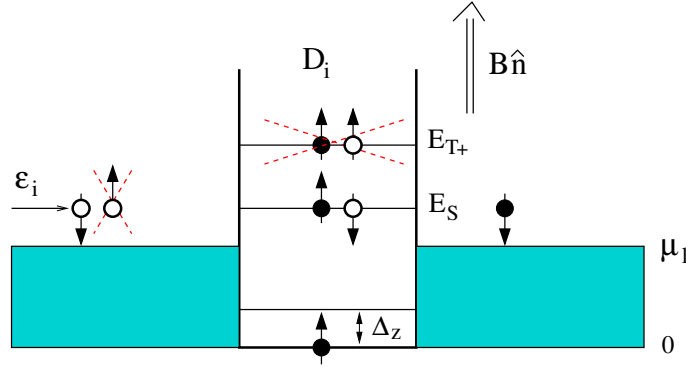


Figure 3.6: The quantum dot as a spin to charge converter: The electrons are injected with energy ε_i in lead $i = 1, 2$ above the chemical potential μ_l . Since these energies can be tuned, with the entanglers or with the filters itself (see text), such that $\varepsilon_i = E_S$ the transmission amplitude is very close to one if the spin is down (resonant transmission) with respect to direction \hat{n} and strongly suppressed if the spin is up (CT process). Therefore, the dot can act as a spin to charge converter where the spin information is converted to the possibility for the electron to pass the dot.

energy E_S (counted from $E_{\uparrow} = 0$). The electron can now tunnel coherently through the dot (resonant tunneling), but only if its spin is down. If the electron spin is up, it can only pass through the dot via the virtual triplet state $|T_+\rangle$ which is strongly suppressed by energy conservation if $E_{T_+} - E_S > \gamma_D$ and $\gamma_e \leq \gamma_D$. In addition, the Zeeman splitting Δ_z should be larger than $E_S - \mu_l$ in order to prevent excitations (spin down state, see Section 3.3) on the dot induced by the tunnel-injected electron. To repeat, the regime of efficient spin-filtering is

$$\gamma_e \leq \gamma_D < (E_S - \mu_l), E_{T_+} - E_S, \text{ and } k_B T < (E_S - \mu_l) < \Delta_z. \quad (3.22)$$

In general, the incoming spin is in some state $|\alpha\rangle$ and will not point along the quantization axis given by the magnetic field direction, i.e. $|\alpha\rangle = \lambda_+ |\uparrow\rangle + \lambda_- |\downarrow\rangle$. This means that by measuring many electrons, all in the same state $|\alpha\rangle$, only a fraction $|\lambda_-|^2$ will be in the down state and $|\lambda_+|^2 = 1 - |\lambda_-|^2$ in the up state. To be specific: The probability that an electron passes through the filter is $|\lambda_-|^2$, provided that the transmission probability for a spin down electron is one (and zero for spin up), which is the case exactly at resonance $\varepsilon_i = E_S$ and for equal tunneling barriers on both sides of the dot [2]. So

in principle, we have to repeat this experiment many times, i.e. with many singlets to get $|\lambda_+|^2$ or $|\lambda_-|^2$. But this is automatically provided by our entangler which exclusively delivers (pure) singlet states, one by one and such that there is a well defined (average) time between subsequent pairs which is much larger than the delay time within one pair, see Chapter 2. Therefore, we can resolve single singlet pairs. The spin filter acts as a spin to charge converter where the spin information is transferred into the information of the possibility that the electron charge passes through the quantum dot.

But how do we measure the successful passing of the electron through the dot? The joint probability $P(i, j)$ quantifies correlations between spin measurements in lead 1 and 2 of the same entangled pair. Thus, this quantity should be directly related to the current-current fluctuation correlator $\int_{-\infty}^{+\infty} dt \langle \delta I_2(t) \delta I_1(0) \rangle$ measured in the reservoirs R_1 and R_2 if the filters are operated in the regime where only the spin direction to be measured can pass the dot. The current fluctuation operator in reservoir $i = 1, 2$ is defined as $\delta I_i(t) = I_i(t) - \langle I_i \rangle$. This quantity can be measured via the power spectrum of the shot noise $S(\omega) = \int_{-\infty}^{+\infty} dt e^{i\omega t} \langle \delta I_2(t) \delta I_1(0) \rangle$ at zero frequency ω . Indeed, it was shown in Ref. [67] that $P(\hat{\mathbf{a}}\eta, \hat{\mathbf{b}}\eta') \propto S_{\eta, \eta'}(\hat{\mathbf{a}}, \hat{\mathbf{b}})$ where the zero frequency cross correlator is

$$S_{\eta, \eta'}(\hat{\mathbf{a}}, \hat{\mathbf{b}}) = 2 \int_{-\infty}^{+\infty} dt \langle \delta I_{\eta' \hat{\mathbf{b}}}(t) \delta I_{\eta \hat{\mathbf{a}}}(0) \rangle. \quad (3.23)$$

With η and η' we denote the spin directions ($\eta, \eta' = \uparrow, \downarrow$) with respect to the chosen axes $\hat{\mathbf{a}}$ and $\hat{\mathbf{b}}$, respectively. The proportionality factor between $P(\hat{\mathbf{a}}\eta, \hat{\mathbf{b}}\eta')$ (the quantity of interest) and the cross correlator $S_{\eta, \eta'}(\hat{\mathbf{a}}, \hat{\mathbf{b}})$ can be eliminated by deviding $S_{\eta, \eta'}(\hat{\mathbf{a}}, \hat{\mathbf{b}})$ with $\sum_{\eta, \eta'} S_{\eta, \eta'}(\hat{\mathbf{a}}, \hat{\mathbf{b}})$ [67]. It was further pointed out in Ref. [67] that the correlator $\langle \delta I_{\eta' \hat{\mathbf{b}}}(t) \delta I_{\eta \hat{\mathbf{a}}}(0) \rangle$ is only finite within the correlation time⁹ $\tau_c = \hbar/\gamma_e$, i.e. for $|t| \lesssim \tau_c$. This sets some additional requirements to our entangler setups. The average time between subsequent arrivals of entangled pairs should be larger than this correlation time. This leads to the constraint

$$2e/I > \hbar/\gamma_e, \quad (3.24)$$

where I denotes the current of entangled pairs, i.e. the pair-split current I_1 calculated for various entangler systems in Chapter 2. The requirement Eq.

⁹In Ref. [67], γ_e is replaced by the voltage bias $\delta\mu$ since no resonant injection, i.e. no quantum dots, are considered.

(3.24) can always be satisfied in our superconductor entanglers due to the weak tunneling regime.

We conclude that the zero frequency correlator $S_{\eta,\eta'}(\hat{\mathbf{a}}, \hat{\mathbf{b}})$, which is directly related to $P(\hat{\mathbf{a}}\eta, \hat{\mathbf{b}}\eta')$, needed as the input to the Bell inequality Eq. (3.18), combined with the spin filter, can be measured by a coincidence counting measurement of charges in the reservoirs R_1 and R_2 that collects statistics over a large number of pairs, all in the same singlet spin-state.

3.9 Conclusion

In conclusion, we have shown that a quantum dot in the Coulomb blockade regime and attached to leads can be operated as an efficient spin filter at the single-spin level. Conversely, if the leads are spin-polarized, the spin state of the quantum dot can be read-out by a traversing current which is (nearly) blocked for one spin state while it is unblocked for the opposite spin state. We pointed out that carbon nanotubes could be used as switchable spin filters with good control. In the last section of this Thesis, we discussed the possibility to use the spin filter as a spin to charge converter useful for measuring spin-spin correlation functions (Bell inequalities) via charge currents.

Appendix A

Suppression of virtual states with both electrons in the leads

We have stated in Section 2.2 that the contributions of virtual states where two electrons are simultaneously in the leads are negligible. Here, we estimate this contribution and show that indeed it is suppressed by $\gamma_L/\delta\mu < 1$ (here the spin of the electrons is not important, and we set $\gamma_1 = \gamma_2 = \gamma_L$ for simplicity). First we consider the dominant transition from $|DD\rangle$ back to $|DD\rangle$ with the tunneling of only one electron to the lead, i.e. a sequence of the type $|DD\rangle \rightarrow |LD\rangle \rightarrow |DD\rangle$. From now on we impose the resonance condition $\epsilon_l = 0$, and we find for the amplitude [cf. Eqs. (2.18, 2.19)]

$$A_{DL} = \langle DD | H_{DL} \frac{1}{i\eta - H_0} H_{DL} | DD \rangle = -i\gamma_L - \frac{\gamma_L}{\pi} \ln \left(\frac{\epsilon_c}{\delta\mu} \right). \quad (\text{A.1})$$

We compare this amplitude A_{DL} with the amplitude A_{LL} of the lowest-order process of tunneling of two electrons via the virtual state $|LL\rangle$, where both electrons are simultaneously in the leads, i.e. the sequence $|DD\rangle \rightarrow |LD\rangle \rightarrow |LL\rangle \rightarrow |DL\rangle \rightarrow |DD\rangle$. We find for the amplitude of this process

$$\begin{aligned} A_{LL} &= \langle DD | H_{DL} \left(\frac{1}{i\eta - H_0} H_{DL} \right)^3 | DD \rangle \\ &= \sum_{\mathbf{k}\mathbf{k}'} \frac{|T_{DL}|^4}{(i\eta - \epsilon_{\mathbf{k}} - \epsilon_{\mathbf{k}'}) (i\eta - \epsilon_{\mathbf{k}})} \left[\frac{1}{i\eta - \epsilon_{\mathbf{k}}} + \frac{1}{i\eta - \epsilon_{\mathbf{k}'}} \right], \quad (\text{A.2}) \end{aligned}$$

where the first term in the bracket results from the sequence of, say, electron 1 tunneling into lead 1, then electron 2 tunneling into lead 2, then electron

2 tunneling back into dot 2, and finally electron 1 tunneling back into dot 1. While the second term in the bracket results from the sequence where the order of tunneling back to the dots is reversed, i.e. electron 1 tunnels back to its dot before electron 2 does. Note that due to this two terms in the bracket the two-particle pole in Eq. (A.2) cancels. Replacing $\sum_{\mathbf{k}}(\dots)$ with $\nu_L \int_{-\delta\mu}^{\epsilon_c} d\epsilon(\dots)$, we can write

$$\begin{aligned}
 A_{LL} &= \frac{\gamma_L^2}{(2\pi)^2} \int_{-\delta\mu}^{\epsilon_c} \frac{d\epsilon'}{i\eta - \epsilon'} \int_{-\delta\mu}^{\epsilon_c} \frac{d\epsilon}{(i\eta - \epsilon)^2} \\
 &= \frac{\gamma_L^2}{2\pi^2 \delta\mu} \left[i\pi + \ln \left(\frac{\epsilon_c}{\delta\mu} \right) \right]. \tag{A.3}
 \end{aligned}$$

Thus, comparing A_{DL} with A_{LL} , we see that indeed a virtual state involving two electrons simultaneously in the leads is suppressed by a factor of $\gamma_L/\delta\mu$ compared to the one with only one electron in the leads.

Appendix B

Electron hole pair excitation

In this appendix, we consider a tunnel process where the two electrons starting from the superconductor tunnel over different dots but during the process of repeated tunneling from the dots to the leads and back to the dots an electron from the Fermi sea hops on one of the dots (say dot 1) when this dot is empty. In principle, such contributions could destroy the desired entanglement since then a “wrong” spin can hop on the dot and the electron on the other dot (dot 2) would no longer be entangled with this electron (while the original partner electron disappears in the reservoir provided by the Fermi sea). We show now that in the regime $\delta\mu > \gamma_l$ such electron-hole pair processes due to the Fermi sea are suppressed. We start with our consideration when the two electrons, after the Andreev process, are each on a different dot forming the $|DD\rangle$ -state (we neglect spin and set $\gamma_1 = \gamma_2 = \gamma_L$ in this consideration for simplicity). Instead of the amplitude $\langle pq|T'|DD\rangle$ calculated in Eq. (2.17) we consider now the following process

$$\begin{aligned}
 A_{eh} &= \langle \bar{p}\bar{q}|T'|\overline{DD}\rangle \\
 &\times \left\{ \langle \overline{DD}|\frac{1}{i\eta-H_0}H_{D_1L_1} \sum_{n=0}^{\infty} \left(\frac{1}{i\eta-H_0}H_{D_2L_2}\right)^{2n} \right. \\
 &\quad \left. \times \frac{1}{i\eta-H_0}H_{D_1L_1}|DD\rangle \right\} \\
 &\times \langle DD|\sum_{m=0}^{\infty} \left(\frac{1}{i\eta-H_0}H_{DL}\right)^{2m}|DD\rangle. \tag{B.1}
 \end{aligned}$$

The new sequence of interest in Eq. (B.1) is the amplitude containing the sum over n . For instance, let us consider the $n = 0$ term, $\langle \overline{DD}|\left(\frac{1}{i\eta-H_0}H_{D_1L_1}\right)^2|DD\rangle$, where we assume that the electron-hole excitation occurs in, say, lead 1. From

$|DD\rangle$, the tunnel Hamiltonian $H_{D_1L_1}$ takes the electron from dot 1 to the state \mathbf{k} in lead 1. Instead of tunneling back of this electron to dot 1, an electron from the state \mathbf{k}' with energy $\epsilon_{\mathbf{k}'} < -\delta\mu$ from the Fermi sea of lead 1 hops on dot 1. Now the dot-lead system is in the state $|\overline{DD}\rangle = d_1^\dagger d_2^\dagger a_{1\mathbf{k}'} a_{1\mathbf{k}}^\dagger |i\rangle$. The sum over n resums the hopping back and forth of electron 2 from D_2 to D_2 , resulting in the replacement of η in $H_{D_1L_1}(i\eta - H_0)^{-1}H_{D_1L_1}$ by $\gamma_L/2$. We perform the further resummation in Eq. (B.1) with this Fermi sea electron on dot 1 and the other electron still on dot 2, assuming that electron 1 in the state \mathbf{k} in lead 1 is in its final state (and not a virtual state). All the resummation processes in Eq. (B.1) are similar to the ones already explained in the main text, except for having now an excitation with energy $\epsilon_{\mathbf{k}} - \epsilon_{\mathbf{k}'} > 0$. The final state $|\overline{pq}\rangle$ consists of two electrons in the lead states \mathbf{p} and \mathbf{q} (their multiple tunneling is resummed in T') and of the excitation with energy $\epsilon_{\mathbf{k}} - \epsilon_{\mathbf{k}'}$, so $|\overline{pq}\rangle = a_{1\mathbf{p}}^\dagger a_{2\mathbf{q}}^\dagger a_{1\mathbf{k}'} a_{1\mathbf{k}}^\dagger |i\rangle$. The normalized correction to the current, I_{eh}/I_1 , can be obtained by summing $|A_{eh}|^2/I_1$ over the final states $|\overline{pq}\rangle$, and thus we arrive at the following integral for $\epsilon_l = 0$, retaining only leading terms in $\gamma_L/\delta\mu$, and using energy conservation, $\epsilon_{\mathbf{k}} - \epsilon_{\mathbf{k}'} + \epsilon_{\mathbf{p}} + \epsilon_{\mathbf{q}} = 0$,

$$\begin{aligned} \frac{I_{eh}}{I_1} &= \left(\frac{\gamma_L}{2\pi}\right)^3 \iiint_{-\delta\mu}^{+\infty} d\epsilon_{\mathbf{k}} d\epsilon_{\mathbf{p}} d\epsilon_{\mathbf{q}} \\ &\times \frac{1 - \Theta(\epsilon_{\mathbf{k}} + \epsilon_{\mathbf{p}} + \epsilon_{\mathbf{q}} + \delta\mu)}{[\epsilon_{\mathbf{k}}^2 + (\gamma_L/2)^2][\epsilon_{\mathbf{p}}^2 + (\gamma_L/2)^2][\epsilon_{\mathbf{q}}^2 + (\gamma_L/2)^2]}. \end{aligned} \quad (\text{B.2})$$

We evaluate the integral in leading order and find

$$\frac{I_{eh}}{I_1} = \frac{3}{2\pi^2} \left(\frac{\gamma_L}{\delta\mu}\right)^2 \ln\left(\frac{\delta\mu}{\gamma_L}\right). \quad (\text{B.3})$$

We see now that the current involving an electron-hole pair, I_{eh} , is suppressed compared to the main contribution I_1 (see Eq. (2.24)) by a factor of $(\gamma_L/\delta\mu)^2$.

Appendix C

Finite size diagonalization of the LL-Hamiltonian

Here, we derive the diagonalized form of the Luttinger liquid Hamiltonian [Eq. (2.55)] including terms of order $1/L$, which describe integer charge and spin excitations. For simplicity, we consider only one Luttinger liquid and will therefore suppress the subscript n for the leads. We start with the exact bosonization dictionary for the Fermi-operator for electrons on branch $r = \pm$ [86, 87],

$$\begin{aligned} \psi_{rs}(x) = \lim_{\alpha \rightarrow 0} \frac{U_{r,s}}{\sqrt{2\pi\alpha}} \exp \left\{ ir(p_F - \pi/L)x + \frac{ir}{\sqrt{2}} \left(\phi_\rho(x) \right. \right. \\ \left. \left. + s\phi_\sigma(x) - r(\theta_\rho(x) + s\theta_\sigma(x)) \right) \right\}. \end{aligned} \quad (\text{C.1})$$

The $U_{r,s}$ -operator (often denoted as Klein factor) is unitary and decreases the number of electrons with spin s on branch r by one. This operator also ensures the correct anticommutation relations for $\psi_{rs}(x)$. The normal ordered charge density operator is $\rho(x) = \sum_{sr} : \psi_{rs}^\dagger(x) \psi_{rs}(x) :$, where $: \cdot :$ measures the corresponding quantity relative to the ground state \cdot . The normal ordered spin density operator is defined by $\sigma^z(x) = \sum_{sr} s : \psi_{rs}^\dagger(x) \psi_{rs}(x) :$. In addition, one can define (bare) current density operators for charge $j_\rho(x) = \sum_{sr} r \psi_{rs}^\dagger(x) \psi_{rs}(x)$, and for the spin $j_\sigma(x) = \sum_{sr} rs \psi_{rs}^\dagger(x) \psi_{rs}(x)$, respectively. Note that the current density has not to be normal ordered since its ground state expectation value vanishes. The normal ordered product $: \psi_{rs}^\dagger(x) \psi_{rs}(x) :$ is calculated according to

$$: \psi_{rs}^\dagger(x) \psi_{rs}(x) := \lim_{\Delta x \rightarrow 0} : \psi_{rs}^\dagger(x + \Delta x) \psi_{rs}(x) : \cdot \quad (\text{C.2})$$

By expanding the operator product in Eq. (C.2) within the normal-order sign, the right-hand side of Eq. (C.2) equals $(1/2\pi)\partial_x(\phi_\rho(x) + s\phi_\sigma(x) - r(\theta_\rho(x) + s\theta_\sigma(x)))/\sqrt{2}$, from which one easily finds

$$\rho(x) = \frac{\sqrt{2}}{\pi}\partial_x\phi_\rho(x), \quad \sigma^z(x) = \frac{\sqrt{2}}{\pi}\partial_x\phi_\sigma(x), \quad (\text{C.3})$$

and for the current densities

$$j_\rho(x) = -\sqrt{2}\Pi_\rho(x), \quad j_\sigma(x) = -\sqrt{2}\Pi_\sigma(x). \quad (\text{C.4})$$

The field $\Pi_\nu(x)$ is related to $\theta_\nu(x)$ by $\partial_x\theta_\nu(x) = \pi\Pi_\nu(x)$. We decompose the phase fields into $\phi_\nu(x) = \phi_\nu^P(x) + \phi_\nu^0(x)$ and $\Pi_\nu(x) = \Pi_\nu^P(x) + \Pi_\nu^0(x)$, where the part with non-zero momentum ϕ_ν^P and Π_ν^P can be expanded in a series of normal modes

$$\phi_\nu^P(x) = \frac{1}{\sqrt{L}} \sum_{p \neq 0} \frac{1}{\sqrt{2\omega_{p\nu}}} e^{ipx} e^{-\alpha|p|/2} (b_{\nu p} + b_{\nu-p}^\dagger), \quad (\text{C.5})$$

and for the canonical momentum

$$\Pi_\nu^P(x) = \frac{-i}{\sqrt{L}} \sum_{p \neq 0} \sqrt{\frac{\omega_{p\nu}}{2}} e^{ipx} e^{-\alpha|p|/2} (b_{\nu p} - b_{\nu-p}^\dagger). \quad (\text{C.6})$$

These fields have to satisfy bosonic commutation relations $[\phi_\nu^P(x), \Pi_\mu^P(x')] = i\delta_{\nu\mu}(\delta(x-x') - 1/L)$, which in turn demands $[b_{\nu p}, b_{\mu p'}^\dagger] = \delta_{\nu\mu}\delta_{pp'}$ and $[b_{\nu p}, b_{\mu p'}] = [b_{\nu p}^\dagger, b_{\mu p'}^\dagger] = 0$. The zero mode parts ϕ_ν^0 and Π_ν^0 can be found by considering the integrated charge (spin) and charge- (spin)-currents, respectively. For instance the integrated charge density $\sum_{rs} N_{rs} = \int dx \rho(x) = (\sqrt{2}/\pi)(\phi_\rho(L/2) - \phi_\rho(-L/2)) = (\sqrt{2}/\pi)(\phi_\rho^0(L/2) - \phi_\rho^0(-L/2))$. Similar results are obtained for the other density operators, which then implies the zero modes to be $\phi_\nu^0(x) = (\pi/L)(N_{+\nu} + N_{-,\nu})x$ and $\Pi_\nu^0 = -(1/L)(N_{+\nu} - N_{-,\nu})$, where $N_{r\rho/\sigma} = (N_{r\uparrow} \pm N_{r\downarrow})/\sqrt{2}$. The Luttinger liquid-Hamiltonian [Eq. (2.55)] is then diagonalized by the following expansion of the bosonic fields

$$\begin{aligned} \phi_\nu(x) = & \sum_{p \neq 0} \sqrt{\frac{\pi K_\nu}{2|p|L}} e^{ipx} e^{-\alpha|p|/2} (b_{\nu p} + b_{\nu-p}^\dagger) \\ & + \frac{\pi}{L}(N_{+\nu} + N_{-,\nu})x, \end{aligned} \quad (\text{C.7})$$

and for the canonical conjugate momentum operator,

$$\begin{aligned} \Pi_\nu(x) &= -i \sum_{p \neq 0} \sqrt{\frac{|p|}{2\pi L K_\nu}} e^{ipx} e^{-\alpha|p|/2} (b_{\nu p} - b_{\nu-p}^\dagger) \\ &\quad - \frac{1}{L} (N_{+\nu} - N_{-,\nu}), \end{aligned} \quad (\text{C.8})$$

where we have used $\omega_{p\nu} = |p|/K_\nu\pi$. For the operator $K_L = H_L - \mu_l N$ we then obtain

$$\begin{aligned} K_L &= \sum_{\nu=\rho,\sigma} \left\{ \sum_{p \neq 0} u_\nu |p| b_{\nu p}^\dagger b_{\nu p} + \frac{2\pi}{L} \left[\frac{u_\nu}{K_\nu} (N_{+\nu} + N_{-,\nu})^2 \right. \right. \\ &\quad \left. \left. + u_\nu K_\nu (N_{+\nu} - N_{-,\nu})^2 \right] \right\}. \end{aligned} \quad (\text{C.9})$$

In Eq. (C.9) we have subtracted the zero point energy $(1/2) \sum_{p \neq 0, \nu} u_\nu |p|$, which originates from an infinite filled Dirac sea of negative energy particle states in the Luttinger liquid-model. The zero modes in Eqs. (C.7) and (C.8) give rise to contributions of order $1/L$ in the Hamiltonian (C.9), and they are also responsible for a shift of the Fermi wavenumber p_F , appearing in the Fermionic field operator $\psi_{ns}(x)$, by a contribution of the same order. Since we are only interested in the thermodynamic limit, we have neglected the zero mode contributions in explicit calculations in the main text.

Appendix D

Two-particle correlation function for a LL

In this appendix, we outline the calculation of the two-particle correlation functions appearing in Eqs. (2.81) and (2.83). We start by writing the Luttinger liquid electron operator for an electron at position x at time t and in branch $r = \pm$ with spin s as¹

$$\psi_{rs}(x, t) = \lim_{\alpha \rightarrow 0} \frac{\eta_{rs}}{\sqrt{2\pi\alpha}} e^{i\Phi(x,t)}. \quad (\text{D.1})$$

Since $\Phi(x, t)$ is linear in Bose operators (see Eqs. (2.56), (2.64) and (2.65)) we can use the following properties: For operators A and B linear in Bose creation and annihilation operators we have

$$e^A e^B = e^{A+B} e^{\frac{1}{2}[A,B]} \quad (\text{D.2})$$

and the relation [78]

$$\langle e^A \rangle = e^{\frac{1}{2}\langle A^2 \rangle}. \quad (\text{D.3})$$

From these two properties it is easily seen that

$$\begin{aligned} \langle e^A e^B \rangle &= \langle e^{A+B} \rangle e^{\frac{1}{2}[A,B]} \\ &= e^{\frac{1}{2}\langle (A+B)^2 \rangle + \frac{1}{2}[A,B]} \\ &= e^{\langle AB + \frac{A^2+B^2}{2} \rangle}. \end{aligned} \quad (\text{D.4})$$

¹The lead index $n = 1, 2$ is not necessary here.

The last line in (D.4) follows from the fact that $[A, B]$ is a C-number and therefore $[A, B] = \langle [A, B] \rangle = \langle AB \rangle - \langle BA \rangle$. Similar, for a four-point correlation function we can write

$$\langle e^A e^B e^C e^D \rangle = \langle e^{A+B} e^{C+D} \rangle e^{\frac{1}{2}[A,B] + \frac{1}{2}[C,D]} \quad (\text{D.5})$$

and we can again perform the average in the exponent, i.e. $\langle e^{A+B} e^{C+D} \rangle = e^{\langle ZQ + \frac{Z^2 + Q^2}{2} \rangle}$ since $Z \equiv A + B$ and $Q \equiv C + D$ are still linear in Bose creation and annihilation operators. We can use these results to calculate the two-particle Luttinger liquid correlation functions appearing in Eqs. (2.80) and (2.82). For a general correlator of the form as presented in Eq. (2.80) we then obtain

$$\begin{aligned} & \left\langle \psi_{rs}(x_4, t_4) \psi_{r'-s}(x_3, t_3) \psi_{r'-s}^\dagger(x_2, t_2) \psi_{rs}^\dagger(x_1, t_1) \right\rangle \\ &= \frac{1}{(2\pi\alpha)} e^{\left\langle \Phi_{r'-s}(x_3, t_3) \Phi_{r'-s}(x_2, t_2) - \left(\frac{\Phi_{r'-s}^2(x_3, t_3) + \Phi_{r'-s}^2(x_2, t_2)}{2} \right) \right\rangle} \\ & \times \frac{1}{(2\pi\alpha)} e^{\left\langle \Phi_{rs}(x_4, t_4) \Phi_{rs}(x_1, t_1) - \left(\frac{\Phi_{rs}^2(x_4, t_4) + \Phi_{rs}^2(x_1, t_1)}{2} \right) \right\rangle} \\ & \times e^{\langle \Phi_{rs}(x_4, t_4) \Phi_{r'-s}(x_2, t_2) + \Phi_{r'-s}(x_3, t_3) \Phi_{rs}(x_1, t_1) - \Phi_{rs}(x_4, t_4) \Phi_{r'-s}(x_3, t_3) - \Phi_{r'-s}(x_2, t_2) \Phi_{rs}(x_1, t_1) \rangle}. \end{aligned} \quad (\text{D.6})$$

In the correlator Eq. (2.80) we use $x_1 = x_2 = x_3 = x_4 = 0$ and $t_4 = t - t''$, $t_3 = t$, $t_2 = t'$, $t_1 = 0$. The first two lines in Eq. (D.6) are the single-particle correlation functions presented in Eq. (2.67) with the result Eq. (2.68).

We continue the calculation for the general case Eq. (D.6). All we need are correlation functions of the form $\langle \Phi_{rs}(x, t) \Phi_{r's'}(x', t') \rangle$. Using the bosonization dictionary Eq. (2.56) and the Fourier decomposition of the phase fields Eqs. (2.64) and (2.65) we obtain for zero temperature

$$\begin{aligned} & \langle \Phi_{rs}(x, t) \Phi_{r's'}(x', t') \rangle \\ &= \sum_{\substack{p \neq 0 \\ \nu = \rho, \sigma}} \frac{s_\nu s'_\nu \pi K_\nu}{4L|p|} e^{-\alpha|p|} e^{ip(x-x') - iu_\nu|p|(t-t')} \left(r + \frac{\text{sgn}(p)}{K_\nu} \right) \left(r' + \frac{\text{sgn}(p)}{K_\nu} \right). \end{aligned} \quad (\text{D.7})$$

In Eq. (D.7), $p = 2\pi n/L$, $n = \pm 1, \pm 2, \dots$ with L the length of the Luttinger liquid and $s_\nu = 1$ for $\nu = \rho$ and $s_\nu = s$ for $\nu = \sigma$ with $s = +, -$ corresponding to spin \uparrow, \downarrow . To account for the p -dependence of the interaction parameters K_ν we introduce a cut-off Λ which is finite and on the order of the Fermi wavelength in the Luttinger liquid, i.e. $\Lambda \sim 1/p_F$. We then assume that $K_\nu(p) = K_\nu, u_\nu(p) = u_\nu$ for $|p| < 1/\Lambda$ and $K_\nu(p) = 1, u_\nu(p) = v_F$ for $|p| > 1/\Lambda$. Accordingly, we split the sum over wavenumbers p in Eq. (D.7) into terms which are weighted either at small or at large wavenumbers. For instance the term $(K_\nu^{-1} + rr'K_\nu)$ we write as $(K_\nu^{-1} + rr'K_\nu) = (K_\nu^{-1} + rr'K_\nu - (1 + rr')) + (1 + rr')$. The first bracket will only be finite for $|p| < 1/\Lambda$ and we therefore can apply a cut-off function $e^{-\Lambda|p|}$ in the addend containing this term. The remaining part $(1 + rr')$ is treated in a similar fashion: Adding and subtracting $e^{-\Lambda|p|}$ we can write $(1 + rr') = (1 + rr')(1 - e^{-\Lambda|p|} + e^{-\Lambda|p|})$. The term $(1 + rr')(1 - e^{-\Lambda|p|})$ is then weighted at large wavenumbers $|p| > 1/\Lambda$ and we will replace u_ν by v_F in the corresponding p -sum whereas $(1 + rr')e^{-\Lambda|p|}$ is weighted at small wavenumbers $|p| < 1/\Lambda$ and we replace $u_\nu(p)$ by u_ν in the sum involving that term. By applying this cut-off procedure and using the identities (for $L \rightarrow \infty$)

$$\begin{aligned} & \sum_{p \neq 0} \frac{e^{-\alpha|p|}}{|p|} e^{ip(x-x') - iu_\nu|p|(t-t')} \\ &= -\frac{L}{\pi} \ln \left(\frac{2\pi}{L} \prod_{R=+,-} \sqrt{\alpha + i(u_\nu(t-t') - R(x-x'))} \right) \end{aligned} \quad (\text{D.8})$$

and

$$\begin{aligned} & \sum_{p \neq 0} \frac{e^{-\alpha|p|}}{|p|} e^{ip(x-x') - iu_\nu|p|(t-t')} \text{sgn}(p) \\ &= -\frac{L}{2\pi} \ln \left(\frac{\alpha + i(u_\nu(t-t') - (x-x'))}{\alpha + i(u_\nu(t-t') + (x-x'))} \right), \end{aligned} \quad (\text{D.9})$$

true for any cut-off $\alpha > 0$, we obtain for the average

$$\begin{aligned}
& e^{\langle \Phi_{rs}(x,t) \Phi_{r's'}(x',t') \rangle} \\
&= \prod_{\nu=\rho,\sigma} \left(\frac{2\pi}{L} \prod_{R=+,-} \sqrt{\Lambda + i(u_\nu(t-t') - R(x-x'))} \right)^{-\frac{1}{4}s_\nu s'_\nu (K_\nu^{-1} + rr' K_\nu)} \\
&\times \prod_{\nu=\rho,\sigma} \prod_{R=+,-} \left(\frac{\Lambda + i(v_F(t-t') - R(x-x'))}{\alpha + i(v_F(t-t') - R(x-x'))} \right)^{\frac{1}{8}s_\nu s'_\nu (1+rr')} \\
&\times \prod_{\nu=\rho,\sigma} \left(\frac{\Lambda + i(v_F(t-t') - (x-x'))}{\Lambda + i(x-x' + v_F(t-t'))} \right)^{\frac{1}{8}s_\nu s'_\nu (r+r')} \\
&\times \prod_{\nu=\rho,\sigma} \left(\frac{\alpha + i(v_F(t-t') - (x-x'))}{\alpha + i(x-x' + v_F(t-t'))} \right)^{-\frac{1}{8}s_\nu s'_\nu (r+r')} \\
&\times \prod_{\nu=\rho,\sigma} \left(\frac{\Lambda + i(u_\nu(t-t') - (x-x'))}{\Lambda + i(x-x' + u_\nu(t-t'))} \right)^{-\frac{1}{8}s_\nu s'_\nu (r+r')} . \tag{D.10}
\end{aligned}$$

From this general formula we can obtain the two-particle Luttinger liquid correlation function Eq. (D.6) and, as a special case, the Eqs. (2.81), (2.83) and (2.68) in the main text.

The distinction between the cut-off α used in the definition of the field operator Eq. (D.1) and the cut-off Λ used for the interaction dependent parameters K_ν and u_ν is only essential at high energies corresponding to small distances and/or small times $|v_F t, x| \lesssim \Lambda$ (see Eq. (2.68)). Since the relevant energies $k_B T$, $\delta\mu$ and Δ are much smaller than $v_F/\Lambda \sim \varepsilon_F$, our final results Eqs. (2.77) and (2.87) could also be obtained by using a single (and finite) cut-off Λ .

Appendix E

Exact results for time integrals

In this appendix, we give the exact results for the time integrals in Eqs. (2.76) and (2.86). The integrals over the time variable t appearing in Eqs. (2.76) and (2.86) have the form

$$\begin{aligned} & \int_{-\infty}^{\infty} dt \frac{e^{i2\delta\mu t}}{\left(\frac{\Lambda}{u_\rho} + it\right)^Q \left(\frac{\Lambda}{u_\sigma} + it\right)^R} \\ &= \frac{2\pi e^{-2\delta\mu \frac{\Lambda}{u_\rho}} (2\delta\mu)^{Q+R-1}}{\Gamma(Q+R)} {}_1F_1(R; Q+R; 2\Lambda(u_\rho^{-1} - u_\sigma^{-1})\delta\mu). \end{aligned} \quad (\text{E.1})$$

This integral formula is valid for Q, R satisfying $\text{Re}(Q+R) > 1$ (see Ref. [100] p. 345) which is in the range of our interest since we have $Q+R > 2$. The function $\Gamma(x)$ in Eq. (E.1) is the Gammafunction and ${}_1F_1(\alpha; \gamma; z)$ is the confluent hypergeometric function given by

$${}_1F_1(\alpha; \gamma; z) = 1 + \frac{\alpha z}{\gamma 1!} + \frac{\alpha(\alpha+1) z^2}{\gamma(\gamma+1) 2!} + \dots \quad (\text{E.2})$$

In the main text we considered only the leading order term of ${}_1F_1$ since higher order terms are smaller by the parameters $2\delta\mu\Lambda/u_\rho$ and $2\delta\mu\Lambda/u_\sigma$. The integrals over the delay times t' and t'' in Eq. (2.86) contain Hankel functions of the first and second kind which are linear combinations of Bessel functions of the first and second kind, i.e. $H_0^{(1/2)}(t\Delta) = J_0(t\Delta) \pm iY_0(t\Delta)$. The integrals over t' and t'' in Eq. (2.86) are therefore linear combinations of

integrals of the form

$$\begin{aligned} & \lim_{\eta \rightarrow 0^+} \int_0^{\infty} dt e^{-\eta t} Y_0(t\Delta) t^\delta \\ &= \lim_{\eta \rightarrow 0^+} \left[-\frac{2}{\pi} \Gamma(\delta + 1) (\Delta^2 + \eta^2)^{-\frac{1}{2}(\delta+1)} Q_\delta \left(\eta / \sqrt{\eta^2 + \Delta^2} \right) \right], \quad (\text{E.3}) \end{aligned}$$

and

$$\begin{aligned} & \lim_{\eta \rightarrow 0^+} \int_0^{\infty} dt e^{-\eta t} J_0(t\Delta) t^\delta \\ &= \lim_{\eta \rightarrow 0^+} \left[\Gamma(\delta + 1) (\Delta^2 + \eta^2)^{-\frac{1}{2}(\delta+1)} P_\delta \left(\eta / \sqrt{\eta^2 + \Delta^2} \right) \right]. \quad (\text{E.4}) \end{aligned}$$

This result is valid for $\delta > -1$ (see Ref. [100] p. 691). The functions Q and P are Legendre functions. The limit $\eta \rightarrow 0^+$ for $Q_\delta(\eta/\sqrt{\eta^2 + \Delta^2})$ is (see Ref. [100] p. 959)

$$Q_\delta(0) = -\frac{1}{2} \sqrt{\pi} \sin(\delta\pi/2) \frac{\Gamma\left(\frac{\delta+1}{2}\right)}{\Gamma\left(\frac{\delta}{2} + 1\right)}, \quad (\text{E.5})$$

and the limit $\eta \rightarrow 0^+$ for $P_\delta(\eta/\sqrt{\eta^2 + \Delta^2})$ is

$$P_\delta(0) = \frac{\sqrt{\pi}}{\Gamma\left(\frac{\delta}{2} + 1\right) \Gamma\left(\frac{1-\delta}{2}\right)} = \frac{1}{\sqrt{\pi}} \cos(\delta\pi/2) \frac{\Gamma\left(\frac{\delta+1}{2}\right)}{\Gamma\left(\frac{\delta}{2} + 1\right)}. \quad (\text{E.6})$$

Appendix F

Response function $\chi_{\phi\phi}(\omega)$

Here, we calculate the equation of motion for the junction phase fluctuation ϕ and the charge fluctuation Q of the tunnel-junction in the Caldeira Leggett model

$$H_{env} = \frac{Q^2}{2C} + \sum_{n=1}^N \left[\frac{q_n^2}{2C_n} + \frac{(\phi - \varphi_n)^2}{2e^2 L_n} \right]. \quad (\text{F.1})$$

The operators of the system and bath satisfy Bose commutation relations $[\phi, Q] = ie$ and $[\varphi_n, q_n] = ie\delta_{nm}$ with other commutators vanishing¹. In the Heisenberg picture, an operator A evolves according to $\dot{A} = i[H_{env}, A]$. For the system variables Q and ϕ we obtain the equations of motion

$$\dot{Q} = \sum_{n=1}^N \frac{1}{eL_n} (\varphi_n - \phi), \quad \dot{\phi} = e\frac{Q}{C}. \quad (\text{F.2})$$

Similar, for the bath degrees of freedom we have

$$\dot{q}_n = \frac{1}{eL_n} (\phi - \varphi_n), \quad \dot{\varphi}_n = e\frac{q_n}{C_n}. \quad (\text{F.3})$$

To derive an equation of motion for φ_n in terms of the system variables only, we use the equation of motion for \dot{q}_n in the equation for $\dot{\varphi}_n$, and obtain

$$\ddot{\varphi}_n + \omega_n^2 \varphi_n = \omega_n^2 \phi, \quad (\text{F.4})$$

¹We use the convention $\hbar = 1$ like in the main text.

with $\omega_n^2 = 1/L_n C_n$. This inhomogeneous differential equation can be solved with the method of Green's function

$$\varphi_n(t) = \varphi_n^0(t) + \int_{t_0}^t dt' G_n(t-t') f_n(t'), \quad (\text{F.5})$$

where we have defined the force $f_n(t') = \omega_n^2 \phi(t')$ and the solution $\varphi_n^0(t)$ of the problem without the force, which depends on the initial conditions at t_0 . The Green's function $G_n(t-t')$ is the solution of $\ddot{\varphi}_n + \omega_n^2 \varphi_n = 0$ for $t > t'$ and is 0 for $t < t'$ with the boundary condition $G_n(t'+0-t') = 0$, and $\frac{d}{dt} G_n(t-t')|_{t=t'+0} = 1$. We find for $G_n(t-t')$

$$G_n(t-t') = \frac{\sin[\omega_n(t-t')]}{\omega_n} \Theta(t-t'), \quad (\text{F.6})$$

which in turn leads to the result for φ_n after performing a partial integration

$$\varphi_n(t) = \varphi_n^0(t) + \phi(t) - \cos(\omega_n t) \phi(t_0) - \int_{t_0}^t dt' \cos[\omega_n(t-t')] \dot{\phi}(t'). \quad (\text{F.7})$$

Now we use this form of φ_n in Eq. (F.2) for \dot{Q} and, by further using $\dot{\varphi} = eQ/C$, we obtain the equation of motion for Q which can be found in the literature, e.g. in the book of Ref. [114]

$$\dot{Q}(t) + \frac{1}{C} \int_{t_0}^t dt' Y(t-t') Q(t') = I_N(t). \quad (\text{F.8})$$

Here, we have introduced the admittance

$$Y(t) = \sum_{n=1}^N \frac{\Theta(t)}{L_n} \cos(\omega_n t) \quad (\text{F.9})$$

and the quantum mechanical noise current

$$I_N(t) = \sum_{n=1}^N \frac{1}{eL_n} [(\varphi_n(t_0) - \phi(t_0)) \cos(\omega_n t) + e \omega_n^2 q_n(t_0) \sin(\omega_n t)], \quad (\text{F.10})$$

where we have used the solution for the homogeneous problem $\varphi_n^0(t) = \varphi_n(t_0) \cos(\omega_n t) + e \omega_n^2 q_n(t_0) \sin(\omega_n t)$. The current I_N depends on the initial conditions of the bath and system. If we take the ensemble average of Eq. (F.8)

we obtain the classical equation of motion for the charge fluctuation Q on a capacitor with capacitance C which is connected in series to an impedance $Z(\omega)^{-1} = \int_{-\infty}^{+\infty} \exp(-i\omega t) Y(t)$ [114]. Since the admittance can be written in its Fourier representation via Eq. (F.9) we can model any impedance $Z(\omega)$ (including dissipation) with a suitable choice of the bath spectrum (L_n, C_n) . Note that the ensemble average is taken with respect to H_{env} only and therefore $\langle I_N(t) \rangle = 0$ since $I_N(t)$ is linear in the coordinates at time t_0 where we assume that the system (including the bath) is in equilibrium. We can also write down the equation of motion for the phase ϕ

$$C\ddot{\phi}(t) + \int_{t_0}^t dt' Y(t-t') \dot{\phi}(t') = eI_N(t). \quad (\text{F.11})$$

To calculate the response function $\chi_{\phi\phi}(\omega)$ we have to disturb the system with an external current $I(t)$ which is done by the perturbation Hamiltonian

$$H' = -\frac{1}{e}\phi I(t). \quad (\text{F.12})$$

The effect of this additional Hamiltonian changes the equation of motion in the sense that the noise current $I_N(t) \rightarrow I_N(t) + I(t)$. We now assume that in the distant past $t_0 \rightarrow -\infty$ the system and bath are in equilibrium described by the Hamiltonian H_{env} only. We then take the expectation value of Eq. (F.11) and obtain

$$C\langle \ddot{\phi}(t) \rangle + \int_{-\infty}^{+\infty} dt' Y(t-t') \langle \dot{\phi}(t') \rangle = eI(t) \quad (\text{F.13})$$

since $\langle I_N(t) \rangle = 0$. The susceptibility (or response function) is defined via

$$\langle \phi(t) \rangle = \frac{1}{e} \int_{-\infty}^{+\infty} dt' \chi_{\phi\phi}(t-t') I(t'). \quad (\text{F.14})$$

By going over to Fourier space we obtain $\chi_{\phi\phi}(\omega) = e\phi(\omega)/I(\omega)$. By comparison with the Fourier transformed equation (F.13), the susceptibility in terms of the impedance $Z(\omega) = Y^{-1}(\omega)$ becomes

$$\chi_{\phi\phi}(\omega) = e^2 \frac{Z_T(\omega)}{i\omega}. \quad (\text{F.15})$$

Here, we used the total impedance $Z_T = (i\omega C + Z^{-1}(\omega))^{-1}$. We have succeeded in relating the microscopic quantity $\chi_{\phi\phi}(\omega)$ to the phenomenological impedance $Z(\omega)$. We are mostly interested in the correlation function $\langle\phi(t)\phi(0)\rangle$ with $\phi(t) = \exp(iH_{env}t)\phi(0)\exp(-iH_{env}t)$. This connection is achieved by relating the correlation function to the dissipative part $\chi_{\phi\phi}^d(\omega) \equiv -\text{Im}(\chi_{\phi\phi}(\omega))$ of the susceptibility via the fluctuation dissipation theorem

$$\int_{-\infty}^{+\infty} dt e^{-i\omega t} \langle\phi(0)\phi(t)\rangle = \frac{2}{1 - e^{-\frac{\omega}{k_B T}}} \chi_{\phi\phi}^d(\omega). \quad (\text{F.16})$$

We then obtain our desired relation between the fluctuation correlator $\langle\phi(t)\phi(0)\rangle$ and the impedance of the electrical circuit [114]

$$\langle\phi(t)\phi(0)\rangle = 2 \int_{-\infty}^{+\infty} \frac{d\omega}{\omega} \frac{\text{Re}Z_T(\omega)}{R_Q} \frac{e^{-i\omega t}}{1 - e^{-\frac{\omega}{k_B T}}}. \quad (\text{F.17})$$

The quantum resistance R_Q is given here as $R_Q = 2\pi/e^2$ ($\hbar = 1$).

References

- [1] C.W.J. Beenakker and H. van Houten, “Quantum Transport in Semiconductor Nanostructures” in *Solid State Physics*, **44**, eds. H. Ehrenreich and D. Turnbull, Academic Press, New York, 1991.
- [2] S. Datta, *Electronic Transport in Mesoscopic Systems*, Cambridge University Press, London, 1995.
- [3] L.P. Kouwenhoven, G. Schön, and L.L. Sohn, *Mesoscopic Electron Transport*, NATO ASI Series E, Vol. 345, Kluwer Academic Publishers, 1997.
- [4] G.A. Prinz, *Phys. Today* **45**(4), 58 (1995); *Science* **282**, 1660 (1998).
- [5] S.A. Wolf, D.D. Awschalom, R.A. Buhrman, J.M. Daughton, S. von Molnár, M.L. Roukes, and A.Y. Chtchelkanova, *Science* **294**, 1488 (2001).
- [6] *Semiconductor Spintronics and Quantum Computing*, eds. D.D. Awschalom, D. Loss, and N. Samarth. Series on Nanoscience and Technology, Springer, 2002.
- [7] J.M. Kikkawa and D.D. Awschalom, *Phys. Rev. Lett.* **80**, 4313 (1998); *Nature* **397**, 139 (1999); D.D. Awschalom and J.M. Kikkawa, *Phys. Today* **52**(6), 33 (1999).
- [8] R. Fiederling, M. Keim, G. Reuscher, W. Ossau, G. Schmidt, A. Waag, and L.W. Molenkamp, *Nature* **402**, 787 (1999).
- [9] Y. Ohno, D.K. Young, B. Beschoten, F. Matsukura, H. Ohno, and D.D. Awschalom, *Nature* **402**, 790 (1999).

- [10] M.N. Baibich, J.M. Broto, A. Fert, F. Nguyen van Dau, F. Petroff, P. Etienne, G. Creuzet, A. Friedrich, and J. Chazeles, *Phys. Rev. Lett.* **61**, 2472 (1988).
- [11] S. Datta and B. Das, *Appl. Phys. Lett.* **56**, 665 (1990).
- [12] D. Loss and D.P. DiVincenzo, *Phys. Rev. A* **57**, 120 (1998).
- [13] A. Steane, *Rep. Prog. Phys.* **61**, 117 (1998).
- [14] D.P. DiVincenzo and D. Loss, *J. Magn. Magn. Mater.* **200**, 202 (1999).
- [15] M. Nielsen, I. Chuang, *Quantum Computation and Quantum Information*, Cambridge University Press, 2000.
- [16] C.H. Bennett and D.P. DiVincenzo, *Nature* **404**, 247 (2000).
- [17] P.W. Shor, in *Proc. 35th Symposium on the Foundations of Computer Science*, (IEEE Computer Society Press), 124 (1994).
- [18] L.K. Grover, *Phys. Rev. Lett.* **79**, 325 (1997).
- [19] J.I. Cirac and P. Zoller, *Phys. Rev. Lett.* **74**, 4091 (1995).
- [20] D. Cory, A. Fahmy, and T. Havel, *Proc. Nat. Acad. Sci. U.S.A.* **94**, 1634 (1997).
- [21] I.L. Chuang, N.A. Gershenfeld, and M. Kubinec, *Phys. Rev. Lett.* **80**, 3408 (1998).
- [22] J.A. Jones, M. Mosca, and R.H. Hanson, *Nature* **393**, 344 (1998).
- [23] E. Knill, R. Laflamme, R. Martinez, and C.-H. Tseng, *Nature* **404**, 368 (2000).
- [24] L.M.K. Vandersypen, R. Hanson, L.H. Willems van Beveren, J.M. Elzerman, J.S. Greidanus, S. De Franceschi, and L.P. Kouwenhoven, *quant-ph/0207059*.
- [25] B.E. Kane, *Nature* **393**, 133 (1998).
- [26] R. Virijen, E. Yablonovitch, K. Wang, H.W. Jiang, A. Balandin, V. Roychowdhury, T. Mor, and D.P. DiVincenzo, *Phys. Rev. A* **62**, 012306 (2000).

- [27] C.H.W. Barnes, J.M. Shilton, and A.M. Robinson, *Phys. Rev. B* **62**, 8410 (2000).
- [28] A. Barenco, D. Deutsch, A. Ekert, and R. Josza, *Phys. Rev. Lett.* **74**, 4083 (1995).
- [29] R. Landauer, *Science* **272**, 1914 (1996).
- [30] J.A. Brum and P. Hawrylak, *Superlattices and Microstructures* **22**, 431 (1997).
- [31] P. Zanardi and F. Rossi, *Phys. Rev. Lett.* **81**, 4752 (1998).
- [32] T. Tanamoto, *Phys. Rev. A* **61**, 022305 (2000).
- [33] T.P. Orlando, J.E. Mooij, L. Tian, C.H. van der Wal, L. Levitov, S. Lloyd, and J.J. Mazo, *Phys. Rev. B* **60**, 15398 (1999).
- [34] D. Averin, *Solid State Commun.* **105**, 659 (1998).
- [35] A. Shnirman, G. Schön, and Z. Hermon, *Phys. Rev. Lett.* **79**, 2371 (1997).
- [36] D.V. Averin and C. Bruder, *Phys. Rev. Lett.* **91**, 057003 (2003).
- [37] L.B. Ioffe, V.B. Geshkenbein, M.V. Feigel'man, A.L. Fauchère, and G. Blatter, *Nature* **398**, 679 (1999).
- [38] D. Pfannkuche, V. Gudmundson, P. A. Maksym, *Phys. Rev. B* **47**, 2244 (1993).
- [39] G. Burkard, D. Loss, and D.P. DiVincenzo, *Phys. Rev. B* **59**, 2070 (1999).
- [40] A. Einstein, B. Podolsky, and N. Rosen, *Phys. Rev.* **47**, 777 (1935).
- [41] J.S. Bell, *Speakable and unspeakable in quantum mechanics*, Cambridge University Press, Melbourne, 1993.
- [42] J.S. Bell, *Rev. Mod. Phys.* **38**, 447 (1966).
- [43] A. Aspect, J. Dalibard, and G. Roger, *Phys. Rev. Lett* **49**, 1804 (1982).

- [44] K. Mattle, H. Weinfurter, P. G. Kwiat, and A. Zeilinger, *Phys. Rev. Lett.* **76**, 4656 (1996).
- [45] D. Bouwmeester, J.-W. Pan, K. Mattle, M. Eibl, H. Weinfurter, and A. Zeilinger, *Nature* **390**, 575 (1997).
- [46] D. Boschi, S. Branca, F. De Martini, L. Hardy, and S. Popescu, *Phys. Rev. Lett.* **80**, 1121 (1998).
- [47] G. Burkard, D. Loss, and E. V. Sukhorukov, *Phys. Rev. B* **61**, R16 303 (2000). Subsequent considerations in this direction are discussed in Refs. J.C. Egues, G. Burkard, and D. Loss, *Phys. Rev. Lett.* **89**, 176401 (2002); G. Burkard and D. Loss, *Phys. Rev. Lett.* **91**, 087903 (2003). For a comprehensive review on noise of spin-entangled electrons, see: J.C. Egues, P. Recher, D.S. Saraga, V.N. Golovach, G. Burkard, E.V. Sukhorukov, and D. Loss, in *Quantum Noise in Mesoscopic Physics*, pp 241-274, Kluwer, The Netherlands, 2003; cond-mat/0210498.
- [48] P. Recher, E.V. Sukhorukov, and D. Loss, *Phys. Rev. Lett.* **85**, 1965 (2000).
- [49] S. Kawabata, *J. Phys. Soc. Jpn.* **70**, 1210 (2001).
- [50] N.M. Chtchelkatchev, G. Blatter, G. Lesovik, and T. Martin, *Phys. Rev. B* **66**, 161320(R) (2002).
- [51] X. Hu and S. Das Sarma, *Phys. Rev. A* **61**, 062301 (2000).
- [52] X. Hu and S. Das Sarma, cond-mat/0307024.
- [53] C.W.J. Beenakker and C. Schönberger, *Phys. Today*, **56**(5), 37 (2003).
- [54] C. Piermarocchi, P. Chen, L.J. Sham, and D.G. Steel, *Phys. Rev. Lett.* **89**, 167402, (2002).
- [55] A. Imamoglu, D.D. Awschalom, G. Burkard, D.P. DiVincenzo, D. Loss, M. Sherwin, and A. Small, *Phys. Rev. Lett.* **83**, 4204 (1999).
- [56] M.-S. Choi, C. Bruder, and D. Loss, *Phys. Rev. B* **62**, 13569 (2000).
- [57] W.D. Oliver, F. Yamaguchi, and Y. Yamamoto, *Phys. Rev. Lett.* **88**, 037901 (2002).

- [58] D.S. Saraga and D. Loss, *Phys. Rev. Lett.* **90**, 166803 (2003).
- [59] J.R. Schrieffer, *Theory of Superconductivity*, Benjamin/Cummings, New York, 1964; M. Tinkham, *Introduction to Superconductivity* 2nd ed., McGraw-Hill, Inc., New York, 1996.
- [60] F.W.J. Hekking, L.I. Glazman, K.A. Matveev, and R.I. Shekhter, *Phys. Rev. Lett.* **70**, 4138 (1993).
- [61] P. Recher, E.V. Sukhorukov, and D. Loss, *Phys. Rev. B* **63**, 165314 (2001).
- [62] P. Recher and D. Loss, *Phys. Rev. B* **65**, 165327 (2002).
- [63] C. Bena, S. Vishveshwara, L. Balents, and M.P.A. Fisher, *Phys. Rev. Lett.* **89**, 037901 (2002).
- [64] P. Recher and D. Loss, *Phys. Rev. Lett.* **91**, 267003 (2003).
- [65] G.B. Lesovik, T. Martin, and G. Blatter, *Eur. Phys. J. B* **24**, 287 (2001).
- [66] S. Bose and D. Home, *Phys. Rev. Lett.* **88**, 050401 (2002).
- [67] P. Samuelsson, E.V. Sukhorukov, and M. Büttiker, *Phys. Rev. Lett.* **91**, 157002 (2003).
- [68] C.W.J. Beenakker, C. Emary, M. Kindermann, and J.L. van Velsen, *Phys. Rev. Lett.* **91**, 147901 (2003).
- [69] P. Recher and D. Loss, *Journal of Superconductivity: Incorporating Novel Magnetism* **15** (1): 49 (2002).
- [70] H.-A. Engel, P. Recher, and Daniel Loss, *Solid State Commun.* **119**, 229 (2001).
- [71] H. Takayanagi, T. Akazaki, and J. Nitta, *Phys. Rev. Lett.* **75**, 3533 (1995).
- [72] S. De Franceschi, F. Giazotto, F. Beltram, L. Sorba, M. Lazzarino, and A. Franciosi, *Appl. Phys. Lett.* **73**, 3890 (1998).
- [73] L.C. Venema, J.W.G. Wildöer, J.W. Janssen, S.J. Tans, H.L.T. Tuinstra, and L.P. Kouwenhoven, *Science* **283**, 52 (1999).

- [74] W. Liang, M. Bockrath, and H. Park, Phys. Rev. Lett. **88**, 126801 (2002); D.H. Cobden and J. Nygård, Phys. Rev. Lett. **89**, 046803 (2002).
- [75] M.R. Buitelaar, A. Bachthold, T. Nussbaumer, M. Iqbal, and C. Schönberger, Phys. Rev. Lett. **88**, 156901 (2002).
- [76] G.D. Mahan, *Many-Particle-Physics, third edition*, Kluwer Academic/Plenum Publishers, New York, 2000.
- [77] E. Merzbacher, *Quantum Mechanics* 3rd ed., John Wiley and Sons, New York, 1998, ch. 20.
- [78] N.W. Ashcroft and N.D. Mermin, *Solid State Physics*, (Holt, Rinehart, and Winston, New York, 1976).
- [79] A.F. Volkov, P.H.C. Magne, B.J. van Wees, and T.M. Klapwijk, Physica C **242**, 261 (1995).
- [80] J. Eroms, M. Tolkiehn, D. Weiss, U. Rössler, J. De Boeck, and G. Borghs, Eur. Phys. Lett. **58**, 569 (2002).
- [81] M. Kociak, A. Yu. Kasumov, S. Guron, B. Reulet, I.I. Khodos, Yu.B. Gorbatov, V.T. Volkov, L. Vaccarini, and H. Bouchiat, Phys. Rev. Lett. **86**, 2416 (2001).
- [82] S. Tarucha, D.G. Austing, T. Honda, R.J. van der Hage, and L.P. Kouwenhoven, Phys. Rev. Lett. **77**, 3613 (1996).
- [83] D. Loss and E.V. Sukhorukov, Phys. Rev. Lett. **84** 1035 (2000).
- [84] D. Pines and P. Nozieres, *The Theory of Quantum Liquids*, Benjamin, Reading, Mass., 1966.
- [85] J.M. Luttinger, J. Math. Phys. **4**, 1154 (1963).
- [86] F.D.M. Haldane, J. Phys. C. **14**, 2585 (1981).
- [87] R. Heidenreich, R. Seiler, and A. Uhlenbrock, J. Stat. Phys. **22**, 27 (1980).
- [88] M. Bockrath, D.H. Cobden, J. Lu, A.G. Rinzler, R.E. Smalley, L. Balents, and P.L. McEuen *Nature* **397**, 598 (1999).

- [89] O.M. Auslaender, A. Yacoby, R. de Picciotto, K.W. Baldwin, L.N. Pfeiffer, and K.W. West, *Phys. Rev. Lett.* **84**, 1764 (2000).
- [90] M.R. Geller and D. Loss, *Phys. Rev. B* **62**, R16 298 (2000).
- [91] R. Egger and A. Gogolin, *Phys. Rev. Lett.* **79**, 5082 (1997); R. Egger, *Phys. Rev. Lett.* **83**, 5547 (1999).
- [92] C. Kane, L. Balents, and M.P.A. Fisher, *Phys. Rev. Lett.* **79**, 5086 (1997).
- [93] H.J. Schulz, G. Cuniberti, and P. Pieri, in *Field Theories for Low-Dimensional Condensed Matter Systems*, G. Morandi et al. Eds. Springer, 2000.
- [94] R. Fazio, K.H. Wagenblast, C. Winkelholz, and G. Schön, *Physica B*, **222**, 364 (1996).
- [95] J. Sólyom, *Adv. Phys.* **28**, 201 (1979).
- [96] Y. Suzumura, *Prog. Theor. Phys.* **63**, 5 (1980).
- [97] H.J. Schulz, *J. Phys. C* **16**, 6769 (1983).
- [98] J. Voit, *J. Phys. CM* **5**, 8305 (1993).
- [99] P. Recher and D. Loss, unpublished.
- [100] I.S. Gradshteyn and I.M. Ryzhik, *Table of Integrals, Series, and Products, Sixth Edition*, Academic Press, San Diego, 2000.
- [101] J. Nygård, Ph.D. Thesis, Faculty of Science University of Copenhagen (2000).
- [102] A. Bachthold, M. de Jonge, K. Grove-Rasmussen, and P.L. McEuen, M. Buitelaar and C. Schönenberger, *Phys. Rev. Lett.* **87**, 166801 (2001).
- [103] D. Rugar, B.C. Stipe, H.J. Mamin, C.S. Yannoni, T.D. Stowe, K.Y. Yasumura, and T.W. Kenny, *Appl. Phys. A* 72 [Suppl.], S3-S10 (2001).
- [104] H.-A. Engel and D. Loss, *Phys. Rev. Lett.* **86**, 4648 (2001); *Phys. Rev. B* **65**, 195321 (2002).

- [105] H.-A. Engel, V. Golovach, D. Loss, L.M.K. Vandersypen, J.M. Elzerman, R. Hanson, and L.P. Kouwenhoven, cond-mat/0309023.
- [106] L. Balents and R. Egger, Phys. Rev. B **64** 035310 (2001).
- [107] M.R. Geller and D. Loss. Phys. Rev. B **56** 9692 (1997).
- [108] J. Nitta, T. Akazaki, H. Takayanagi, and K. Arai, Phys. Rev. B **46**, 14286 (1992); C. Nguyen, H. Kroemer, and E.L. Hu, Phys. Rev. Lett. **69**, 2847 (1992).
- [109] A.M. Marsh, D.A. Williams, and H. Ahmed, Phys. Rev. B **50**, 8118 (1994).
- [110] A.J. Rimberg, T.R. Ho, Ç. Kurdak, and J. Clarke, Phys. Rev. Lett. **78**, 2632 (1997).
- [111] L.S. Kuzmin, Yu.V. Nazarov, D.B. Haviland, P. Delsing, and T. Claesson, Phys. Rev. Lett. **67**, 1161 (1991).
- [112] J.J. Hesse and G. Diener, Physica B **203**, 393 (1994).
- [113] A. Huck, F.W.J. Hekking, and B. Kramer, Eur. Phys. Lett. **41**, 201 (1998).
- [114] M.H. Devoret, D. Esteve, H. Grabert, G.-L. Ingold, H. Pothier, and C. Urbina, Phys. Rev. Lett. **64**, 1824 (1990); see also G.-L. Ingold and Y.V. Nazarov, ch. 2 in H. Grabert and M.H. Devoret (eds.), *Single Charge Tunneling*, Plenum Press, New York, 1992.
- [115] A.O. Caldeira and A.J. Leggett, Ann. Phys. (N.Y.) **149**, 374 (1983).
- [116] F.G. Monzon and M.L. Roukes, J. Mag. Magn. Mater. **198**, 632 (1999).
- [117] S. Lüscher, T. Heinzel, K. Ensslin, W. Wegscheider, and M. Bichler, Phys. Rev. Lett. **86**, 2118 (2001).
- [118] Y. Kato, R.C. Myers, D.C. Driscoll, A.C. Gossard, J. Levy, and D.D. Awschalom, Science **299**, 1201 (2003).
- [119] R. Hanson, B. Witkamp, L.M.K. Vandersypen, L.H. Willems van Beveren, J.M. Elzerman, and L.P. Kouwenhoven, cond-mat/0303139.

- [120] M. Ciorga, A.S. Sachrajda, P. Hawrylak, C. Gould, P. Zawadzki, S. Jullian, Y. Feng, and Z. Wasilewski, Phys. Rev. B **61**, R16315 (2000); Physica E **11**, 35 (2001).
- [121] L.P. Kouwenhoven, D.G. Austing, and S. Tarucha, Rep. Prog. Phys. **64**, 701 (2001).
- [122] R. Hanson, L.M.K. Vandersypen, L.H. Willems van Beveren, J.M. Elzerman, I.T. vink, and L.P. Kouwenhoven, cond-mat/0311414.
- [123] J.C. Egues, Phys. Rev. Lett. **80**, 4578 (1998).
- [124] M. Popp, D. Frustaglia, and K. Richter, Nanotechnology **14**, 347 (2003).
- [125] E.R. Mucciolo, C. Chamon, and C.M. Marcus, Phys. Rev. Lett. **89**, 146802 (2002).
- [126] M. Governale, D. Boese, U. Zülicke, and C. Schroll, Phys. Rev. B **65**, 140403(R) (2002).
- [127] T. Koga, J. Nitta, H. Takayanagi, and S. Datta, Phys. Rev. Lett. **25**, 126601 (2002).
- [128] J.A. Folk, R.M. Potok, C.M. Marcus, and V. Umansky, Science **299**, 679 (2003).
- [129] H. Ohno, Science **281** 951 (1999).
- [130] C.W.J. Beenakker, Phys. Rev. B **44**, 1646 (1991).
- [131] J.J. Sakurai, *Modern Quantum Mechanics*, Addison Wesley, New York, 1985.
- [132] D.V. Averin and Yu.V. Nazarov, in *Single Charge Tunneling*, eds. H. Grabert and M.H. Devoret, NATO ASI Series B: Physics Vol. 294, Plenum Press, New York, 1992.
- [133] M. Pustilnik, Y. Avishai, and K. Kikoin, Phys. Rev. Lett. **84**, 1756 (2000).
- [134] S. Tarucha, D.G. Austing, Y. Tokura, W.G. van der Wiel, and L.P. Kouwenhoven, Phys. Rev. Lett. **84**, 2485 (2000).

- [135] D. Weinmann, W. Häusler, W. Pfaff, B. Kramer, and U. Weiss, *Europhys. Lett.* **26**, 467 (1994); D. Weinmann, W. Häusler, and B. Kramer, *Phys. Rev. Lett.* **74**, 984 (1995).
- [136] S.J. Tans, M.H. Devoret, H. Dai, A. Thess, R.E. Smalley, L.J. Geerligs, and C. Dekker, *Nature* **386**, 474 (1997).
- [137] M. Bockrath, D.H. Cobden, P.L. McEuen, N.G. Chopra, A. Zettl, A. Thess, and R.E. Smalley, *Science* **275**, 1922 (1997); D.H. Cobden, M. Bockrath, P.L. McEuen, A.G. Rinzler, and R.E. Smalley, *Phys. Rev. Lett.* **81**, 681 (1998).

Curriculum Vitae

Ausbildung

30. Juli 1973	Geboren in Basel
1980-1985	Besuch der Primarschule in Basel und Gossau SG (erstes Schulhalbjahr 1983)
1985-1986	Besuch der Realschule in Basel
1986-1993	Besuch des mathematisch-naturwissenschaftlichen Gymnasiums (MNG) in Basel
1993	Matura (Typus C)
1993-1994	Militärdienst in der Schweizerischen Armee
1994-1999	Studium der Physik an der Universität Basel
November 1999	Diplom in Theoretischer Physik. Diplomarbeit mit Thema <i>Magnetization of a one-dimensional antiferromagnetic spin-chain in a uniform magnetic field</i> unter Anleitung von Prof. Daniel Loss
1999-2003	Doktorand und Assistent von Prof. Daniel Loss am Institut für Physik an der Universität Basel
November 2003	Dissertation in Theoretischer Physik mit Titel <i>Correlated Spin Transport in Nanostructures: Entanglement Creation and Spin Filtering</i> unter Anleitung von Prof. Daniel Loss

Meine universitäre Ausbildung verdanke ich den Professoren:

N. A'Campo, C. Bandle, G. Bauer, B. Binggeli, C. Bruder, R. Buser, O. Gerhard, H. -J. Güntherodt, D. Kotschick, D. Loss, E. Meyer, H. Rudin, B. Scarpellini, C. Schönenberger, I. Sick, G. -A. Tammann, L. Tauscher, F. -K. Thielemann, D. Trautmann und C. Ullrich,

und den Privatdozenten:

U. Aeschbacher, T. Ahrend, W. Belzig, H. Mühry und H. Walser.

Publikationen

Dynamical Coulomb blockade and spin-entangled electrons

P. Recher and D. Loss, Phys. Rev. Lett. 91, 267003 (2003)

Towards Quantum Communication with Electron Spins

D.S. Saraga, G. Burkard, J.C. Egues, H.-A. Engel, P. Recher, D. Loss
Turk. J. Phys. 27, 427 (2003)

Shot noise for entangled and spin-polarized electrons

J.C. Egues, P. Recher, D.S. Saraga, V.N. Golovach, G. Burkard,
E.V. Sukhorukov, and D. Loss

Quantum Noise in Mesoscopic Physics, ed. Yu. Nazarov, Kluwer,
The Netherlands, 2003; cond-mat/0210498

*Superconductor coupled to two Luttinger liquids as an
entangler for electron spins*

P. Recher and D. Loss
Phys. Rev. B 65, 165327 (2002)

*Creation of nonlocal spin-entangled electrons via Andreev tunneling,
Coulomb blockade, and resonant transport*

P. Recher and D. Loss
Journal of Superconductivity: Incorporating Novel Magnetism 15, 49 (2002)

*Electron spins for spintronics and quantum communication
in quantum dots and wires*

D. Loss, P. Recher, and H.-A. Engel
XXXVI Rencontres de Moriond, Electronic Correlations: From meso- to
nano-physics, 525 (2001)

Electron spins in quantum dots for spintronics and quantum computation

H.-A. Engel, P. Recher, and D. Loss
Solid State Commun. 119, 229 (2001)

Andreev tunneling, Coulomb blockade, and resonant transport of nonlocal spin-entangled electrons

P. Recher, E.V. Sukhorukov, and D. Loss
Phys. Rev. B 63, 165314 (2001)

Quantum dot as spin filter and spin memory

P. Recher, E.V. Sukhorukov, and D. Loss
Phys. Rev. Lett. 85, 1962 (2000)

Spintronics and quantum computing with quantum dots

P. Recher, D. Loss, and J. Levy
Macroscopic Quantum Coherence and Quantum Computing, eds. D.V. Averin, B. Ruggiero, and P. Silvestrini, Kluwer Academic/Plenum Publishers, New York, 2001; cond-mat/0009270

Patent

Titel: A Spin Filter and a Memory using such a Spin Filter

Erfinder: P. Recher, E.V. Sukhorukov, and D. Loss

Inhaber: Scientific Generics Limited

Patent Nr.: 00958807.0-2203-GB0003422